The Pennsylvania State University
The Graduate School
College of Agricultural Science

HENIPAVIRUS ASSEMBLY AND BUDDING

A Dissertation in
Pathobiology
by
Weina Sun

Submitted in Partial Fulfillments
of the Requirements
for the Degree of

Doctor of Philosophy

May 2015

The dissertation of Weina Sun was reviewed and approved* by the following:

Anthony P. Schmitt

Associate Professor of Molecular Virology

Dissertation Advisor

Chair of the Committee

Director of Pathobiology Graduate Program

K. Sandeep Prabhu

Professor of Immunology and Molecular Toxicology

Pamela A. Hankey Giblin

Professor of Immunology

Immunology and Infectious Disease Undergraduate Advisor

Robert F. Paulson

Professor of Veterinary and Biomedical Science

Craig E. Cameron

Professor of Biochemistry and Molecular Biology

Eberly Chair in Biochemistry and Molecular Biology

*Signatures are on file in the Graduate School

ABSTRACT

The emergence of a group of paramyxoviruses called henipavirus has caused fatal illness such as severe vasculitis and encephalitis which resulted in high fatality rate in both humans and animals since 1990's in south Asia and Australia. Like other paramyxoviruses, the essential viral protein that organizes the process of henipavirus assembly and budding is the matrix protein (M), where it functions to link together the viral glycoproteins and ribonucleoprotein complex (RNPs). Current studies have sought out to investigate the host factors that are involved in virus assembly and budding by interacting with M protein to facilitate M functions.

In an effort to identify host factors that are important for henipavirus assembly and budding, proteomics-based approach was performed to identify host proteins that interact with viral M protein. Here, we affinity purified viral M proteins by FPLC and identified co-purifying host proteins by mass spectrometry. Co-immunoprecipitation was used as a secondary screening of protein candidates identified from mass spec results. One of the host proteins candidates, AP3B1, the beta subunit of AP-3 complex, was selected for further investigations. Importantly, a 29 amino acids polypeptide derived from AP3B1 hinge domain was identified as the minimal fragment to bind M protein as well as effectively inhibit henipavirus-like particles (VLPs) production. This inhibitory effect is due to disruption of M protein association with membrane. Additionally, in AP3B1 depleted cells by siRNA knockdown, Nipah VLP production is significantly reduced. By immunofluorescence

microscopy, M protein colocalization with endogenous AP3B1 was also observed in mammalian cells. Our results suggested that AP-3 might play an important role in M protein functions.

Henipaviruses have two types of surface glycoproteins, the attachment protein (G) and fusion protein (F). They were responsible for virus entry by mediating virus attachment to cell receptors and fusion with cell membrane. Numerous studies have illustrated how the virus entry occurs under the coordination of G and F proteins. However, little is known about how glycoproteins assemble into virions or VLPs. We know that M protein is the main driving force of particles formation, so we wondered how M protein coordinates with G protein and F protein to facilitate their trafficking and assembly into virions or VLPs. Here, under the unique pathway of HeV F protein identified by our collaborator Dr. Rebecca Dutch at University of Kentucky, we have found that HeV M protein, F protein and G protein all partially colocalized with Rab11a-REs, and overexpression of a DN Rab11a could significantly inhibit Hendra M-VLPs as well as F-VLPs formation in the cells. Interestingly, in cells that express inhibitory AP3B1 Hinge domain, M colocalization with Rab11-REs was disrupted. Unlike M protein or F protein, G proteins releases poorly into particles when expressed alone in cells. We observed that G incorporation into VLPs could be facilitated by co-expression of M protein but not F protein, likely through G-M interaction at the plasma membrane. Moreover, we have found that F protein incorporation into VLPs depended on its endocytic trafficking event regardless its cleavage status, as an endocytosis defective mutant F S490A that was retained on

the cell surface was shown to be significantly defective on particles assembly. On the other hand, HeV F protein still well incorporated into VLPs when its cleavage was prevented by a cathepsin L inhibitor, E-64d. Therefore, we hypothesized that henipavirus M and F proteins have separate mechanisms for trafficking to Rab11-REs, with the M protein trafficking facilitated by its interaction with AP3B1. M and cathepsin-cleaved F proteins must then assemble together within these compartments prior to their delivery to the cell surface for particle budding and assemble with G protein through G-M interaction at the plasma membrane.

TABLE OF CONTENTS

LIST OF FIGURES ..... **ix**

LIST OF TABLES ..... **xi**

LIST OF ABBREVIATIONS ..... **xii**

CHAPTER 1 ..... **1**

Introduction **1**

1.1 Paramyxovirus classification and significance 1

1.2 Paramyxovirus genome and replication 6

1.3 Paramyxovirus matrix (M) protein and virus assembly 10

1.4 Virus-like particles production 15

1.5 Trafficking of paramyxovirus glycoproteins 17

1.6 Adaptor protein (AP) complexes 20

1.7 Adaptor protein 3 (AP-3) complex 23

1.8 AP-3 complex and viral trafficking 24

1.9 Rab11 GTPase in negative-strand RNA virus assembly 26

1.10 Identification of protein-protein interactions between virus and host 29

1.11 Preview 31

CHAPTER 2 ..... **34**

Materials and Methods **34**

Plasmids 34

Henipavirus M protein affinity purification and mass spectrometry 37

Coimmunoprecipitation 38

Measurements of VLP production 39

Membrane flotation assays to measure M protein membrane association 41

RNA interference (RNAi) 41

Immunofluorescence microscopy 42

Brefeldin A (BFA) treatment 44

Cathepsin L inhibition VLP assay 45

Phosphoinositide 3-kinase (PI3K) inhibition VLP assay 46

Sedimentation gradient analysis of Hendra VLPs density 46

Subcellular fractionation 47

CHAPTER 3 49

Matrix Proteins of Nipah and Hendra Viruses Interact with Beta Subunits of AP-3 Complexes 49

3.1 Introduction 49

3.2 Results 51

Identification of henipavirus M-associating host proteins by affinity purification and mass spectrometry 51

AP3B1 interacts with Henipavirus M proteins via its hinge domain 55

Overexpression of M-binding, AP3B1-derived polypeptides blocks production of henipavirus VLPs 61

Depletion of AP3B1 from cells impairs Nipah VLP production 66

Partial co-localization of Nipah virus M protein with endogenous AP3B1 in transfected cells 68

3.3 Discussion 70

CHAPTER 4 75

Trafficking and Assembly of Hendra Virus Glycoproteins with Matrix Protein 75

4.1 Introduction 75

4.2 Results 81

M trafficking to Rab11a recycling endosomes is important for Hendra M-VLPs production 81

F trafficking to Rab11a recycling endosomes is important for Hendra F-VLPs production 85

Endocytic trafficking of Hendra virus F protein is required for assembly into M-VLPs 88

Evidence for M-mediated recruitment of HeV G into VLPs 91

Hendra virus G protein colocalizes with M protein in transfected cells 93

4.3 Discussion 95

CHAPTER 5 101

Summary and Future Directions 101

5.1 Summary 101

5.2 Future Directions 103

Develop antiviral-strategies against henipaviruses using inhibitory polypeptides derived from AP3B1 103

Explore the biological role of AP-3 complex in M protein functions 105

Identify other M-interacting host factors in both human cells and bat cells ... 108

Explore the trafficking of HeV M and assembly of HeV M protein with G and F proteins 109

APPENDICES 114

Appendix A: Brefeldin A treatment disrupts M protein intracellular localization and impairs M-VLP productions 114

Appendix B: Mapping AP3B1 binding sites within NiV M protein 117

Appendix C: Generating M mutants that fail to bind AP3B1 119

Appendix D: Mutations within Hinge 1B screen for amino acids residues that are more important for M-binding 123

Appendix E: Hendra F and M VLPs productions are inhibited upon PI3P depletion….. 127

Appendix F: HeV M and F are in vesicles resembling Rab11a positive compartments 129

BIBLIOGRAPHY 132

LIST OF FIGURES

Figure 1-1. Phylogenetic tree of the paramyxovririnae subfamily. 5

Figure 1-2. Genome organization of representative members from genera of paramyxoviridae. 8

Figure 1-3. Paramyxovirus particle and life cycle. 9

Figure 1-4. Budding of paramyxovirus particles. 14

Figure 1-5. Classical trafficking pathway of viral surface glycoproteins. 19

Figure 1-6. Overview of AP complexes. 22

Figure 1-7. Model of interactions between negative-strand RNA viruses and the Rab11 pathway. 28

Figure 3-1. Identification of henipavirus M-associating host proteins by affinity purification and mass spectrometry. 55

Figure 3-3. Small AP3B1-derived polypeptides bind Nipah virus M protein. 60

Figure 3-4. Small AP3B1-derived polypeptides inhibit henipavirus VLP production.. 63

Figure 3-5. AP3B1 Hinge polypeptide inhibits the membrane-binding ability of Nipah virus M protein 65

Figure 3-6. siRNA knockdown of endogenous human AP3B1 decreases Nipah VLP production 67

Figure 3-7. Partial colocalization of Nipah virus M protein with endogenous AP3B1 in 293T cells. 69

Figure 4-1. Schematic illustration of paramyxovirus glycoproteins domain structures. 77

Figure 4-2. Unique trafficking pathway of Hendra virus F protein. 80

Figure 4-4. Rab11-REs co-localize with Hendra virus glycoproteins and are necessary for F-VLPs production. 87

Figure 4-5. Endocytosis but not proteolytic processing of F protein is required for Hendra virus M and F proteins assembly into the same particles. 90

Figure 4-6. Hendra virus G protein incorporation into VLPs is enhanced by M protein instead of F protein. 92

Figure 4-7. Colocalization of Hendra virus G protein with M protein in transfected Vero cells. 94

Figure 4-8. An overall model for Hendra virus M assembly with Hendra virus glycoproteins 97

Figure A-1. Brefeldin A treatment impaires Nipah M-VLPs production by disrupting M membrane association 116

Figure B-1. Mapping AP3B1-binding region within Nipah virus M protein. 118

Figure C-1. Identification of Nipah virus M mutants that are defective on AP3B1 binding. 121

Figure C-2. Mutant Nipah virus M proteins that fail to bind AP3B1 are also defective on VLP production..... 122

Figure D-1. Generating Hinge 1B mutants that are defective on M-binding. 125

Figure D-2. Hinge 1B mutant that fail to bind M protein do not inhibit Nipah M-VLPs production..... 126

Figure E-1. PI3K inhibitor LY294002 treatment severely impairs both Hendra virus M-VLPs and F-VLPs. 128

Figure F-1. Subcellular fractionation in an iodixanol gradient to examine HeV M and F localization to Rab11 positive compartments. 131

LIST OF TABLES

Table 1-1. Different requirements of paramyxovirus VLPs productions. 16
Table 4-1. Proteolytic cleavages sites of viral type I glycoproteins. 78

LIST OF ABBREVIATIONS

AMOTL1 – Angiomotin like 1
AP – Adaptor protein
AP-3 – Adaptor protein 3
AP3β1 – Adaptor protein complex AP-3 subunit beta 1
CT – Cytoplasmic tail
DN – Dominant-negative
EBOV - Ebola virus
EGFP- Enhanced green fluorescence protein
ESCRT – Endosomal sorting complex required for transport
EXOSC10 - Exosome component 10
F – Fusion
FPLC - Fast protein liquid chromatography
G – Glycoprotein
H – Hemagglutinin
HBV – Hepatitis B virus
HERC5 - HECT And RLD domain containing E3 ubiquitin protein ligase 5
HeV – Hendra virus
HeV SH-M – Strep (II), 6xHis-tagged Hendra virus M protein
HIV-1 – Human immunodeficiency virus-1
hMPV- Human metapneumovirus
HN – Hemagglutinin-neuraminidase
hPIV – Human parainfluenza virus
HPV – Human papillomavirus
hRSV – Human respiratory syncytial virus
HTATSF1 - HIV-1 Tat specific factor 1
IAV – Influenza A virus
ILF2/3 - Interleukin enhancer binding factor 2/3
ILV – Intralumenal vesicles
L – Large
LC/LC-MS/MS – Multidimensional liquid chromatography and tandem mass Spectrometry
LROs – Lysosome- related organells
M - Matrix
MeV – Measles virus
MS – Mass spectrometry

MuV – Mumps virus
MVB – Multivesicular body
N/NP – Nucleocapsid
NDV – Newcastle disease virus
NiV – Nipah virus
NiV SH-M – Strep (II), 6xHis-tagged Nipah virus M protein
NKRF - NF-KappaB repressing factor
P – Phosphoprotein
PIV5 – Parainfluenza virus 5
PI3K - Phosphoinositide 3-kinase
P. *alecto* – Pteropus Alecto
Rab11-FIPs – Rab11-family-interacting proteins
RdRP – RNA-dependent RNA polymerase
RNP – Ribonucleoprotein complex
RPS3 - Ribosomal protein S3
RSV – Respiratory syncytia Virus
SeV – Sendai virus
SDS-PAGE - Sodium dodecyl sulfate polyacrylamide gel electrophoresis
SH – Small hydrophobic
SIV – Simian immunodeficiency virus
TCOF1 - Treacher Collins-Franceschetti syndrome 1
TGN – Trans-Golgi network
TM – Trans-membrane
TSG101 - Tumor susceptibility gene 101
Ub - Ubiquitin
VLP – Virus-like particle
VPRBP - Vpr (HIV-1) Binding Protein
VPS – Vacuolar protein sorting
VSV – Vesicular stomatitis virus
Y2H – Yeast two-hybrid
ZC3HAV1 - Zinc Finger CCCH-Type, antiviral 1

CHAPTER 1

Introduction

1.1 Paramyxovirus classification and significance

Paramyxoviruses are a group of enveloped viruses that consist of many nonpathogenic and pathogenic viruses. There are two sub-families in the family of *paramyxovirdae*: *paramyxovirinae* and *pneumovirinae*. *Paramyxovirinae* is then divided into five genera: *rubulavirus, respirovirus*, *mobilivirus*, *avulavirus* and newly emerged *henipavirus* (Fig. 1-1), whereas *pneumovirinae* consists of two genera: *pneumovirus* and *metapneumovirus*. Many paramyxoviruses are important pathogens in humans and animals such as Measles virus (MeV), Mumps virus (MuV), Newcastle disease virus (NDV), Nipah virus (NiV) and Hendra virus (HeV) as well as human Parainfluenza virus (hPIV), human Respiratory Syncytial virus (hRSV) and human Metapneumovirus (hMPV).

In the subfamily of paramyxovirinae, some human pathogens such as MeV and MuV are still posing a huge threat to the health of the populations in developing countries where vaccination is not as easily available as it is in developed countries. Although the routine vaccination with MMR (Measles, Mumps and Rubella) was introduced to United States since 1967 (167), and most people were protected against the diseases caused by these viruses, several outbreaks still occurred in United States during the last decade due to incomplete protection of the vaccine (~88% effective of two dose MMR; ~78% effective of one dose MMR) and

unvaccinated groups (167). For example, in 2006, the United States experienced a multi-state outbreak involving more than 6500 reported cases of Mumps (167); In July 2009, more than 4000 cases were involved in a Mumps outbreak in North America including New York, New Jersey and Quebec in Canada (167). For Measles viruses, Centers for Disease Control and Prevention (CDC) has reported that from Jan 1st to Jan 30th of 2015, 102 people from 14 states in United States have been diagnosed with Measles (36). Since the Measles elimination from 2000, outstanding reemergence of Measles has reached a record of 644 cases from 27 states during 2014 (36). As these viruses are transmitted by aerosol route, unvaccinated individuals and international travel are likely to be the main routes for the virus to spread worldwide. More efforts are suggested for appropriate vaccination of people against the diseases.

In the subfamily of pneumovirinae, there are also important human pathogens, such as hRSV and hMPV. Both viruses cause respiratory tract disease in infants and young children. They could also infect adults and immunocompromised individuals (61, 212). The clinical manifestations of hMPV range from a mild upper respiratory tract infection to severe pneumonia and bronchiolitis, but usually, they are indistinguishable from hRSV infection (215). Currently, there are no commercially available vaccines for hRSV and hMPV prevention, and there are limited therapeutic approaches against them, even though ribavirin showed some effectiveness (22, 202).

In addition, newly emerged zoonotic paramyxoviruses cause severe illness in both animals and humans. Examples include NiV and HeV, the two members in the genus of henipavirus. Cedar virus (CedV) was recently identified as the third member of henipavirus (121). These viruses naturally infect fruit bats (*Pteropodidae* family) (40, 77), but spillover events sometimes lead to the transmission of the viruses to other species. During the 1990s, numerous outbreaks occurred, in which the viruses first transmitted from bats to domesticated animals (horses and pigs) and then transmitted to humans (133, 161, 216). In humans, the viruses cause fatal illnesses such as acute respiratory disease, severe vasculitis and encephalitis (40, 41, 72, 132, 133). Most human cases were among swine and equine handlers who have occupational exposure to the affected animals. However, human-to-human transmission has been observed for NiV during outbreaks in Bangladesh in 2004 (75). Epithelial cells from the lower respiratory tract, endothelial cells, and neurons are thought to be the main targets of NiV and HeV infection as they bear ephrin-B2/3 receptors for virus attachment (26, 63, 120, 131, 211). As ephrin-B2/3 are conserved among mammalian species, both NiV and HeV infect a wide range of hosts. NiV and HeV outbreaks have created public health emergencies in Australia and southern Asia, and have caused significant economic loss in the agricultural sectors. Given the lack of both preventive and therapeutic treatments against henipavirus infection, both NiV and HeV are classified as category C priority agents and are BSL-4 restricted (59). Currently, studies on vaccine development against lethal henipaviruses have made impressive progress based on the study on HeV G protein (23). For example, a

licensed horse vaccine Equivac ® HeV developed by CSIRO's Australian Animal Health Laboratory (AAHL) and Pfizer Animal Health is commercially available to immunize horses against HeV since Nov. 1st 2012, which provides a possibility to significantly minimize the diseases caused by HeV infection in both animals and their handlers (50, 126). Here, HeV G protein is modified to generate a soluble HeV G subunit (HeV-sG), which was used as the main vaccine components (23, 50, 126). In addition, neutralizing human monoclonal antibodies have been developed using HeV-sG as the antigen (226). One of these antibodies called m102.4 was demonstrated to be able to protect animal models such as ferrets and African green monkeys from both NiV and HeV lethal challenges (24, 29, 70, 225, 226). Meanwhile, HeV-sG has also been tested for its potential as vaccine in these animal models, and protection was observed after challenge with either NiV or HeV (23, 25, 128, 149). These studies showed that HeV-sG could be a promising vaccine candidate not just for horses, but for humans as well, although more efforts are required to solidify its effectiveness in humans.

Several other paramyxoviruses only affect animals, such as NDV. It belongs to *avulavirus* genus. Infection of NDV in avian species caused influenza-like symptoms, which resulted in significant loss in poultry industry (68). In spite of the fact that it poses no health hazards to humans, NDV is known to infect a wide variety of birds with varying degree of susceptibility and becomes one of the most widespread animal diseases (68). Currently, NDV remains a constant threat to the poultry industry worldwide, although NDV vaccination generated by a low virulent strain

was available decades ago. Interestingly, other studies have found that the vaccine strain of NDV can efficiently and selectively infect and kill cancer cells. It is consequently being investigated as a promising novel oncolytic virotherapy agent (222).

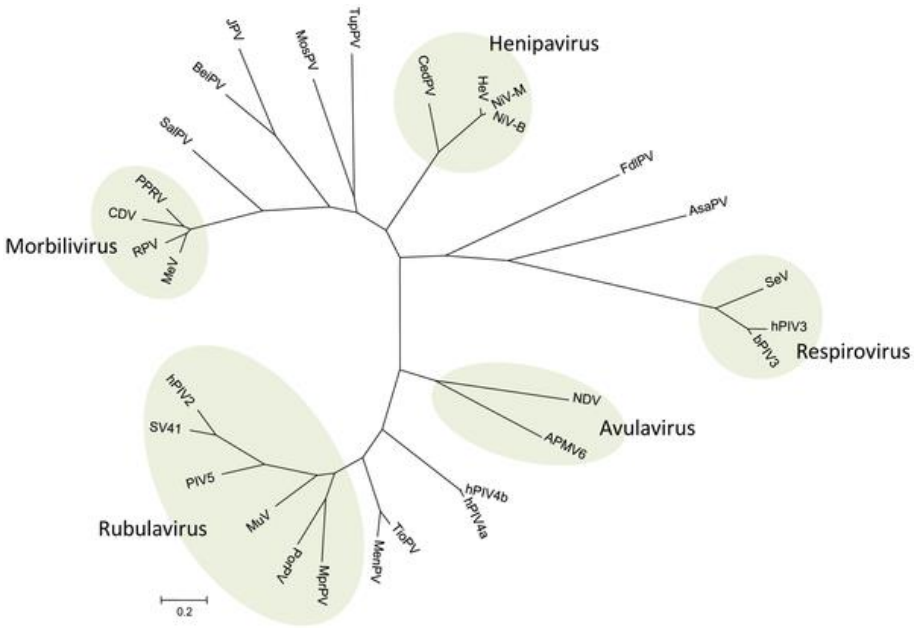

Figure 1-1. Phylogenetic tree of the paramyxovririnae subfamily. This phylogenetic tree is based on the N protein sequence of selected paramyxoviruses. Viruses were grouped according to genus as followed. *Henipavirus* genus: CedPV (Cedar virus), HeV (Hendra virus), NiV (Nipah virus). *Respirovirus* genus: SeV (Sendai virus), hPIV3 (Human parainfluenza virus 3), bPIV3 (Bovine parainfluenza virus 3). *Avulavirus* genus: NDV (Newcastle disease virus), APMV6 (Avian paramyxovirus type 6). *Rubulavirus* genus: hPIV2 (Human parainfluenza virus 2), SV41 (Simian parainfluenza virus 41), PIV5 (Parainfluenza virus 5), MuV (Mumps virus), PorPV (Porcine rubulavirus), MprPV (Mapeura virus). *Morbilivirus* genus: PPRV (Peste-des-Petits-Ruminants virus), CDV (Canine distemper virus), RPV (Rinderpest virus), MeV (Measles virus).This figure was adapted from (121).

1.2 Paramyxovirus genome and replication

The paramyxovirus genome is non-segmented, negative-stranded RNA ranging from 15kb~19kb in length. Genome of *paramyxovirnae* usually contains 6 or 7 genes encoding 6 to 9 proteins, in the relatively conserved order N/NP-P-M-F-(SH)-HN/H/G-L from 3' to 5', whereas genome of *pneumovirunae* contains 8 to 10 genes with extra genes to encode non-structural (NS) proteins and M2 protein (Fig. 1-2). Paramyxovirus replication and spreading starts with the attachment of virus particles to the sailic acids or protein receptors on the target cell surface. This is achieved by interaction of cellular receptor with viral attachment protein called HN, H or G, depending on the virus (Fig. 1-3A, B). Then the fusion between virus envelope and plasma membrane is mediated at neutral pH by the fusion (F) protein encoded by F gene. N/NP gene encodes the nucleocapsid protein that encapsidates the viral genome to form ribonucleoprotein complexes (RNPs) (Fig. 1-3A, B). After membrane fusion, the viral RNPs are released into the cytoplasm. The intact RNPs serve as template for subsequent transcription. Transcription occurs in the cytoplasm mediated by RNA-dependent RNA polymerase (RdRP). RdRP contains two critical viral protein components, the phosphoprotein encoded by P gene, and large protein encoded by L gene. L protein possesses the catalytic activities of the polymerase whereas P protein mediates the interaction of L protein with RNPs (Fig. 1-3A, B). In addition to P protein, the P genes of some viruses also encodes C, V and W proteins resulting from polymerase stuttering during transcription (V and W) and leaky ribosomal scanning during translation (C) (85, 106, 116) (Fig. 1-2).

Transcription proceeds from 3’ to 5’ of viral genome to produce a gradient of mRNA, where the highest level of mRNA is produced from the gene closest to the 3’ end of the genome. This is due to a “stop-start” transcription mechanism employed by these viruses (108), in which transcription terminates as RdRP recognizes “stop” signals after each gene and re-starts as RdRP recognizes the “start” signals before the very first gene or the next gene, and in rare cases, the same gene. Genome replication also occurs in the cytoplasm when sufficient protein components are accumulated. (+) RNA antigenomes are synthesized by RdRP that serve as templates to produce viral genomic (-) RNA (Fig. 1-3B). Matrix (M) protein is produced by M gene, and it is the main driving force for the last step of the paramyxovirus life cycle, assembly and budding of viral particles. As viral components are trans-located to assembly sites at the plasma membrane, M proteins coordinate virus assembly by linking together the viral RNPs and glycoproteins (Fig. 1-3A, B). At last, RNPs containing virus particles are released from the cell membrane by budding (Fig. 1-3B).

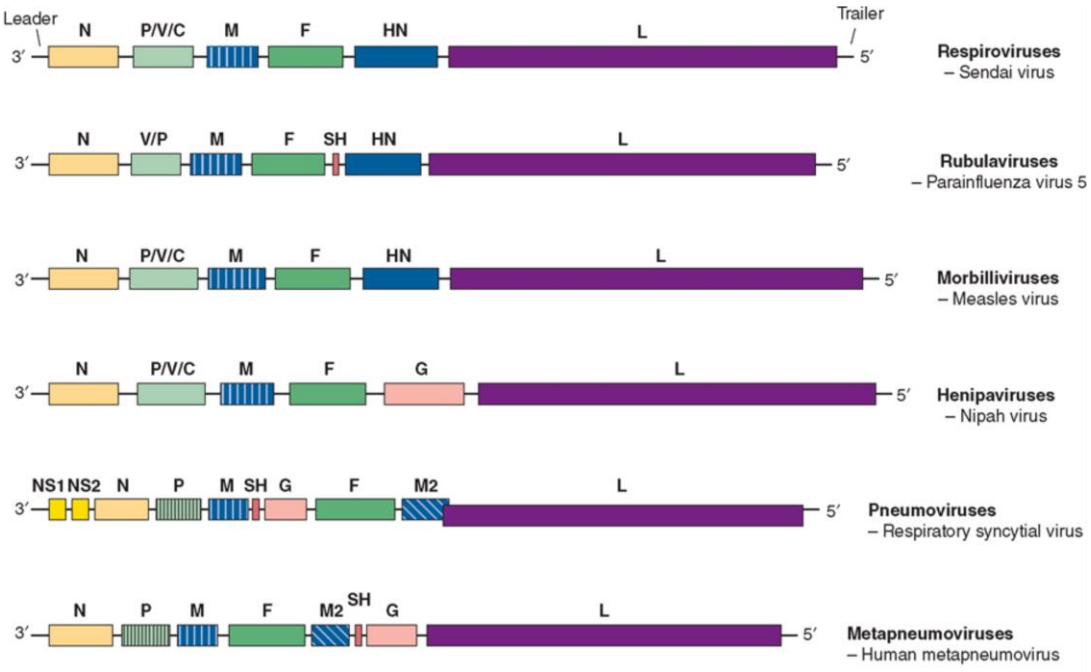

Figure 1-2. Genome organization of representative members from genera of paramyxoviridae. Representative viruses show genome organization of genera of respirovirus, rubulavirus, morbillivirus, henipavirus, pneumovirus and metapneumovirus. This figure was adapted from (151).

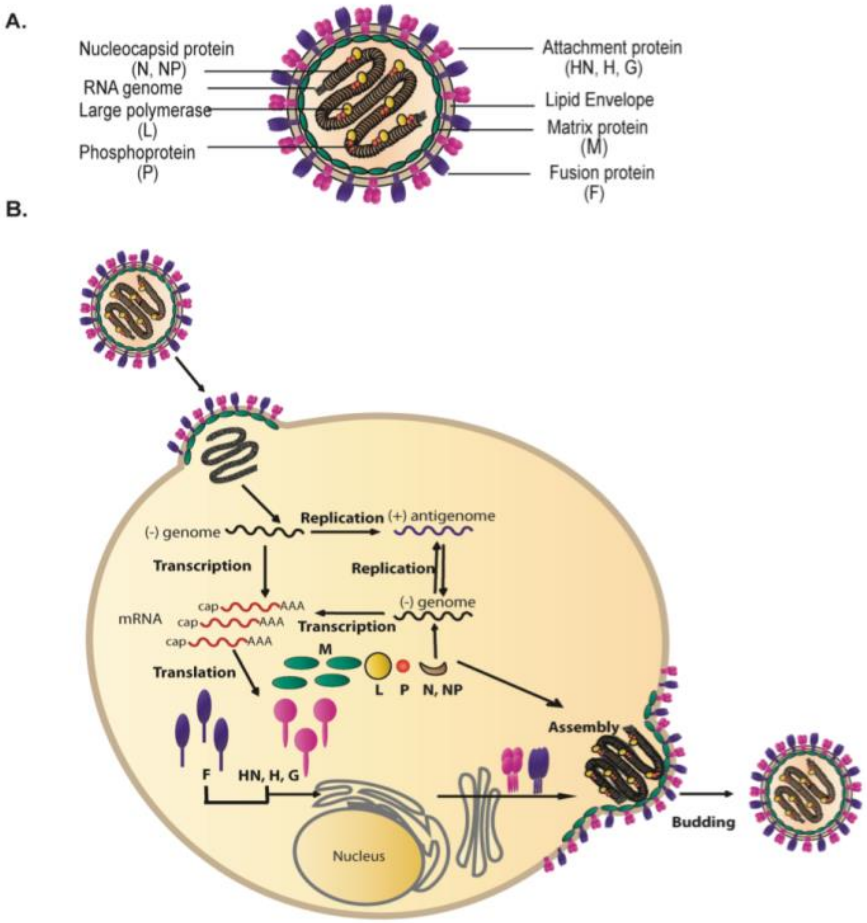

Figure 1-3. Paramyxovirus particle and life cycle. (A) Schematic representation of paramyxovirus particles. **(B)** Paramyxovirus life cycle. Virus entry is initiated by receptor binding to the attachment protein, fusion is mediate by fusion protein at neutral pH to release viral components. Genome transcription and replication occurs in the cytoplasm using viral RdRP. Viral components assemble at plasma membrane and particles are released by budding. This figure was adapted from (62).

1.3 Paramyxovirus matrix (M) protein and virus assembly

Paramyxovirus M protein is the organizer of virus assembly and budding. M proteins were firstly identified as the main driving force of virus assembly and budding by studies using reverse genetics system, where it showed that the recombinant paramyxoviruses such as SeV (104, 221) and MeV (10, 87) with deletion or loss-of-function mutated M proteins were unable to efficiently produce infectious virus particles. In the absence of M protein, viral components could only spread cell-to-cell due to the expression of fusion active glycoproteins on the cell surface (35).

Paramyxovirus M protein is a membrane-binding protein. When henipavirus M is expressed alone in the cells, for example, more than 50% of M protein is found to associate with cellular membrane (210). This property of paramxyovirus M proteins is likely due to the electrostatic interaction between the basic residues within M protein and negatively charged membrane, as there is an absence of hydrophobic stretches within M protein that could penetrate membrane for anchoring (181). Also, unlike myristoylation of retrovirus gag protein, which would be used for membrane anchoring, there is a lack of such post-translational modification on paramyxovirus M protein (95). A recently determined atomic structure of NDV M protein also suggested possible electrostatic interactions with membrane as positive charged residues are mostly found at the surface of the protein (14). In terms of what cellular membrane that M proteins bind, it has been suggested that “lipid rafts” microdomains that are rich in cholesterol and sphingolipids play an important role. In some cases, M protein is found to associate with lipid rafts only in the presence of

its homologous glycoproteins, such as SeV (4), while in other cases, M association with lipid rafts occurs regardless of the presence of glycoproteins, such as MeV (164).

Numerous studies have indicated a role for ubiquitin in enveloped virus assembly and budding, as depletion of the free ubiquitin by proteasome inhibitors such as MG-132 (127) in the cells impaired virions budding. Therefore, ubiquitination of viral protein has been studied, and it was found that mono-ubiquitination of some enveloped virus matrix proteins could serve as sorting signals to direct virus assembly and budding (83, 84, 155, 185). This likely is true for paramyxoviruses as well, as our group has found mono-ubiquitination of PIV5 M at multiple lysine sites and also found the release of PIV5 VLPs or virions could be inhibited upon treatment of proteasome inhibitors (81), or upon removal of lysine residues from M protein (81, 182). M protein of NiV has also been reported to be mono-ubiquitinated, and Nipah M-VLP production is sensitive to protease inhibitor MG-132 (210). It is thought that NiV M protein undergoes nuclear-cytoplasmic trafficking and membrane association that are highly dependent on M protein ubiquitination (210).

Paramyxovirus M proteins likely recruit host machinery to assist with the bending and pinching off of membranes during the budding process. This would be analogous to the host factors recruitment mediated by the late domains of retroviruses and Ebola virus (17). Several late domains have been identified within the matrix protein of enveloped RNA viruses such as HIV-1, VSV and EBOV (17). The typical late-domain amino acids motifs include P(T/S)AP, YP(X_n)L or PPxY, and they were found to recruit ESCRT components such as Tsg101, AIP1/ALIX or Nedd4-like E3

ubiquitin ligases (17). These proteins are normally responsible for trafficking membrane receptor protein cargos into lysosomes through multivesicular bodies (MVBs) (8, 9, 118, 169, 186). Paramyxoviruses do not have above-mentioned late domains in the matrix proteins. However, a novel sequence identified in PIV5 M protein, FPIV, is found to functionally compensate for the lack of PTAP within HIV-1 gag protein (182). Also, NiV M protein is reported to possess amino acids motifs that are indispensable for M protein functions, such as YMYL and YPLGVG within its N-terminal domain (43, 154). Mutations or deletions of these two motifs resulted in Nipah M-VLPs budding defects and displayed aberrant subcellular localization of M protein (43, 154). Additionally, both YMYL and YPLGVG can complement, at least partially, the budding defect of Ebola virus VP40 late-domain mutants, suggesting that they quite likely act as the late-domains of NiV M proteins for budding (43, 154).

It is thought that M protein organizes assembly by directly interacting with viral glycoprotein cytoplasmic tails (Fig. 1-4). If one or both of the glycoprotein cytoplasmic tails are truncated, the viruses bud poorly. In some cases, M protein is found to bind both glycoproteins through interactions with their cytoplasmic tails for efficient assembly, such as SeV, and hMPV (4, 65, 117, 180), whereas M proteins of some other paramyxoviruses are reported to interact with only one of the glycoproteins, such as NDV, RSV (13, 150). In addition, glycoproteins also appeared to define the membrane region as budding sites where M would associate with, as one study showing the ultrastructure of NDV found that M proteins were mainly concentrated to the plasma membrane where the glycoproteins were enriched (14)

For the incorporation of viral RNPs, M proteins are found to interact with the nucleocapsid (N/NP) protein (Fig. 1-4). Typically, this interaction between M protein and N/NP proteins is thought to occur within assembly and budding sites at plasma membrane. However, many evidences have supported another scenario where M protein preassembles with N/NP protein in the cytoplasm and the M-RNP complexes are transported together to the plasma membrane for some paramyxoviruses, such as SeV (191) and MeV (178). Often, interaction between M and N/NP is selective between homologous proteins (46) and is directed to the C-terminus of viral N/NP protein, such as in the case of PIV5 (184), and MeV (94).

A

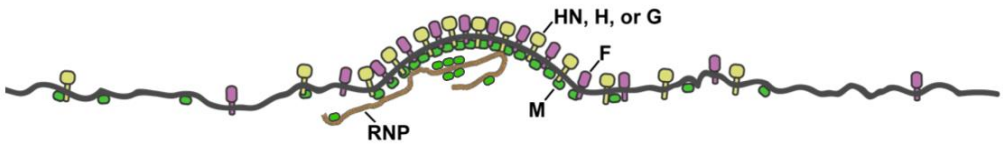

B

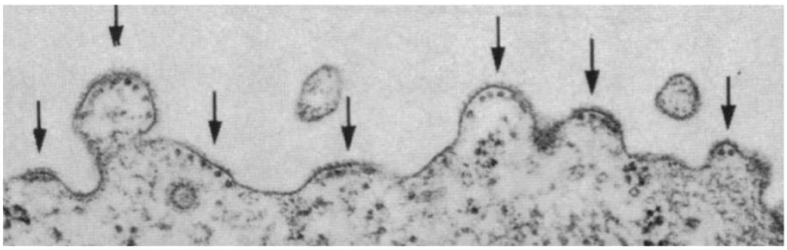

Rodriguez-Boulan and Sabatani, PNAS, 1978

Figure 1-4. Budding of paramyxovirus particles. (A) Schematic representation of paramyxovirus budding, where M protein function to link together the cytoplasmic tails of surface glycoproteins and RNPs. **(B)** Thin section of SeV budding from infected MDCK cells under electro-microscope. This figure was adapted from (80).

1.4 Virus-like particles production

Virus-like particles (VLPs) are the particles composed of one or more viral protein(s) and envelope that resemble authentic viruses produced from the cells, but lacking the viral genome, which is indispensable for the virus infectivity. Since VLPs are thought to bud in a similar way as the real viruses do, they are usually manipulated in the lab for the studies of viral particles formation and budding. For other enveloped viruses, such as retroviruses, expression of HIV-1 gag protein alone in the cells could result in VLPs production (71). In the case of paramyxoviruses-like particles, many of them could be produced upon M protein expression alone in the cells, such as hPIV1, NDV, MeV, SeV, NiV and HeV, etc (80) (Table 1-1). For some paramyxoviruses including PIV5 and MuV, M protein is not sufficient to form virus-like particles. Other viral proteins such as nucleocapsid protein or glycoproteins are required for VLPs production (80)(Table 1-1). For example, PIV5 VLPs could be produced efficiently through co-expression of M, NP and either F or HN. The closely related MuV shares a similar requirement for VLP production (Table 1-1). In other cases, expression of glycoprotein alone could induce release of VLPs such as the fusion protein of NiV (152) and SeV (192).

Virus	Viral proteins needed for efficient VLP production	Notes	References
hPIV1	M	Nucleocapsid-like structures are incorporated into the VLPs when NP protein is expressed	Coronel et al. (1999)
Sendai virus	M	F protein enhances VLP production, but HN protein does not; C protein enhances VLP production, likely through recruitment of the host protein Aip1/Alix	Takimoto et al. (2001), Sugahara et al. (2004)
NDV	M	Glycoproteins and NP protein can be incorporated into VLPs, but do not enhance M-driven VLP production; incorporation of glycoproteins into VLPs becomes efficient when both glycoproteins are expressed	Pantua et al. (2006)
PIV5	M, NP, and F; or M, NP, and HN	M protein expressed alone does not result in VLP production; F and HN proteins are necessary but redundant for VLP production	Schmitt et al. (2002)
Mumps virus	M, NP, and F	M protein expressed alone results in very little VLP production; F protein strongly enhances VLP production, but HN protein does not	Li et al. (2009)
Measles virus	M	F protein does not enhance M-driven VLP production	Pohl et al. (2007), Runkler et al. (2007)
Nipah virus	M	Glycoproteins and N protein can be incorporated into VLPs when expressed, but do not enhance M-driven VLP production	Ciancanelli and Basler (2006), Patch et al. (2007)

Table 1-1. Different requirements of paramyxovirus VLPs productions. A brief overview of viral proteins requirements for efficiently VLPs production of several paramyxoviruses. For some paramxyoviruses such as hPIV1, SeV, NDV, MeV and NiV, matrix protein expressed by itself could form VLPs, whereas other viruses such as PIV5 and MuV, efficient VLP production required co-expression of NP and at least one of the surface glycoproteins. This table was adapted from (80).

VLP systems are useful as virus assembly and budding could be separated from other events in virus life cycle. It is even more convenient when the authentic viruses are highly bio-safety restricted, such as zoonotic henipaviruses. Two members from this genus, HeV and NiV, are highly pathogenic to both humans and animals. However, by employing a VLP system, studies on virus assembly and budding could be extended to less restricted conditions. Although VLPs are not infectious, they are still immunogenic. Therefore, VLP systems also provide an opportunity for effective vaccination against pathogenic viruses. For example, VLPs could act as potent adjuvants to induce both innate and adaptive immune response (15, 209). Since VLPs could be manipulated in terms of its lipids and proteins composition, they could be engineered to form particles that meet with diverse epitopes requirements (39). Meanwhile, VLPs could act directly as vaccines, although many of them are in still in hypothesis stage, some of them have already entered clinical trials. Examples include HPV L1 VLP vaccine, Norovirus VLP vaccine, Chikungunya VLP vaccine and Influenza VLP vaccine (39). Encouragingly, some VLP vaccines have already been commercialized. This has been demonstrated by the development of human papillomavirus (HPV) vaccine to help preventing cervical cancer, as well as VLP-based Hepatitis B virus (HBV) vaccine to prevent Hepatitis B and Hepatocellular carcinoma (39).

1.5 Trafficking of paramyxovirus glycoproteins

Paramyxoviruses possess two types of membrane integral glycoproteins, the attachment protein and the fusion protein, on the host-derived envelope membrane. The attachment protein is a type II glycoprotein and the fusion protein is a type I glycoprotein. The attachment protein is found to be mainly responsible for receptor binding and F protein mediates fusion of viral envelope with cellular plasma membrane at neutral pH. Different paramyxoviruses might have attachment proteins with different functions, so that they are termed as HN, H and G. In the case of henipaivirus, the attachment protein is called G protein as it neither has hemagglutinin nor neuraminidase activities. The G protein of henipavirus binds to the protein receptors such as ephrin-B2/3 on the cell surface instead of sialic acids (21, 137, 138). Paramyxovirus F proteins need to be proteolytically processed for the progeny viruses to be infectious.

The typical trafficking pathway of viral type I glycoproteins has been characterized including paramyxovirus F protein. In general, the viral glycoproteins are synthesized in the ER and transported to the plasma membrane through secretory pathways (33) (Fig. 1-5). The biologically active paramyxovirus F protein consists of two disulfide-linked subunits, F_1 and F_2, that are generated from proteolytic cleavage of the precursor F_0 (129). The fusion proteins are usually processed as they traffic through the secretory pathway either by endoprotease, such as furin that cleaves PIV5 F or at the plasma membrane by exoprotease, such as extracellular amniotic endoprotease that cleaves SeV F when grown in eggs (74, 101). At last, viral glycoproteins assemble with other viral components at the plasma membrane (Fig. 1-5). In the case of

henipavirus F protein, the trafficking pathway is fundamentally different from the standard paramyxoviruses trafficking pathway. Here, uncleaved F_0 is transported to the plasma membrane through the secretory pathway, and is not cleaved until additional endocytic trafficking events take place. F_0 is endocytosed back into the cell mediated by a tyrosine-based motif (Yxxϕ) within its cytoplasmic tail (124, 205). Within early endosome compartments, it is proteolytically cleaved into F_1 and F_2 by an endosomal protease called cathepsin L. The fusion active F protein is then recycled back to the plasma membrane (148, 165).

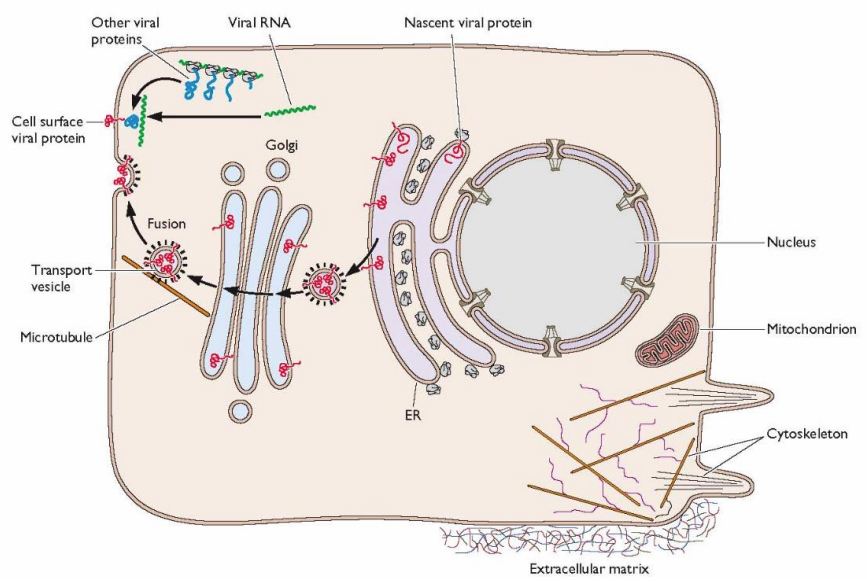

Figure 1-5. Classical trafficking pathway of viral surface glycoproteins. Viral glycorproteins are synthesized in the ER and transported to plasma membrane through secretory pathway, where they assemble with other viral components. This figure was adapted from (96).

1.6 Adaptor protein (AP) complexes

During vesicle biogenesis and trafficking in mammalian cells, protein coats were used to generate bristle-coated pits, which subsequently pinched off to form protein-coated vesicles containing incorporated protein cargos. Among the protein coats identified, the firstly characterized and most well studied was clathrin coat (156). In order to recruit protein cargos to the vesicles, additional adaptor proteins are required to link together the protein cargo and the protein coat. There are two main classes of protein cargo-binding adaptors that are characterized: 70kD golgi-localized, γ-ear-containing Arf-binding (GGAs) proteins (20) and 300kD adaptor protein (AP) complexes. Adaptor protein complexes are heterotetramers consist of one large subunit (β), a second large subunit (γ/α/δ/ε/ζ), a medium subunit (μ) and a small subunit (σ) that assemble into a "Mickey mouse face" shape (88, 134) (Fig. 1-6A, B). At present, there are five distinct AP complexes that have been identified, AP-1, AP-2, AP-3, AP-4 and AP-5 (88, 89, 99, 166, 189). Among the five AP complexes, only AP-1 and AP-3 have another isoform whose expression is tissue and cell specific (134). AP complexes were firstly identified when people observed unknown ~100kD molecules involved in clathrin coat association with vesicles (199, 204). They were later recognized as the components of AP-1 and AP-2 complex (99). AP complexes function to sort membrane proteins as they are shuttled between cellular organelles. How these adaptors perform their sorting functions is linked to the donor organelle where they localize. For example, AP-1 transports protein between tubular endosomes and TGN (197); AP-2 is specifically involved in clathrin-mediated

endocytosis (90); AP-3 is present in the TGN/tubular endosomes and traffics protein cargos to late endosomes, lysosomes or lysosomes related organelles (LROs) (157); AP-4 localizes to the TGN, and it can produce vesicles that transport specific endosomal proteins (89). The exact function of AP-5 is not clear yet, but it is found to localize to a late endosomal compartment in certain cell types (88)(Fig. 1- 6C)

Interaction between AP complexes and protein cargos are mediated by tyrosine-based sorting signal and dileucine-based sorting signals. Almost all μ subunits of AP complexes have been found to recognize tyrosine-based sorting signals such as Yxxϕ motif, however with distinct specificity and affinity (3, 145). For example, both AP-1 and AP-2 μ subunits could bind HIV-1 Env YSPL motif (218). On the other hand, other subunits could recognize dileucine-based sorting signal such as [DE]XXXL[LI]/DXXLL. For example, AP-3 was found to bind its protein cargos such as lysosome integral membrane protein LIMP-II through a DERAPLI sequence as well as tyrosinase through a EEKQPLL sequence (91).

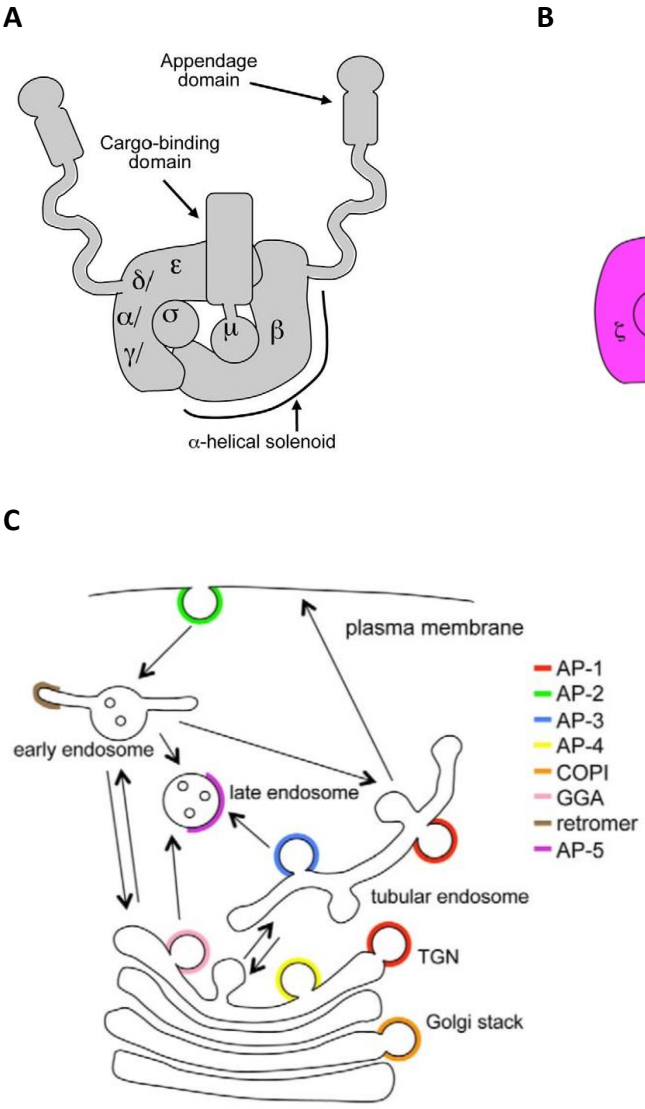

Figure 1-6. Overview of AP complexes. (A) Structure of AP-1, 2, 3, 4 complexes **(B)** Structure of a more distinct AP-5 complex **(C)** Diagram of trafficking pathways and machinery of AP complexes. This figure was adapted from (88).

1.7 Adaptor protein 3 (AP-3) complex

AP-3 complex was firstly identified in the yeast (*Saccharomyces cerevisiae*) when genetically screening for protein factors that transport alkaline phosphatase (ALP) to yeast vacuoles, the yeast homologue of mammalian lysosomes or lysosome-related organelles (LROs) (144). Two genes encoding yeast homologues of AP-3 beta and delta subunits, Ap16p and Ap15, were first isolated (47, 190). The role of AP-3 complex in vacuole trafficking in yeasts as well as its sequence and structural similarity with known AP complexes established AP-3 as a new member in AP complex family (188, 189). Two isoforms of AP-3 complex are characterized, where AP-3A is ubiquitously expressed in all cell types, while AP-3B is only expressed in neurons (53, 54, 140, 189). It is been well demonstrated that the homologous AP-3 complex in yeast is required for protein transport to vacuoles including the trafficking of soluble carboxypeptidase Y (CPY) and ALP, and mutations of AP-3 subunits resulted in sorting defects of these proteins (48, 190). Meanwhile, mutations within genes encoding AP-3 components in other organisms are found to cause defects in LROs biogenesis. For example, pigmentation defects in fruit fly (*Drosophila melanogaster*) caused by defective mutations of AP-3 delta subunit resulted in eye-color mutant, *garnet* (115). In addition, defective mutations within genes encoding beta and delta subunits in mice resulted in murine mutant lines, *pearl* (224) and *mocha* (98) respectively. Importantly, it is found that mutations in the human gene encoding the AP3B1 subunit resulted in Hermansky-Pudlak Syndrome (HPS) type II, a Mendelian disorder characterized as the combination of

albinism and bleeding diathesis (55, 86). In mammalian cells, several proteins were identified as the protein cargos of AP-3 complexes, examples include melanosomal enzymes tyrosinase (TYR) and tyrosinase-related protein 1 (TYRP1) (91, 196), lysosomal membrane protein endolyn/CD164 (92) and Lysosomal-associated protein III (CD63) (157). Depletion of AP-3 in cells renders sorting defects or changes in steady-state localization of its protein cargos to lysosomes or LROs. For instance, in AP-3-deficient melanocytes, TYR is mis-distributed to early endosomes and late endosomes instead of melanosomes (196). lysosome-associated membrane protein LAMP-1 and CD63, whose traffic pathways from tubular endosomes to lysosomes are dependent on AP-3 complexes, were significantly recycled to the cell surface in AP-3-depleted cells (157). Similarly, CD63 mutants that were defective in AP-3 binding were re-localized to the cell surface instead of lysosomes (176). During these sorting processes, other host proteins that interact with AP-3 complexes were shown to regulate its sorting function such as Arf1 GTPase (146), phosphatidylinositol 4 kinase type II alpha (PI4KII) (179)， BLOC-1/BLOC-2 (57) and clathrin (52).

1.8 AP-3 complex and viral trafficking

As discussed earlier, viruses often hijack host machinery for their own purposes. While AP-3 is mainly involved in endosomal/lysosomal trafficking, membrane-binding viral protein cargos could be often found within AP-3 pathway or AP-3 containing vesicles. In some cases, this occurred through direct interaction between

viral protein and AP-3 subunits. For example, the μ subunit of AP-3 bound to HIV-1 Nef protein through a dileucine-based sorting motif within Nef, and the recruitment of AP-3 by Nef was required by optimal viral replication (49). Additionally, Gag protein of HIV-1, which is equivalent to paramyxovirus M protein, was also shown to bind the δ subunit of AP-3 complex. Either overexpression of Gag-binding AP3D1-polypeptides or the depletion of AP-3 complex resulted in defective HIV-1 budding (58). Interaction of AP3B1 with a subunit of a microtubule kinesin motor protein complex, Kif3A, was also been characterized. In this study, it was shown that not only Kif3A but also the interaction between AP3B1 with Kif3A, which was regulated by pyrophosphorylation of AP3B1 hinge region, was required for HIV-1 Gag budding (7). Importantly, HIV-1 particle assembly was found to be defective in cells derived from human patients with AP-3 deficiency, caused by mutation to AP3B1 (114).

In other enveloped virus trafficking, AP-3 is also reported to be necessary, such as VSV. It has been shown that the δ subunit of AP-3 is required for VSV-G trafficking from trans-Golgi network to cell surface (141). During this process, VSV-G was thought to recruit AP-3 complexes through interactions between the YTDIE motif within its cytoplasmic tail and the δ subunit of AP-3 complex. AP-3 thereby facilitated the export of G from the TGN and allowed trafficking to the plasma membrane (141). Other examples include flavivirus, such as Japanese encephalitis virus and dengue virus, where AP-3 was found to co-localize with RNA replication compartments of these viruses, and initiation of RNA replication was shown to be

delayed in AP-3 deficient cells, suggesting trafficking of viral components that are required for RNA replication might be delayed (1).

1.9 Rab11 GTPase in negative-strand RNA virus assembly

Vesicular trafficking regulates membrane protein sorting within eukaryotic cells, which is coordinated by small GTPases. Rab GTPases (21-25kD) belong to Ras superfamily of monomeric G proteins and are also the main regulators of vesicular trafficking. At present, there have been about 70 Rab GTPases identified in human cells. Most of the Rab proteins are ubiquitously expressed in the cells, while certain Rabs are cell-type restricted. Different Rabs usually associate with different endocytic or exocytic membrane compartments as well as vesicles derived from them, and could often act as protein markers of these compartments. For example, Rab1 and Rab2 localize to the ER, while Rab4 and Rab5 represent early endosomes; Rab7 is the marker of late endosome, and traffics protein from early endosomes to late endosomes, whereas Rab8 is mainly found in the Golgi apparatus and functions to transport protein from TGN to plasma membrane; Rab11 is associated with recycling endosome, and Rab12 is found to target perinuclear centrosome.

As described earlier, many enveloped negative-strand RNA viruses are dependent on host machinery for budding, such as ESCRT machinery. However, many others are ESCRT-independent. As Rab GTPases play a very important role in sorting cellular proteins, they could also been hijacked by viruses for the purpose of directing newly synthesized viral proteins to the sites of assembly. It is noteworthy that although

various Rab GTPases have been suggested to influence negative RNA virus assembly and budding, numerous studies in recently years have pointed a more important role for Rab11 or Rab11 effectors, including Rab11- family-interacting proteins (FIPs), myosin Vb or Rab-BP, in being required during negative-strand RNA virus trafficking. For example, vRNPs of influenza A virus (IAV) are found to associate with Rab11 positive vesicular compartments and vRNPs distribution is disrupted upon Rab11 depletion by siRNA or overexpression of DN Rab11 effectors (6). Similar observation is also obtained for paramyxoviruses, such as SeV and MeV, where vRNPs were found to colocalize as well as simultaneously move with Rab11 positive vesicles (37, 135). These data suggested a possible role of Rab11 in directing vRNPs to the site of assembly (Fig. 1-7B). Furthermore, other evidences also support a functional role of Rab11 in virus budding. For example, depletion of Rab11 was found to block hantavirus particles release (177). Similarly, it is observed that upon depletion of Rab11 by siRNA, IAV release was substantially impaired as abnormal particles were formed and they failed to pinch off from plasma membrane (31). In the case of paramyxovirus, when overexpressing a dominant negative Rab11 effector, Rab11-FIP2, a huge reduction was observed for RSV budding from apical side of polarized cells (30) (Fig. 1-7A). Interestingly, as ANDV has been suggested to bud into internal compartment, Rab11 likely facilitated ANDV budding by transporting vesicles containing assembled virus particles (177) (Fig. 1-7 C). However, it is still yet to be determined that how Rab11 facilitates these virus assembly and budding and if Rab11 would have similar effects on many other negative-strand RNA viruses.

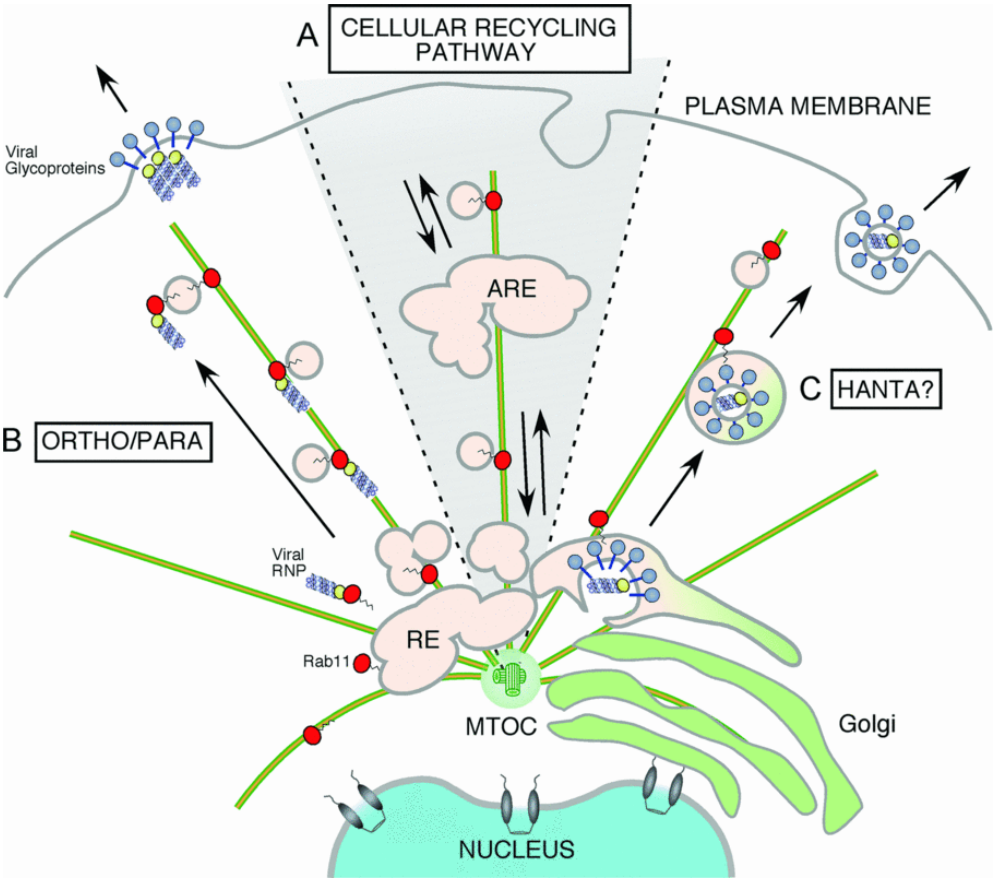

Figure 1-7. Model of interactions between negative-strand RNA viruses and the Rab11 pathway. (A) Rab11 pathway between perinuclear recycling endosome or apical recycling endosome and the plasma membrane. **(B)** Microtubule-mediated transport of vRNPs to plasma membrane. **(C)** Possible secretion route for the ANDV from MTOC to plasma membrane mediated by Rab11. This figure was adapted from (32).

1.10 Identification of protein-protein interactions between virus and host

Investigations on virus-host interaction are important as they could provide insights on the host factors that are required for virus life cycle as well as those restricting the viruses. Protein-protein interactions (PPIs) between virus and host have been extensively studied using different approaches. In general, methods to identify protein-protein interactions (PPIs) have been classified as three types: *in vitro*, *in vivo*, and *in silico*. Examples for *in vitro* identification include tandem affinity purification-mass spectrometry (TAP-MS), affinity chromatography, co-immunoprecipitation, protein microarrays, phage display. One classical approach for *in vivo* PPIs identification is yeast two-hybrid (Y2H) and its derivative, such as yeast three-hybrid (Y3H). The most recently emerging *in silico* identification of PPIs approaches are based on development of bioinformatics and public protein-protein interaction database. For instance, phylogenetic tree method could predict the protein-protein interaction based on the evolution history of the protein, and ortholog-based sequence method could use pairwise local sequence algorithm to identify the homologous nature of the query protein in the annotated protein databases (170).

When studying PPIs, *in vitro* proteomics-based approaches such as co-immunoprecipitation, affinity chromatography mass spectrometry or tandem affinity purification mass spectrometry have been frequently used, where a protein of interest is single or double affinity tagged, followed by a one or two-step purification process either by incubating with resin conjugated with the ligands of

affinity tag(s) or by running through a solid matrix packed in the column that would specifically bind the affinity tag(s), and mass spectrometry is used to analyze the co-purifying polypeptides. These approaches are high through-put and are very responsive to detect even weak interactions, and have been used to establish virus-host interactome networks, such as host proteins bound to Ebola virus VP40, where the component of COPII transportation system, Sec24C, was identified as a VP40 interacting protein using coimmunoprecipitation approach (219). This discovery contributed to the characterization of the important role of COPII transportation system in assembly and budding of Ebola virus (219). Another example is influenza virus, where TAP-MS was used to identify host proteins that bind viral RNPs or RdRP. The result provided important information for newly discovered host interacting candidates as well as confirmed several previously identified virus-host interactions (123). Similar approach was also applied to paramyxovirus. For example, Measles virus V protein was affinity tagged in the context of recombinant virus. MeV V interactome was established after co-purifying of V-interacting host protein and analyzing them by MS (103).

Alternatively, the genetics-based approach Y2H is also broadly used to identify PPIs. This approach has been used to reveal many important virus-host interactions since 1990s, such as interaction between Tsg101 and HIV-1 gag protein (203), as it was well suited for high through-put screening of direct physical interactions, even though false positive results were often found. On the other hand, *in silico* or computational methods is gaining popularity in the field of virus research today, as

they are much less time-consuming and costly. These methods are mainly used to predict PPIs by analyzing the query protein sequences or structural information relative to existing protein databases. For example, *in silico* approaches have been used to analyze HIV-1 human PPIs network constructed from HIV-1 human protein interaction database (HHPID)(162), which provide data for 5127 interaction between 19 HIV-1 protein and 1432 host proteins. Existing problems for this approach include insufficiency of negative samples, however, *in silico* approach is still believed to be of great importance to reveal insights towards virus and host interactions (12).

1.11 Preview

Genetics or proteomics-based approaches have successfully identified host proteins that were involved in enveloped virus assembly and budding. This led us to investigate what host factors could facilitate henipavirus assembly and budding by interacting with their matrix proteins, the main organizer for henipavirus assembly and budding. We employed affinity purification of viral M proteins followed by mass spectrometry analysis to identify co-purifying host factors. We selected one of host protein candidates identified by this approach, AP3B1, for further study. We mapped M binding region to the hinge domain of AP3B1, and generated small polypeptides derived from AP3B1 hinge domain that are rich in serine and acidic amino acids. These polypeptides also proved to be potent inhibitors against henipavirus-like particles production by driving M protein away from cellular membrane. Defects of henipavirus-like particle production in AP3B1 depleted cells

as well as colocalization of M protein with endogenous AP3B1 in protein clusters suggested AP-3 complex is likely specifically involved in M protein trafficking and budding. This study allowed us to identify virus-host proteins interface that could be potentially targeted for future development of antivirals against lethal henipaviruses infection.

Henipaviruses fusion protein has a unique trafficking pathway that differs from many other paramyxoviruses. Based on the characterization of Hendra virus F and G trafficking by the Dutch group, we collaborated to further investigate how Hendra virus M protein assembles with glycoproteins. We found all three proteins M, F and G were observed in Rab11-REs. DN Rab11 expression in the cells impaired both Hendra M-VLP and F-VLP. However, M protein was no longer in Rab11-REs in the presence of AP3B1 Hinge domain, suggesting AP-3 is necessary for M trafficking to Rab11-REs. Furthermore, M co-expression significantly increased G incorporation into M-VLPs, which was supported by colocalization of the two proteins in transfected cells. We know that F protein is proteolytically cleaved by endosomal protease cathepsin L after it is endocytosed following trafficking to plasma membrane through secretory pathway. We wanted to explore if endocytosis of F protein or the cleavage of F protein is required for F protein incorporation into M-VLPs. Here, we examined a HeV F mutant S490A, which is defective on endocytosis, for particle assembly, and found this mutant F protein failed to assemble into M-VLPs, indicating endocytotic trafficking of F is required for its incorporation into particles. On the other hand, we prevented F cleavage using a cathepsin L inhibitor

E-64d, which allowed complete endocytosis of F protein. We found uncleaved but endocytosis competent F could incorporate into M-VLPs, indicating proteolytically processing of F protein is not required. Based on these observations, we hypothesized that HeV M and F protein have separate mechanisms for trafficking to Rab11-REs, with the M protein trafficking facilitated by its interaction with AP3B1. Then M and cathepsin-cleaved F proteins must then assemble together within these compartments prior to their delivery to the cell surface for particle budding.

CHAPTER 2

Materials and Methods

Plasmids

cDNA corresponding to the Nipah virus M protein was a kind gift of Dr. Paul Rota (Centers for Disease Control and Prevention, Atlanta, GA), and cDNA corresponding to the Hendra virus M protein was a kind gift of Dr. Christopher Broder (Uniformed Services University, Bethesda, MD). These cDNAs were modified using PCR to encode N-terminal Strep6His tags (amino acid sequence WSHPQFEKHHHHHH), or N-terminal Myc tags (amino acid sequence EQKLISEEDL). The resulting cDNAs were subcloned into the eukaryotic expression vector pCAGGS (142) to generate pCAGGS-NiV M, pCAGGS-HeV M, pCAGGS-SH-NiV M, pCAGGS-SH-HeV M, pCAGGS-Myc-NiV M, and pCAGGS-Myc-HeV M. cDNA corresponding to Nipah virus M and Hendra virus M was also modified by PCR to encode an N-terminal Flag tag (amino acid sequence DYKDDDDK), and subcloned into the expression vector pcDNATM3.1/myc-His (-)A (Invitrogen, Carlsbad, CA) for use in fluorescence microscopy experiments. (the pcDNA vector was used in this case because it results in a more moderate level of M protein expression, making M protein localization easier to define and visualize). cDNA corresponding to the PIV5 and Mumps virus M proteins, subcloned into the pCAGGS vectors, have been described before (110, 183). cDNA corresponding to Sendai virus M protein (Z strain), subcloned into the pCAGGS vector, was a kind gift from Takemasa Sakaguchi. Mutagenesis within NiV M was generated by PCR. Like

the wild type NiV M, mutant M protein sequences were modified with PCR to encode an N-terminal Myc-tag. The resulting cDNAs were subcloned into expression vector pCAGGS.

cDNA corresponding to full-length human AP3B1 was purchased from Open Biosystems (Thermo Fisher Scientific, Waltham, MA; clone ID 3914400). This sequence was modified using PCR to incorporate an N-terminal Flag tag, and subcloned into the pCAGGS vector to generate plasmid pCAGGS-AP3B1. Subfragments of AP3B1, each with N-terminal Flag tag, were generated by PCR using the full-length AP3B1 cDNA as template and subcloned into pCAGGS, with boundaries as illustrated in Fig. 3-3A. To obtain cDNA corresponding to full-length *P. alecto* AP3B1, RNA was isolated from immortalized *P. alecto* kidney (PaKiT) cells, and cDNA was synthesized using the Superscript III First-Strand Synthesis System (Life Technologies, Grand Island, NY) according to the manufacturer's recommendations. The AP3B1 sequence was PCR amplified using primers designed based on the published *P. vampyrus* sequence (64) (sense primer 5' ATGTCCAGTAACAGCTTCG 3' and antisense primer 5' TTACCCCTGGGACAGGACAGG 3'). The sequence was modified to encode an N-terminal Flag tag, and subcloned into the pCAGGS expression vector. Amino acid sequences of the human and *P. alecto* AP3B1 proteins were aligned using ClustalW2 (109) to define Head, Hinge, and Ear domains. These subfragments of *P. alecto* AP3B1 were modified to encode N-terminal Flag tags, and subcloned into the pCAGGS vector. Mutagenesis within Hinge 1B was generated by PCR. Like the wild type Hinge 1B, mutant Hinge 1B sequences were

modified with PCR to encode an N-terminal Flag-tag. The resulting cDNAs were subcloned into expression vector pCAGGS.

The plasmid pCAGGS-AmotL1-m has been described previously (159). The SH-EGFP sequence was generated by PCR using the pEGFP-C1 vector (Clontech, Mountain View, CA) as template and modified to encode the N-terminal Strep6His tags. The resulting cDNA was subcloned in pCAGGS vector to generate plasmid pCAGGS-SH-EGFP. cDNA for host protein candidates EXOSC10 (clone ID 5505500), NKRF (clone ID 5228666), ILF2 (clone ID 2820505), ZC3HAV1 (clone ID 5418915), HTATSF1 (clone ID 3504952) and VPRBP (clone ID 4853730) were all purchased from Open Biosystems (Thermo Fisher Scientific, Waltham, MA). Each cDNA was amplified and modified by PCR to append an N-terminal Flag tag and was subsequently subcloned into the pCAGGS vector.

The plasmid pCAGGS-HeV F was a kind gift from Dr. Rebecca Dutch (University of Kentucky). The plasmid pcDNA-S-tag-HeV G was kindly provided by Dr. Christopher Broder (Uniformed Services University of Health Science). pEGFP-C1-Myc-Rab11a wild type and pEGFP-C1-Myc-Rab11a S25N were gifts from Dr. Wei Guo (University of Pennsylvania).

cDNA of GST was obtained from pGEX-4T-1 (GE Healthcare Life Science, Pittsburgh, PA). Truncated NiV M cDNAs were generated by PCR from full-length NiV M sequence. They were subcloned into pGEX-4T-1 with GST sequence at 5'. cDNA of GST-NiV M fragments were subsequently amplified by PCR and further subcloned into pCAGGS to generate pCAGGS-GST-NiV M 1-282, pCAGGS-GST-NiV M 283-352,

pCAGGS-GST-NiV M 1-190, pCAGGS-GST-NiV M 191-352, pCAGGS-GST-NiV M 1-128, pCAGGS-GST-NiV M 129-352, pCAGGS-GST-NiV M 191-282. pCAGGS plasmids encoding smaller NiV M subfragments within NiV M 191-282 including pCAGGS-GST-NiV M 191-236, pCAGGS-GST-NiV M 191-262, pCAGGS-GST-NiV M 237-262, pCAGGS-GST-NiV M 263-282 were also generated in a similar way.

Henipavirus M protein affinity purification and mass spectrometry

For affinity purification of viral M proteins and M-interacting host factors, 293T cells (in groups of five 10-cm-diameter dishes) were transfected with pCAGGS plasmids corresponding to SH-M, SH-EGFP, or untagged M, at 3 µg/dish. At 24 h posttransfection (p.t)., cells were harvested and lysed in StrepTactin lysis buffer (100 mM Tris-HCl, 150 mM NaCl, 1 mM EDTA, 1% NP-40, pH 8.0). Cell lysates were clarified by centrifugation and further passed through 0.45 µm syringe filters to remove debris. For RNase treated samples, clarified lysates were incubated with 200 µg/ml RNase A at room temperature for 30 min. RNase A treated samples were clarified a second time by centrifugation before passing through the syringe filter. Purification of M protein was done using the ÄKTAprime Plus FPLC system (GE Lifesciences, Pittsburgh, PA) equipped with a 1 ml StrepTrap-HP column. Proteins were eluted from the column using a solution containing 100 mM Tris-HCl, 150 mM NaCl, 1 mM EDTA, and 2.5 mM desthiobiotin, pH 8.0. Eluted proteins were concentrated using 500-3 U-Tube concentrators (Novagen, Madison, WI). Concentrated samples were resolved by SDS-PAGE using either 10% or 15% gels, and

stained with Coomassie Brilliant Blue (American Bioanalytical, Natick, MA) for gel excision. Additional SDS-PAGE gels run in parallel were stained with either Sypro Orange or Lucy 506 (Bio-Rad Laboratories, Hercules, CA) for documentation of protein bands. Excised bands were submitted to the Taplin Mass Spectrometry Facility (Harvard Medical School, Boston, MA) for protein identification by liquid chromatography and tandem mass spectrometry (LC/LC-MS/MS).

Coimmunoprecipitation

Coimmunoprecipitation of viral M proteins with AP3B1 and other host proteins was performed using modifications of methods that have been previously described (160). HEK 293T cells grown in 6-cm-diameter dishes to 70-80% confluency in Dulbecco's modified Eagle medium (DMEM) supplemented with 10% fetal bovine serum (FBS), were transfected with pCAGGS plasmids encoding Myc-tagged viral M proteins (0.4 μg/dish), GST or GST-fused M fragments (1.5ug/dish) with or without pCAGGS plasmids encoding Flag-tagged candidate host proteins or AP3B1 derivatives (1.0 μg/dish). Cells were transfected with Lipofectamine-Plus reagents (Invitrogen, Carlsbad, CA) per manufacturer's protocol. At 24 h p.t., cells were starved for 30 min in DMEM containing 2% FBS and 1/10 the normal amount of methionine and cysteine followed by labeling for 3-5 hrs in the same medium supplemented with 40 μCi of [35S] Promix/ml (Perkin Elmer, Waltham, MA). Cells were harvested and mixed with lysis buffer (20 mM Tris-HCl, 150 mM NaCl, 1 mM EDTA, 1% NP-40, 1 mM PMSF, pH 8.0). The resulting cell lysates were clarified by

centrifugation, followed by rocking for 2 h at 4°C in the presence of anti-myc monoclonal antibody (Life Technologies, Grand Island, NY), Glutathione Sepharose®4B (BioWORLD, Dublin, OH) or anti-Flag M2 magnetic beads (Sigma-Aldrich, St. Louis, MO). Immune complexes were collected by centrifugation after incubation with protein A sepharose beads for 0.5-1 hr, and washed 3x with lysis buffer. Proteins were separated by SDS-PAGE using 10%, 15% or 17.5% gels, and were detected using a Fuji FLA-7000 phosphorimager (FujiFilm Medical Systems, Stamford, CT).

Measurements of VLP production

To generate VLPs, HEK 293T cells grown in 6-cm dishes were transfected with pCAGGS plasmids encoding Myc-tagged NiV M protein or Myc-tagged HeV M protein (0.4 μg/dish), together with various plasmids encoding AP3B1-derived polypeptides (Full-length AP3B1/Head/Hinge/Ear: 0.75 μg/dish; Hinge 1/Hinge 2/Hinge 3: 1 μg/dish; Hinge 1A/Hinge 1B: 1.5 μg/dish). Transfections were carried out in Opti-MEM using Lipofectamine-Plus reagents. At 24 h p.t., the culture medium was replaced with DMEM containing 2% FBS, 1/10 the normal amount of methionine and cysteine, and 40 μCi of [35S] Promix/ml. After an additional 18 h, cell and media fractions were collected. VLPs from the culture media fractions were pelleted through 20% sucrose cushions, resuspended, floated to the tops of sucrose flotation gradients, pelleted again, and then resuspended in SDS-PAGE loading buffer containing 2.5% (wt/vol) dithiothreitol, as described previously (184). Cell lysate

preparation and immunoprecipitation of proteins from the cell lysate fraction was carried out as described previously (183). Anti-Myc monoclonal antibody was used to immunoprecipitate viral M proteins, and anti-Flag M2 magnetic beads were used to immunoprecipitate AP3B1 and AP3B1-derived polypeptides. The precipitated proteins and VLPs were separated on 10% SDS gels and detected using a Fuji FLA-7000 phosphorimager. VLP production efficiency was calculated as the quantity of M protein in purified VLPs divided by the quantity of M protein in the corresponding cell lysate fraction, normalized to the value obtained in the positive control experiment.

To generate Hendra M, F and G VLPs, HEK293T cells in 6-cm dishes were transfected with pCAGGS plasmid encoding Myc-HeV M (0.2 ug/dish) together with pcDNA plasmid encoding S-tagged HeV G (0.2 ug/dish), or pCAGGS plasmid encoding HeV F (0.8 ug/dish) together with pcDNA plasmid encoding S-tagged HeV G (0.2 ug/dish). Cells transfected to express only S-tag-HeV G were used as a control. 24 h p.t., the culture medium was replaced with DMEM containing 2% FBS. 18 h later, cells were harvested and lysed in 100 ul PLB, and VLPs were purified as described earlier and re-suspended in 50 ul PLB. 1/10 of the cell lysates and 1/5 of the VLPs were resolved on 10% SDS-PAGE. HeV G protein, F protein and HeV M protein were detected by western blot using a rabbit anti-HeV G pAb SVL 10006-11 provided by Dr. Christopher Broder (Uniformed Services University of Health Science), a rabbit anti-HeV F pAb provided by Dr. Rebecca Dutch (University of Kentucky) and a mouse anti-Myc mAb. Images were captured using a Fuji FLA-7000 phosphorimager.

Membrane flotation assays to measure M protein membrane association

HEK293T cells in 10-cm dishes were transfected with pCAGGS plasmids encoding NiV M protein (0.8 µg/dish) together with AP3B1-derived polypeptides (1.5 µg/dish). At 24 h p.t. cells were harvested, re-suspended in 600 µl of hypotonic buffer (25 mM NaCl, 50 mM Na2HPO4, pH 7.3, 1 mM phenylmethylsulfonyl fluoride), and incubated for 30 min at 4°C. The cells were subjected to 40 strokes of Dounce homogenization followed by microcentrifugation at 200 x g for 5 minutes to remove debris and nuclei. The resulting homogenates were mixed with 1.5 ml of 80% sucrose in NTE (0.1 M NaCl; 0.01 M Tris-HCl, pH 7.4; 1 mM EDTA). Layers of 50% sucrose (2.4ml) and 10% sucrose (0.6ml) in NTE were placed on top of the Dounced mixtures, and samples were centrifuged at 160,000 x g for 4 h in a Sorvall AH650 swinging bucket rotor. Six equal fractions were collected from the top of each gradient. Proteins from the gradient fractions were separated by SDS-PAGE using 10% gels and subjected to immunoblot analysis using a polyclonal antibody to NiV M that has been described previously (110). Protein bands were detected and quantified using a Fuji FLA-7000 laser scanner. The fraction of membrane-bound M protein was calculated as the amount of M protein detected in the top three fractions of the gradient, divided by the total amount of M protein detected in all six fractions.

RNA interference (RNAi)

Three 19-nt siRNAs for human AP3B1 (SASI_Hs01_00018424, SASI_Hs01_00018425, SASI_Hs01_00018426) were purchased from Sigma-Aldrich

(St. Louis, MO), together with the Universal Negative Control siRNA. HEK293T cells in 6-cm dishes were cotransfected with pCAGGS plasmid encoding Myc-tagged NiV M (0.4 μg per dish) and 100 nM siRNA (either the negative control siRNA or a mixture of SASI_Hs01_00018424 (50 nM) plus SASI_Hs01_00018426 (50 nM). SASI_Hs01_00018424 targets the sequence CGAAUCUAGUUCAAUAGAA, and SASI_Hs01_00018426 targets the sequence GCAACAAAGAUUCUGCUAA. siRNA and plasmid cotransfection was performed using Lipofectamine-Plus reagents. VLPs were collected and VLP production was calculated as described above. Additional transfections were carried out in parallel to measure the efficiency of AP3B1 depletion. HEK293T cells in 6-well plates were transfected with siRNA (100 nM) using Lipofectamine-Plus reagents as above. At 24 h p.t, the culture medium was replaced with DMEM supplemented with 2% FBS. At 42 h p.t, cells were harvested and lysed in SDS-PAGE loading buffer containing 2.5% (wt/vol) dithiothreitol. Proteins were fractionated by SDS-PAGE using 10% gels, and the levels of endogenous AP3B1 protein were measured by immunoblot analysis using the AP3B1-specific polyclonal antibody AP3B1 13384-1-AP (Proteintech Group, Chicago, IL).

Immunofluorescence microscopy

HEK293T cells seeded on poly-D-lysine-coated glass coverslips and grown to 50% confluency were transfected with plasmid pcDNATM3.1-Flag-NiV M (50 ng/well) using Lipofectamine-Plus. At 24 h p.t., cells were washed three times with warm PBS

for 10 min per wash, fixed with 4% paraformaldehyde in PBS for 15 min, then washed three additional times. Cells were then permeabilized using 0.1% saponin, incubated in a blocking solution containing 1% BSA and 0.1% fish gelatin, and incubated with primary and secondary antibody solutions as described previously (81). Nipah virus M protein was visualized using anti-DDK monoclonal antibody specific to the Flag tag (Origene, Rockville, MD), and endogenous AP3B1 was visualized using anti-AP3B1 rabbit polyclonal antibody (Proteintech Group, Chicago IL). Secondary antibodies used were: Alexa Fluor 594 goat anti-mouse IgG2a for detection of M protein and Alexa Fluor 488 goat anti-rabbit for detection of AP3B1 (Life Technologies). Washes were done after each antibody incubation and cell nuclei were stained using ProLong Gold antifade reagent with DAPI (Invitrogen). Cells were visualized with a Zeiss AxioImager M1 fluorescence microscope (Carl Zeiss Inc., Thornwood, NY) and images were captured using an Orca R2 digital camera (Hamamatsu Photonics, Bridgewater, NJ). Images were deconvolved using iVision software (BioVision Technologies, Exton PA).

To visualize HeV M, F, G and Rab11a, Vero cells seeded on poly-D-lysine-coated glass coverslips and grown to 50% confluency were transfected with plasmid pcDNA-Flag-HeV M (0.1 ug/well) alone, pcDNA-Flag-HeV M (0.1 ug/well) together with pcDNA-S-tag-HeV G (50 ng/well), pCAGGS-HeV F (0.2 ug/well) together with pEGFP-C1-Rab11a (0.2 ug/well) or pcDNA-S-tag-HeV G (50 ng/well) together with GFP-Rab11a. Hendra virus M protein was visualized using anti-DDK monoclonal antibody specific to the Flag tag. Hendra virus F protein was visualized by mouse anti-HeV F

mAb 7F7 provided by Dr. Rebecca Dutch (University of Kentucky), whereas Hendra virus G protein was detected using mouse anti-HeV G mAb 5B1 provided by Dr. Christopher Broder (Uniformed Services University of Health Science). Endogenous Rab11a or GFP-Rab11a was detected using rabbit anti-Rab11a pAb (Proteintech group) as GFP photo-bleach too fast to capture stack images. Secondary antibodies used were: Alexa Fluor 594 goat anti-mouse IgG2a for detection of M protein, Alexa Fluor 594 goat anti-mouse IgG1 to detect F and G, and Alexa Fluor 488 goat anti-rabbit for detection of Rab11a. The rest of the procedure is the same as described above.

Brefeldin A (BFA) treatment

For immunofluorescence microscopy, Vero cells grown in 12-well plates were transfected with pcDNA3.1 plasmid encoding Flag-NiV M (50 ng/well) in duplicates. They were either mock treated with DMSO or treated with 20 ug/ml BFA in DMSO at 4 h p.t. 24 h p.t, cells were fixed, and experiments were performed as described earlier. Flag-HeV M protein was visualized using anti-DDK monoclonal antibody specific to the flag tag and endogenous AP3B1 was visualized using anti-AP3B1 rabbit polyclonal antibody. Secondary antibodies used were: Alexa Fluor 594 goat anti-mouse IgG2a for detection of M protein and Alexa Fluor 488 goat anti-rabbit for detection of AP3B1. Images were captured using an Orca R2 digital camera. Images were deconvolved using iVision software. For membrane flotation assay, HEK293T cells grown in 6-cm dishes were transfected with pCAGGS encoding Myc-NiV M (0.4

ug/dish) in duplicates. They were either mock treated with DMSO or treated with 20 ug/ml BFA in DMSO at 4 h p.t. 24 h. p.t, cells were harvested and homogenized, membranes and membrane binding proteins were floated as described earlier. Myc-NiV M protein was visualized using mouse anti-Myc mAb by western blot. Images were captured using a Fuji FLA-7000 phosphorimager. For VLPs budding assay, HEK293T cells grown in 6-cm dishes were transfected with pCAGGS encoding Myc-NiV M (0.2 ug/dish) or pGFP plasmid encoding GFP-HIV-1 Gag (0.2 ug/dish) in duplicates. They were either mock treated with DMSO or treated with 20 ug/ml BFA in DMSO at 24 h p.t. 18 h later, cells were harvested and VLPs were purified as describe earlier. Myc-NiV M protein was visualized using mouse anti-Myc mAb and GFP-Gag was visualized using rabbit anti-GFP pAb by western blot. Images were captured using a Fuji FLA-7000 phosphorimager.

Cathepsin L inhibition VLP assay

To generate Hendra M and F VLPs, HEK 293T cells grown in 6-cm dishes were transfected with pCAGGS plasmids encoding Myc-tagged HeV M protein (0.2 ug/dish) together with wild type HeV F protein or HeV F S490A protein (0.8 µg/dish) in duplicates, where one group was treated with 10 uM cathepsin L inhibitor E-64d starting at transfection. 24 h p.t, the culture medium was replaced with DMEM containing 2% FBS with 10 uM E-64d for the pretreated group, and without E-64d for the non-pretreated group. 18 h later, cells were harvested and lysed in 100 ul PLB, and VLPs were purified as described earlier and re-suspended in 50 ul PLB. 1/10 of

the cell lysates and 1/5 of the VLPs were resolved on 10% SDS-PAGE. HeV F proteins and HeV M protein were detected by western blot using rabbit anti-HeV F pAb provided by Dr. Rebecca Dutch (University of Kentucky), and a mouse anti-Myc mAb. Images were captured using a Fuji FLA-7000 phosphorimager.

Phosphoinositide 3-kinase (PI3K) inhibition VLP assay

Hendra M and F VLPs and HIV-1 Gag-VLP were produced as described before. HEK 293T cells grown in 6-cm dishes were transfected with pCAGGS plasmids encoding Myc-tagged HeV M protein (0.2 ug/dish), HeV F protein (0.8 µg/dish) or pGFP plasmid encoding HIV-1 GFP-Gag (0.2 ug/dish) in replicates. 24 h p.t, they were mock treated with DMSO or with 25 uM or 50 uM PI3K inhibitor LY294002 in replacing DMEM containing 2% FBS. 18 h later, cells were harvested and lysed in 100 ul PLB. VLPs were purified as described earlier and re-suspended in 50 ul PLB. 1/10 of the cell lysates and 1/5 of the VLPs were resolved on 10% SDS-PAGE. HeV F proteins and HeV M protein were detected by western blot using a rabbit anti-HeV F pAb, and a mouse anti-Myc mAb. HIV-1 Gag protein was detected using a rabbit anti-GFP pAb. Images were captured using a Fuji FLA-7000 phosphorimager.

Sedimentation gradient analysis of Hendra VLPs density

HEK293T cells in 10-cm dishes were transfected with pCAGGS plasmids encoding Myc-HeV M (0.4 ug/dish), HeV F (1.6 ug/dish), or Myc-HeV M together with HeV F. Transfections were carried out in Opti-MEM using Lipofectamine-Plus reagents. At

24 h p.t., the culture medium was replaced with DMEM containing 2% FBS. 18hr later, media were collected to purify VLPs on 20% sucrose cushion and VLPs were re-suspended in 200 ul 1x NTE buffer. 5%-45% continuous sucrose gradients were created by laying 1.85 ml 5% sucrose in 1x NTE onto 1.85 ml 45% sucrose in 1x NTE followed by diffusing for 24 h in the fridge at 4C. 200 ul. VLP suspension were added on top of the gradients and spun for 16 h at 4C, 40k rpm in a Sorvall AH650 swinging bucket rotor. 12x 300 ul fractions were collected from top to bottom, 15 ul of each fraction were resolved on 10% SDS-PAGE, HeV M and F proteins were detected by western blot using a mouse anti-Myc mAb and a rabbit anti-HeV F pAb. Density of each fraction was determined by weighing, and calculated based on weight (g)/0.3 (ml).

Subcellular fractionation

HEK 293T cells in 10-cm dish were mock transfected or transfected with pCAGGS plasmids encoding Myc-HeV M or HeV F. 24 h p.t., cells were washed three times with lysis buffer (10 mM Tris [pH 7.5], 0.25 M sucrose, 1 mM EDTA, 200 μM orthovanadate, and 1 mM phenylmethylsulfonyl fluoride) at 4°C. They were subsequently scraped off the dish in 1ml lysis buffer, aspirated with a syringe, and destroyed by passaging 20 times through a needle (23 gauge). Nuclei were pelleted at 800 × *g* for 5 min at 4°C. The supernatant was subjected to subcellular fractionation in discontinuous iodixanol gradients which was modified from the methods of Yeaman et al (220). Briefly, the separation of different membrane

compartments was achieved by centrifugation of three-step 10 to 20 to 30% (wt/vol) iodixanol gradients. One third (300ul) of the cell lysates were mixed with Opti-Prep (60% [wt/vol]) iodixanol (Sigma), and lysis buffer to generate solutions containing 10, 20, or 30% iodixanol. Equal volumes (1.5 ml) of these three solutions were layered in centrifuge tubes, and samples were centrifuged at 40k rpm for 10 h at 4°C. Fractions (300 µl) were collected and proteins were separated by sodium dodecyl sulfate-polyacrylamide gel electrophoresis (SDS-PAGE) and detected by western blot using mouse anti-LAMP-1 mAb (BD Bioscience, San Jose, CA), anti-Rab11a, anti-Myc and anti-HeV antibodies. Images were captured using a Fuji FLA-7000 phosphorimager.

CHAPTER 3

Matrix Proteins of Nipah and Hendra Viruses Interact with Beta Subunits of AP-3 Complexes

(This is a reprint of the published paper (Sun, W., McCrory, T. S., Khaw, W. Y., Petzing, S., Myers, T., & Schmitt, A. P. (2014). Matrix Proteins of Nipah and Hendra Viruses Interact with Beta Subunits of AP-3 Complexes. *Journal of virology*, *88*(22), 13099-13110.))

3.1 Introduction

Hendra virus and Nipah virus are zoonotic paramyxoviruses belonging to the henipavirus genus (18, 60, 105) Natural hosts for these viruses are pteropid fruit bats such as flying foxes, which suffer no apparent illness from the infections, but act as reservoirs allowing spillover transmissions that can be deadly to other animals and to people (44, 76). Hendra virus was first identified in Australia in 1994, after causing fatal infections in multiple horses and in one person who was exposed to an infected horse (143, 217). Numerous spillovers of Hendra virus to horses in Australia have occurred since that initial outbreak, and these have led to 7 human cases and 4 human fatalities to-date (5, 163). Nipah virus was discovered after a Malaysian outbreak in 1998-1999, in which the virus was transmitted from bats to domesticated pigs. The virus circulated among the pigs and ultimately infected over 200 pig farmers, resulting in more than 100 fatalities (40). Like Hendra virus, Nipah virus has caused repeated spillovers in the years since its initial emergence, with many of the subsequent Nipah virus outbreaks occurring in Bangladesh and India (5).

Paramyxoviruses and other negative-strand RNA viruses encode matrix proteins

that function to organize the assembly and release of virus particles (111). Once formed, the particles are membrane-enveloped and covered with a layer of glycoprotein spikes, consisting of the viral attachment and fusion proteins. In addition, the particles contain negative-sense RNA genomes that are encapsidated by nucleocapsid proteins to form the viral ribonucleoprotein complexes (RNPs). During paramyxovirus assembly, the matrix (M) proteins accumulate at sites on cellular membranes from which the particles will bud, and recruit other components to these locations, including the viral glycoproteins, the viral RNPs, and in many cases host budding machinery (80, 194).

The assembly and budding process that leads to the formation of enveloped virus particles can often be reconstituted in transfected cells, allowing for the production of virus-like particles (VLPs) that resemble virions morphologically, but lack viral genomes and many of the other viral components necessary for infectivity. For the paramyxoviruses, M protein expression in mammalian cells is necessary, and in many cases sufficient, to trigger the budding and release of VLPs with size and shape that is consistent with authentic virions. For example, the M proteins of Sendai virus (192, 193), human parainfluenza virus type 1 (45), Newcastle disease virus (150), Measles virus (164, 178), and Nipah virus (42, 152, 153) are sufficient to induce the formation and release of VLPs from transfected cells. In many cases, the viral glycoproteins and/or nucleocapsid proteins become incorporated into the VLPs if those proteins are co-expressed with M protein (80). In the cases of parainfluenza virus 5 (PIV5) (183) and Mumps virus (110), efficient VLP release necessitates

expression of viral glycoprotein and nucleocapsid protein, in addition to M protein.

Recruitment of host machinery via the matrix and Gag proteins of negative-strand RNA viruses and retroviruses is critical in many cases for proper formation and release of virus particles (79, 119, 175, 206), yet for many paramyxoviruses, including the henipaviruses, M protein:host protein interactions remain largely unexplored. In this study, we have identified the Beta subunit of the AP-3 adapter protein complex, AP3B1, as a binding partner for the Nipah virus and Hendra virus M proteins. Binding was mapped to the serine-rich and acidic Hinge domain of the AP3B1 protein. Budding of Nipah VLPs was significantly impaired upon siRNA-mediated depletion of AP3B1 from cells. VLP budding could also be inhibited through expression of short M-binding polypeptides derived from the AP3B1 Hinge region. Our findings suggest that AP-3 directed trafficking processes are important during henipavirus particle formation, and identify a new host-protein:virus protein binding interface that could prove useful as a target in future efforts aimed at developing therapeutics to treat these viral infections.

3.2 Results

Identification of henipavirus M-associating host proteins by affinity purification and mass spectrometry

To define host factors involved in henipavirus particle formation, we affinity-purified Hendra virus M protein from the lysates of transfected cells, and identified co-purifying host factors using mass spectrometry. This approach employed a

modified M protein, SH-HeV M, that harbors tandem N-terminal Strep(II) and 6xHis tags. We found that placing these affinity tags at the N-terminus of Hendra virus M protein had minimal effects on M protein stability and VLP production function, whereas addition of the same tags to the C-terminal end of M protein caused substantial stability and VLP production defects (data not shown). SH-HeV M protein was expressed in 293T cells using transient transfection, and M protein was affinity-purified from cell lysates by FPLC via the Strep(II) tag. SDS-PAGE and whole protein staining revealed a complex mixture of polypeptides which co-purified with Hendra virus M protein (Fig. 3-1A). A parallel purification using the highly similar Nipah virus M protein (SH-NiV M) in place of the Hendra virus M protein led to a near-identical profile of co-purifying polypeptides visualized by SDS-PAGE (Fig. 3-1A). These co-purifying polypeptides were almost completely absent in control experiments using either tagged eGFP (SH-EGFP) or untagged Nipah virus M protein (Fig. 3-1A). 15 bands resulting from the Hendra virus M co-purification procedure were selected for analysis. These were excised from the gel and subjected to in-gel trypsinization and multidimensional liquid chromatography and tandem mass spectrometry (LC/LC-MS/MS) for peptide identification. Results of this analysis revealed multiple distinct polypeptides associated with each of the excised bands (Fig. 3-1B). Several proteins involved in intracellular trafficking were identified (TCOF1, AP3B1, EXOSC10) as well as some that have previously been linked to virus replication (ZC3HAV1, AP3B1, HERC5, ILF2/3). More than half of the host proteins identified through this analysis are RNA-associated proteins, including RNA helicases,

splicing factors, nuclear ribonucleoproteins, and ribosomal proteins.

We speculated that the large proportion of RNA-associated proteins identified after M protein co-purification might have been a consequence of an M protein interaction with cellular RNA. Under this scenario, a large number of proteins might co-purify with M protein not because they interact with M protein itself, but rather because they directly or indirectly interact with the cellular RNA that M protein has bound. Although the henipavirus M proteins have not previously been shown to bind RNA, matrix proteins from related viruses such as respiratory syncytial virus (173), Ebola virus (73), and influenza virus (208) have been shown to bind cellular RNA. We reasoned that treatment of cell lysates with RNase prior to the FPLC purification step would likely reduce or eliminate any potential RNA-directed interactions, and might serve to facilitate the identification of proteins and/or protein complexes that bind directly to M protein. Indeed, RNase treatment markedly changed the profile of polypeptides co-purifying with Hendra virus M protein as visualized by SDS-PAGE (Fig. 3-1C), and mass spectrometry analysis of excised bands revealed that only a minor fraction of these polypeptides correspond to RNA helicases, splicing factors, and other RNA-associated proteins (Fig. 3-1D).

A

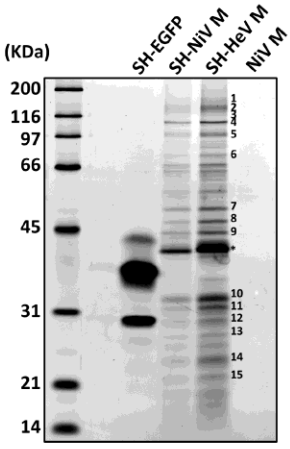

B

Band ID	Unique Peptides	Protein Coverage	Protein Name
1 ~130kD	76	48%	DEAH (Asp-Glu-Ala-His) box polypeptide 9 (DHX9)
	67	46%	Splicing factor 3b, subunit 1 (SF3B1)
	27	15%	Treacher Collins-Franceschetti syndrome 1 (TCOF1)
	23	26%	Protein KRI1 homolog (KRI1)
	21	23%	Replication factor C1 (RFC1)
	16	21%	Putative rRNA methyltransferase 3 (FTSJ3)
	16	18%	Family with sequence similarity 120A (FAM120A)
	16	14%	Structural maintenance of chromosomes 1A (SMC1A)
	15	19%	Squamous cell carcinoma antigen recognized by T cells 3 (SART3)
	12	11%	Polymerase (RNA) III (DNA Directed) polypeptide A (POLR3A)
2 ~120kD	67	48%	Heterogeneous nuclear ribonucleoprotein U (HNRNPU)
	49	43%	DEAH (Asp-Glu-Ala-His) box polypeptide 30 (DHX30)
	31	39%	DEAD (Asp-Glu-Ala-Asp) box polypeptide 24 (DDX24)
	31	35%	Regulator of nonsense transcripts 1 (UPF1)
	29	30%	Splicing factor 3b, subunit 3 (SF3B3)
	22	26%	HNRNPU like protein 2 (HNRNPUL2)
	22	22%	Adaptor-related protein complex 3, beta 1 subunit (AP3B1)
	19	18%	Structural maintenance of chromosomes 2-like 1 protein (SMC2)
	16	23%	Heterogeneous nuclear ribonucleoprotein U-Like 1 (HNRNPUL1)
	13	12%	Polymerase (RNA) III (DNA Directed) polypeptide B (POLR3B)
3 ~115kD	49	37%	Leucine-rich PPR repeat containing protein (LRPPRC)
	38	35%	Pyruvate carboxylase (PC)
	34	36%	Guanine nucleotide binding protein-like 2,nucleolar (GNL2)
	32	28%	DNA-directed RNA polymerase, mitochondria (POLRMT)
	32	32%	N-acetyltransferase 10 (NAT10)
	25	25%	SWI/SNF related, matrix associated, actin dependent regulator of chromatin (SMARCA5)
	24	32%	Tripartite motif containing 28 (TRIM28)
	24	33%	U3 small nucleolar RNA-associated protein 14 homolog A (UTP14A)
	24	29%	Processing of precursor 1 (POP1)
	24	29%	Pre-rRNA-processing protein TSR1 Homolog (TSR1)
4 ~110kD	43	55%	Cell division cycle 5-like protein (CDC5L)
	27	40%	Nucleolin (NCL)
	26	30%	Nucleolar protein 14 homolog (NOP14)
	25	38%	NF-kappaB repressing factor (NKRF)
	22	23%	DEAH (Asp-Glu-Ala-His) box polypeptide 36 (DHX36)
	19	39%	Zinc finger CCCH-type, antiviral 1 (ZC3HAV1)
	18	19%	Polymerase (RNA) I polypeptide B (POLR1B)
	16	24%	Paf1/RNA polymerase II complex component (RTF1)
	15	16%	HECT and RLD domain containing E3 ubiquitin ligase 5 (HERC5)
	15	27%	A kinase (PRKA) anchor protein 8-Like (AKAP8L)
5 ~97kD	57	55%	DEAD (Asp-Glu-Ala-Asp) box polypeptide 21 (DDX21)
	45	56%	Interleukin enhancer binding factor 3 (ILF3)
	42	39%	Topoisomerase (DNA) I (TOP1)
	23	38%	Metastasis adhesion protein (MTDH)
	21	30%	Ribosomal RNA processing 1 homolog B (RRP1B)
	15	20%	Exosome component 10 (EXOSC10)
	13	26%	E3 ubiquitin-protein ligase RAD18 (RAD18)
	12	22%	Pre-mRNA processing factor 3 (PRPF3)
	12	21%	TRM1 tRNA methyltransferase 1-Like (TRM1L)
	12	16%	DEAD (Asp-Glu-Ala-Asp) box polypeptide 27 (DDX27)

Band ID	Unique Peptides	Protein Coverage	Protein Name
6 ~90kD	44	47%	ATP-dependent DNA helicase II 80 kDa subunit (XRCC5)
	41	35%	DEAH (Asp-Glu-Ala-His) box polypeptide 15 (DHX15)
	29	40%	DEAD (Asp-Glu-Ala-Asp) box polypeptide 18 (DDX18)
	25	36%	Heterogeneous nuclear ribonucleoprotein R (HNRNPR)
	19	26%	Spermatid perinuclear RNA binding protein (STRBP)
	17	24%	MAP/microtubule affinity-regulating kinase 3 (MARK3)
	17	22%	General transcription factor IIIC, polypeptide 4 (GTF3C4)
	15	36%	Heterochromatin protein 1 binding protein 3 (HP1BP3)
	13	17%	Testis expressed 10 (TEX10)
	13	24%	Zinc finger protein 768 (ZNF768)
7 ~50kD	18	52%	Y box binding protein 1 (YBX1)
	13	30%	Cold shock domain protein A (CSDA)
	11	23%	ATP synthase, H+ transporting, mitochondrial F1 complex, alpha subunit 1, cardiac muscle (ATP5A1)
8 ~46kD	37	53%	Ribosomal protein L4 (RPL4)
	23	37%	Sjogren syndrome antigen B (SSB)
	15	30%	Mitochondrial trifunctional enzyme, beta subunit (HADHB)
	15	26%	Small subunit (SSU) processome component, homolog (KRR1)
	14	34%	Ly1 antibody reactive homolog (LYAR)
	14	30%	Eukaryotic translation initiation factor 4A, isoform 3 (EIF4A3)
	12	26%	Mitochondrial ribosomal protein L38 (MRPL38)
	11	27%	Mitochondrial ribosomal protein L37 (MRPL37)
9 ~44kD	27	40%	Ribosomal protein L3 (RPL3)
	20	44%	Mitochondrial ribosomal protein S27 (MRPS27)
	19	44%	Tu translation elongation factor, mitochondrial (TUFM)
	18	38%	Mitochondrial ribosomal protein S35 (MRPS35)
	13	37%	Interleukin enhancer binding factor 2 (ILF2)
10 ~35kD	36	67%	Ribosomal protein S3A (RPS3A)
	26	76%	Ribosomal protein S3 (RPS3)
	20	46%	Ribosomal protein S2 (RPS2)
	14	39%	Mitochondrial ribosomal protein L19 (MRPL19)
11 ~30kD	29	73%	Ribosomal protein S4, X-linked (RPS4X)
	21	43%	Ribosomal protein S6 (RPS6)
	16	32%	Ribosomal protein L7A (RPL7A)
	13	53%	Mitochondrial ribosomal protein L24 (MRPL24)
12 ~28kD	19	50%	Ribosomal protein L7 (RPL7)
	15	53%	Ribosomal protein S8 (RPS8)
	14	48%	Mitochondrial ribosomal protein S7 (MRPS7)
	12	40%	Ribosomal protein L10A (RPL10A)
13 ~26kD	18	52%	Ribosomal protein L19 (RPL19)
	10	29%	Ribosomal protein L13 pseudogene 12 (RPL13P12)
	10	35%	Mitochondrial ribosomal protein L9 (MRPL9)
14 ~23kD	23	56%	Ribosomal protein L9 (RPL9)
	18	45%	Ribosomal protein L13A (RPL13A)
	17	59%	Ribosomal protein L17A (RPL17A)
	16	48%	Ribosomal protein L21 pseudogene 19 (RPL21P19)
15 ~22kD	24	78%	Ribosomal protein S11 (RPS11)
	22	66%	Ribosomal protein L26-like 1 (RPL26L1)
	15	60%	Mitochondrial ribosomal protein L11 (MRPL11)
	14	51%	Ribosomal protein L23A (RPL23A)
	11	35%	Ribosomal protein L24 (RPL24)

C

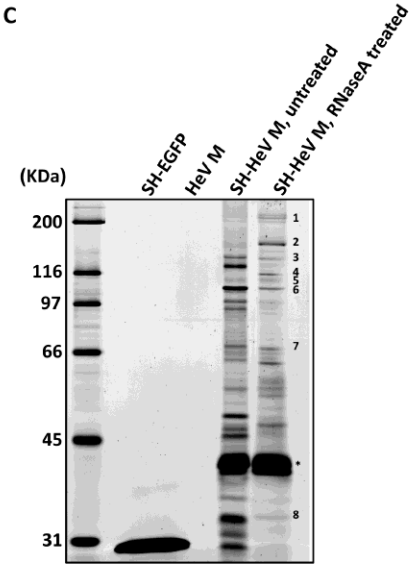

D

Band ID	Unique Peptides	Protein Coverage	Protein Name
1 ~210kD	125	45%	Acetyl-CoA carboxylase 1 (ACACA)
	34	16%	Small nuclear RNP helicase (SNRNP200)
	25	16%	Bromodomain-containing protein 4 (BRD4)
	25	12%	Pre-mRNA processing factor (PRPF8)
	23	12%	Translocated promoter region protein (TPR)
2 ~180kD	111	52%	Eukaryotic translation initiation factor 3, subunit A(EIF3A)
	27	24%	Adaptor-related protein complex 3, delta 1 subunit (AP3D1)
	16	17%	HIV-1 Vpr binding protein (VPRBP)
	13	14%	SIN3 transcription regulator (SIN3A)
	13	12%	TRAF2 and NCK interacting kinase (TNIK)
3 ~130kD	52	39%	FACT complex subunit SPT 16 (SUPT16H)
	34	29%	Treacher Collins-Franceschetti syndrome 1 (TCOF1)
	18	19%	Ubiquitin carboxyl-terminal hydrolase 7 (USP7)
	15	27%	HIV Tat-specific factor 1 (HTATSF1)
	12	12%	Adaptor-related protein complex 3, beta 1 subunit (AP3B1)
4 ~116kD	61	51%	Eukaryotic translation initiation factor 3, subunit B(EIF3B)
	44	41%	U5 small nuclear RNP component (EFTUD2)
	33	26%	DNA damage-binding protein 1 (DDB1)
	17	19%	Pyruvate carboxylase (PC)
	11	11%	Ankyrin repeat domain 28 (ANKRD28)
5 ~113kD	52	43%	Eukaryotic translation initiation factor 3, subunit C-like (EIF3CL)
	13	15%	Superkiller viralicidic activity 2-like 2 (SKIV2L2)
	12	15%	Poly (ADP-ribose) polymerase (PARP1)
	11	12%	Importin-7 (IPO7)
	10	17%	Tripartite motif containing 28 (TRIM28)
6 ~110kD	35	50%	Nucleolin (NCL)
	35	31%	WASH complex subunit strumpellin (KIAA0196)
	31	35%	Lysine-specific histone demethylase 1 (KDM1)
	17	26%	Digestive organ expansion factor homolog (DIEXF)
	11	15%	26S proteasome regulatory subunit (PSMD1)
7 ~70kD	52	51%	Propionyl-CoA carboxylase alpha chain (PCCA)
	46	58%	Heat shock cognate 71 protein(HSPA8)
	34	39%	Trifunctional enzyme subunit alpha (HADHA)
	24	36%	Polyadenylate-binding protein (PABPC1)
	16	35%	Apoptosis-inducing factor, mitochondrion-associated (AIFM1)
8 ~33kD	26	58%	Mitochondrial ribosomal protein L45 (MRPL45)
	22	48%	Acidic (leucine-rich) nuclear phosphoprotein 32 (ANP32B)
	20	70%	Ribosomal protein S3 (RPS3)
	11	39%	Mitochondrial ribosomal protein L15 (MRPL15)
	10	33%	Acidic nuclear phosphoprotein (ANP32A)

Figure 3-1. Identification of henipavirus M-associating host proteins by affinity purification and mass spectrometry. (A) 293T cells were transfected to express affinity-tagged henipavirus M proteins, untagged M protein, or affinity-tagged eGFP, as indicated. Cell lysates were prepared and subjected to FPLC using a StrepTrap-HP column. Eluted proteins were resolved by SDS-PAGE and visualized using Sypro Orange. The asterisk denotes the migrations of SH-NiV M and SH-HeV M. Numbers indicate protein bands that were excised from a duplicate Coomassie Blue-stained SDS gel for MS-based identification of polypeptides. **(B)** Proteins identified by MS from the 15 bands illustrated in Panel A. Coverage indicates the percentage of amino acid residues within the protein that are present in at least one of the identified peptides **(C)** Affinity tagged HeV M protein was purified from cell lysates using FPLC as in Panel A, with an additional RNase A digestion step performed just prior to FPLC. **(D)** Proteins identified by MS from the 8 bands illustrated in Panel C.

AP3B1 interacts with Henipavirus M proteins via its hinge domain

To further interrogate the abilities of HeV M co-purifying host factors to interact with henipavirus M proteins, coimmunoprecipitation experiments were performed. Several candidate M-interacting host factors were selected for these experiments: AP3B1, EXOSC10, HECR5, HTATSF1, ILF2, NKRF, RPS3, TCOF1, VPRBP, YBX1 and ZC3HAV1. cDNAs corresponding to these proteins were obtained, and N-terminal Flag tags were appended. The Flag-tagged host proteins were expressed together with myc-tagged Nipah virus M protein in transfected 293T cells. The host proteins were precipitated with Flag antibody, and co-precipitation of M protein was evaluated (Fig. 3-2 and data not shown). Strong co-precipitation of M protein was observed in the presence of AP3B1. This was the only candidate host factor for which substantial M protein co-precipitation was observed, although TCOF1, ZC3HAV1 and VPRBP each led to a weak level of co-precipitation.

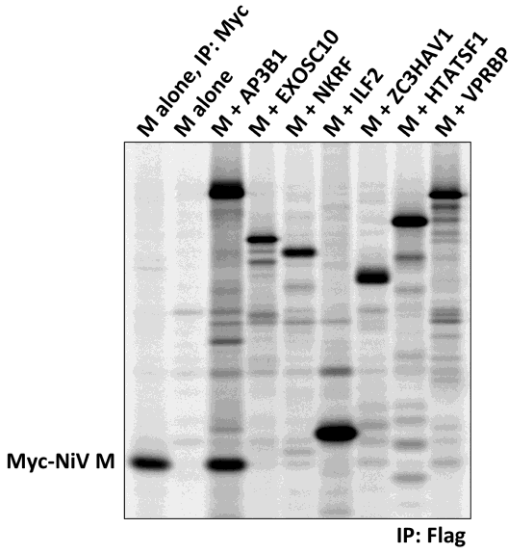

Figure 3-2. Coimmunoprecipitation of Nipah virus M protein with candidate host proteins identified by MS. 293T cells were transfected to produce Myc-tagged NiV M protein together with the indicated Flag-tagged candidate host factors. Proteins synthesized in the transfected cells were ^{35}S-labeled, and cells were lysed in a solution containing 1% NP-40. Immunoprecipitation was carried out using Myc antibody (Lane 1) or Flag-conjugated resin (Lanes 2 to 9), and proteins were detected using a phosphorimager.

AP3B1 forms the Beta subunit of tetrameric AP-3 adapter complexes, which act as cargo adaptors during endosomal trafficking and sorting (54, 139, 157). Trafficking of HIV-1 Gag to multivesicular bodies is mediated in part by AP-3 complexes, and HIV-1 assembly is impaired in AP-3 deficient cells (58, 69, 114). Based on homology with the Beta subunits of other adapter protein complexes, AP3B1 consists of three domains: an N-terminal Head domain that comprises approximately 60% of the protein, a C-terminal Ear domain (approximately 25% of the protein), and a serine-rich, acidic Hinge domain that separates the Head and Ear regions (Fig. 3-3A, B) (7, 54). To more clearly define the binding interface between AP3B1 and henipavirus M proteins, mapping studies were performed. A series of Flag-tagged human AP3B1 protein derivatives were constructed as illustrated in Fig. 3-3A, and these were used to coimmunoprecipitate Nipah virus M protein in transfected 293T cells (Fig. 3-3C, D). M-binding function was localized to the Hinge domain of the protein, as co-immunoprecipitation was observed with the full-length, Head/Hinge, and Hinge constructs, but not with the Head or Ear constructs (Fig. 3-3C). AmotL1-m was used as a negative control in these experiments. This 83 aa-long polypeptide binds to the M protein of another paramyxovirus, PIV5 (159), but fails to interact with henipavirus M proteins. To further localize the M-binding region within AP3B1, its Hinge domain was divided into three roughly equal segments, designated Hinge 1, Hinge 2, and Hinge 3 (Fig. 3-3A, B). Expression of the Hinge 1 segment led to M protein coimmunoprecipitation (Fig.3- 3C). Interestingly, expression of Hinge 3 segment also led to a similar level of M protein coimmunoprecipitation. In contrast,

Hinge 2 segment expression resulted in poor M protein coimmunoprecipitation. Both Hinge 1 and Hinge 3 are highly acidic and serine-rich (Fig. 3-3B). The two sequences are non-overlapping, but each contains an identical ten amino acid sequence "DSSSDSESES". The Hinge 1 sequence was further subdivided (Fig. 3-3A, B). Hinge 1A lacks DSSSDSESES and failed to bind M protein (Fig. 3-3D). The 29 amino acid-long Hinge 1B contains DSSSDSESES and was sufficient for M protein binding (Fig. 3-3D). Thus, a short polypeptide derived from the Hinge region of AP3B1 was sufficient for interaction with Nipah virus M protein in coimmunoprecipitation assays.

The M proteins of other paramyxoviruses (Hendra virus, PIV5, Sendai virus, and Mumps virus) were also tested for interaction with full-length AP3B1 in co-immunoprecipitation assays (Fig. 3-3E). We found the Hendra virus and Nipah virus M proteins to be virtually indistinguishable in these assays, as both exhibited highly efficient co-precipitation with AP3B1. The PIV5, Sendai virus, and Mumps virus M proteins all coimmunoprecipitated with AP3B1 as well, but the efficiency of coimmunoprecipiation appeared to be less. Although it is difficult to assess relative binding affinities using this approach, our results suggest that a diverse group of paramyxovirus M proteins have the potential to interact with AP3B1.

Further binding experiments were performed using AP3B1 protein derived from the henipavirus M proteins bind AP3B1 black flying fox, *Pteropus alecto*, which is a natural host reservoir species for both Nipah virus and Hendra virus. Flag-tagged versions of *P. alecto* AP3B1 were constructed (full-length, Head, Hinge, and Ear), and

coimmunoprecipitation of Nipah virus M protein was evaluated (Fig. 3-3F). Strong coimmunoprecipitation of M protein with the full-length *P. alecto* AP3B1 was observed, similar to the result obtained with human AP3B1. The Hinge domain of *P. alecto* AP3B1 was able to coimmunoprecipitate M protein, but the Head and Ear domains failed to coimmunoprecipitate M protein, again consistent with results obtained using the human-derived AP3B1 constructs and suggesting that the human and *P. alecto* AP3B1 proteins are fundamentally similar to one another with respect to their interactions with henipavirus M proteins. Consistent with this idea, sequence comparisons revealed a high degree of conservation between the human and *P. alecto* AP3B1 proteins (90% amino acid identity overall, 27 out of 29 aa residues identical within the Hinge 1B region, and 10 out of 10 aa residues identical within the DSSSDSESES sequence).

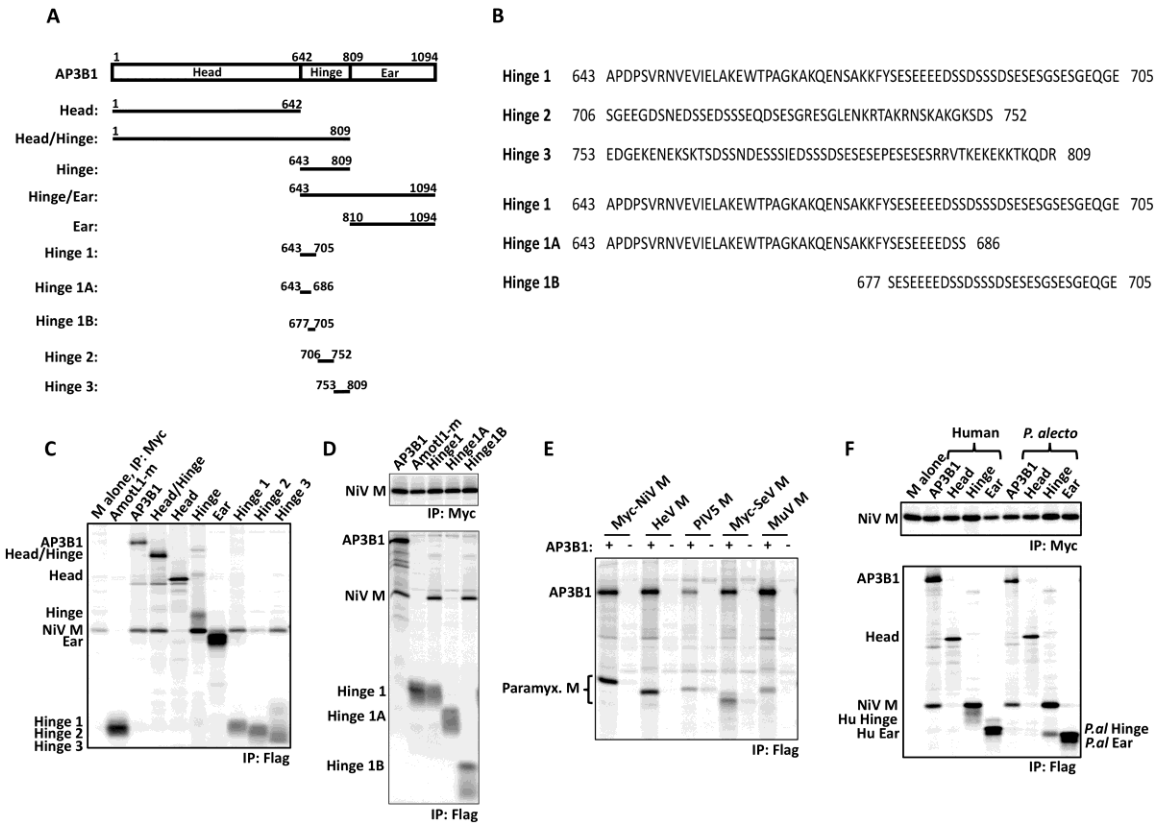

Figure 3-3. Small AP3B1-derived polypeptides bind Nipah virus M protein. (A) Schematic representation of human AP3B1 and AP3B1-derived polypeptides. **(B)** Amino acid sequences of human AP3B1 Hinge-derived polypeptides. (C to F) 293T cells were transfected to produce Myc-tagged NiV M protein **(C, D and F)** or the indicated paramyxovirus M proteins **(E)** together with the indicated Flag-tagged AP3B1-derived polypeptides, and coimmunoprecipitation was carried out as described in the legend to Fig. 2. The bat (*P. alecto*)-derived AP3B1-derived polypeptides used in Panel F are the equivalents of the corresponding human segments illustrated in Panel A, based on ClustalW2 sequence alignment between the human and *P. alecto* AP3B1 proteins. Upper gels in panels D and F correspond to control immunoprecipitations of Myc-M protein using Myc antibody, while lower gels correspond to co-immunoprecipitation experiments using Flag antibody.

Overexpression of M-binding, AP3B1-derived polypeptides blocks production of henipavirus VLPs

Short host factor-derived polypeptides that bind to viral Gag or M proteins can sometimes act as potent inhibitors of virus budding, either because they act as competitive inhibitors and prevent full-length endogenous host proteins from binding, or because they otherwise interfere with budding function when they are bound to the viral proteins (38, 56, 66, 67, 122, 130, 159). To test if AP3B1-derived polypeptides can inhibit henipavirus particle production, these polypeptides were expressed together with henipavirus M proteins in transfected 293T cells for production of VLPs. After metabolic labeling, VLPs were collected from the culture supernatants, pelleted through sucrose cushions, further purified by flotation on sucrose gradients, and analyzed on SDS gels (Fig. 3-4). We found that VLPs were abundantly produced when Nipah virus M protein was expressed in the absence of AP3B1-derived polypeptides (Fig. 3-4A), consistent with observations that have been reported before (42, 152). When the M-binding Hinge polypeptide was expressed together with M protein, VLP production was reduced by more than 20-fold (Fig. 3-4A, B). Similar reductions in VLP production (between 10- and 20-fold) were observed upon expression of the M-binding polypeptides Hinge 1 and Hinge 3. Even the 29 amino-acid Hinge 1B polypeptide was inhibitory, resulting in VLP production that was 10-fold reduced from the normal level (Fig. 3-4A, B). In contrast, the AP3B1-derived polypeptides which did not bind to M protein in coimmunoprecipitation experiments (Head, Hinge 2, and Hinge 1A) affected VLP

production by less than 2-fold (Fig. 3-4A, B). This same pattern was also observed with Hendra VLP production. We found that expression of the Hendra virus M protein in the absence of any other viral proteins (and in the absence of any AP3B1-derived polypeptides) led to abundant VLP formation and release (Fig. 3-4C, D). Co-expression of the Hinge, Hinge 1, Hinge 3, and Hinge 1B polypeptides inhibited production of Hendra VLPs while the Head, Hinge 2, and Hinge 1A polypeptides failed to inhibit (Fig.3- 4C, D, and data not shown). Hence, Hendra virus was found to be quite similar to Nipah virus both in the requirements for VLP production (M protein alone is sufficient), and in the sensitivity to inhibition by AP3B1-derived polypeptides. Additional VLP release experiments were performed using the Nipah virus M protein expressed together with the bat (*P. alecto*) version of the AP3B1 Hinge domain (Fig. 3-4E). We found that expression of the *P. alecto* AP3B1 Hinge domain inhibited VLP production just as effectively as expression of the human AP3B1 Hinge domain. Overall, these experiments have defined small, AP3B1-derived polypeptides that bind henipavirus M proteins and potently inhibit the production of henipavirus-like particles in transfected cells.

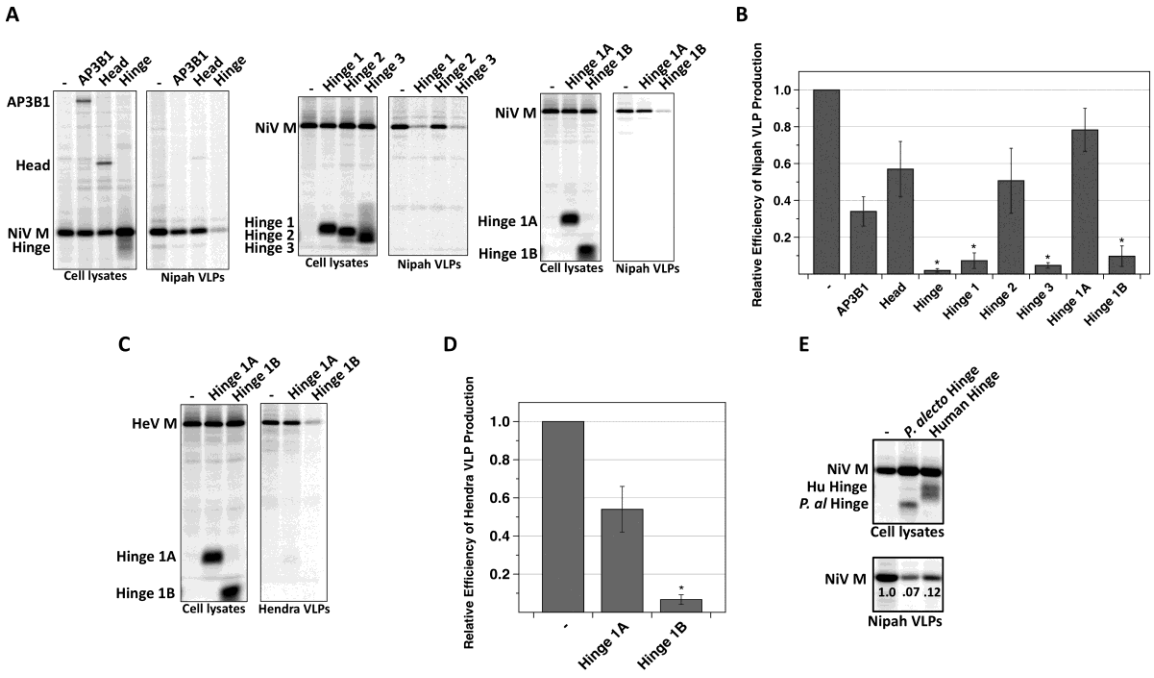

Figure 3-4. Small AP3B1-derived polypeptides inhibit henipavirus VLP production. (A) 293T cells were transfected to produce Nipah virus M protein together with the indicated human AP3B1-derived polypeptides. After metabolic labeling of cells, lysates were prepared and M protein was immunoprecipated using Myc antibody, while AP3B1-derived polypeptides were immunoprecipitated using Flag-conjugated resin. VLPs from culture supernatants were purified by centrifugation through sucrose cushions followed by flotation on sucrose gradients. Purified VLPs were loaded directly onto SDS gels without immunoprecipitation, and proteins were visualized using a phosphorimager. **(B)** Three independent experiments were performed as described for panel A, and VLP production efficiencies were calculated as the amount of viral M protein detected in VLPs divided by the amount of M protein detected in the corresponding cell lysate fraction, and were normalized to the values obtained in the absence of any polypeptide co-expression. Error bars indicate standard deviations. **(C)** VLPs were produced as described for panel A, but using Hendra virus M protein in place of Nipah virus M protein. **(D)** Efficiency of Hendra VLP production was calculated using data obtained from three independent experiments performed as in panel C. **(E)** Nipah VLPs were produced as described for panel A, with co-expression of either the human or the *P. alecto* versions of the AP3B1 Hinge domain. Relative efficiencies of VLP production are indicated.

To gather insight into the mechanism of budding inhibition caused by AP3B1-derived polypeptides, the membrane-binding function of M protein was monitored. Detergent-free lysates were prepared from 293T cells transfected to express Nipah virus M protein together with various AP3B1-derived polypeptides, and membrane-binding of M protein was assessed using sucrose flotation gradients (Fig. 3-5). 50-60% of M protein was found in the membrane-bound (floated) fraction of the gradient when M was expressed alone, and this did not change significantly upon co-expression of either full-length AP3B1 or the AP3B1 Head polypeptide. However, co-expression of AP3B1 Hinge polypeptide reduced the fraction of membrane-bound M protein to less than 20% (Fig. 3-5). This result suggests a mechanism for inhibition in which M protein that is bound to AP3B1-derived polypeptides is subsequently unable to interact with cellular membranes as it normally would.

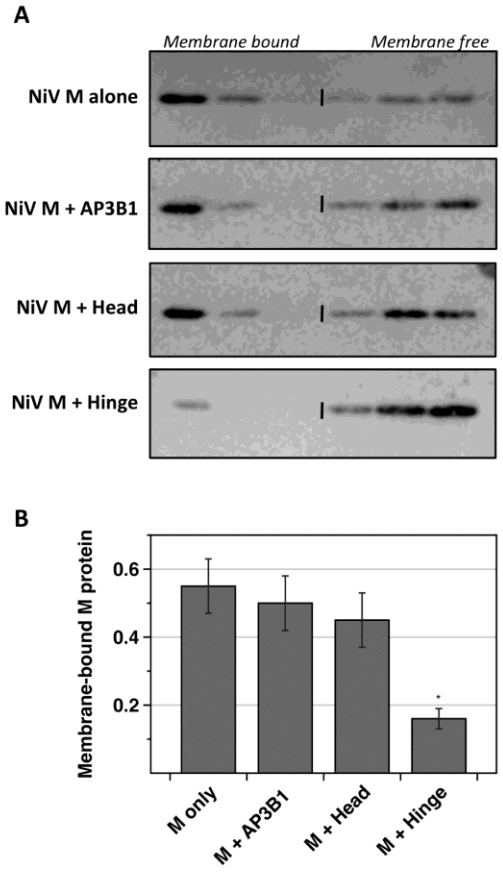

Figure 3-5. AP3B1 Hinge polypeptide inhibits the membrane-binding ability of Nipah virus M protein. (A) 293T cells were transfected to produce Nipah virus M protein together with the indicated human AP3B1-derived polypeptides. Detergent-free cell lysates were prepared and overlaid with sucrose solutions to form flotation gradients. After ultracentrifugation, samples were collected from the tops of the gradients. Proteins from gradient fractions were resolved by SDS-PAGE, and NiV M protein was detected by immunoblotting using M-specific polyclonal antibody. **(B)** Three independent experiments were performed as described in Panel A. The percentage of M protein that was membrane-bound (top three fractions of the gradients) was quantified using a phosphorimager. Results were plotted, with standard deviations indicated as error bars. Differences from the values obtained in the presence of the control siRNA were assessed for statistical significance by using a two-tailed Student *t* test, and *P* values of <0.01 are denoted by asterisks.

Depletion of AP3B1 from cells impairs Nipah VLP production

To investigate the importance of AP-3 complexes for Nipah virus M protein function and particle assembly, siRNAs were used to deplete AP3B1 protein from 293T cells. The efficiency of AP3B1 depletion was monitored in western blot experiments (Fig. 3-6A, B). The quantity of endogenous AP3B1 was reduced to approximately 30% of its normal level in cells transfected with AP3B1-specific siRNAs. To measure the effect of AP3B1 depletion on Nipah VLP production, cells were simultaneously transfected with M-expressing plasmid and siRNA (Fig. 3-6C, D). VLP production was reduced 3-fold in AP3B1-depleted cells, relative to cells that had been transfected with a control siRNA. These results suggest that the ability of Nipah virus M protein to efficiently direct virus-like particle formation is dependent upon the presence of physiological levels of AP3B1 within host cells.

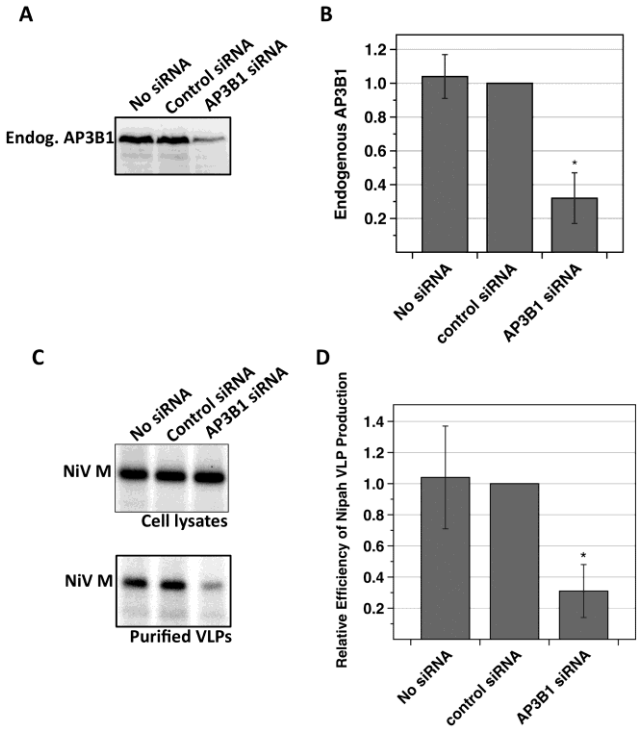

Figure 3-6. siRNA knockdown of endogenous human AP3B1 decreases Nipah VLP production. 293T cells were transfected with plasmid encoding Nipah virus M protein together with 100 nM siRNA as indicated. **(A and B)** Endogenous AP3B1 was detected by immunoblotting using AP3B1-specific antibody, and protein bands were quantified using a laser scanner. Results from three independent experiments were plotted, with standard deviations indicated as error bars. **(C and D)** Nipah VLPs were purified and detected as described in the legend to Fig. 4. Results from three independent experiments were plotted, with standard deviations indicated by error bars. Differences from the values obtained in the presence of the control siRNA were assessed for statistical significance by using a two-tailed Student *t* test, and *P* values of <0.01 are denoted by asterisks.

Partial co-localization of Nipah virus M protein with endogenous AP3B1 in transfected cells

Further evidence for biological relevance of M protein interaction with AP3B1 was obtained by monitoring colocalization of these proteins in cells (Fig. 3-7). 293T cells were transfected to produce Nipah virus M protein, and colocalization between M protein and endogenous AP3B1 was observed by fluorescence microscopy. M protein was found mainly at the plasma membrane and in the cytoplasm (Fig. 3-7), and a smaller amount of M protein was often detected in the cell nucleus, consistent with previous observations (42, 210). The cytoplasmic M protein formed numerous small clusters, and many of these clusters exhibited substantial colocalization with endogenous AP3B1, indicating that a portion of M protein localizes to AP-3 trafficking compartments. It should be noted that this AP3B1-colocalized fraction of M protein represents a minority of the total M protein in the cell, as some of the cytoplasmic M protein and virtually all of the plasma-membrane associated M protein are not AP3B1-colocalized. These observations are consistent with the possibility that M protein associates transiently with AP3B1-positive cellular compartments during its trafficking to the sites of virus assembly.

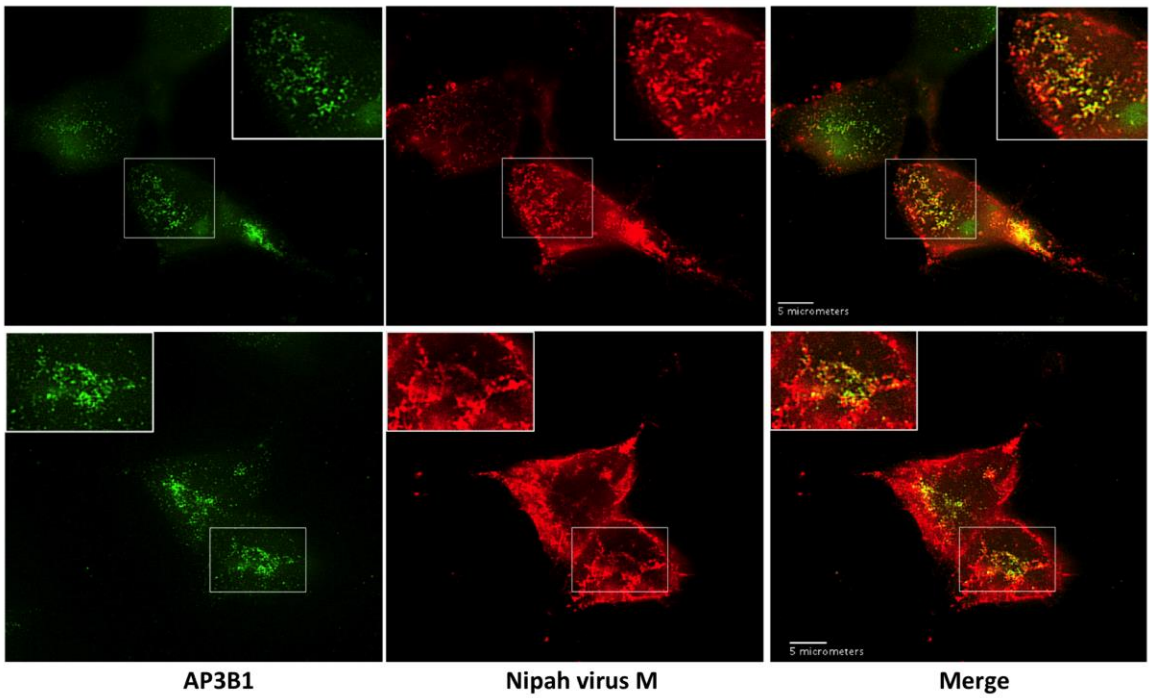

Figure 3-7. Partial colocalization of Nipah virus M protein with endogenous AP3B1 in 293T cells. 293T cells on glass coverslips were transfected to produce Flag-tagged Nipah virus M protein, and subcellular localizations of M protein (red) and endogenous AP3B1 (green) were visualized by immunofluorescence microscopy at 24 h post-transfection. Two representative sets of images are shown in the top and bottom panels. Representative of *n=3* shown.

3.3 Discussion

Here, we have used a co-affinity purification approach to identify the Beta subunit of the AP-3 adapter protein complex as a binding partner for the Nipah and Hendra virus M proteins. M protein binding was mapped to the serine-rich and acidic Hinge domain of AP3B1, and a 29 amino acid-long polypeptide derived from the Hinge domain was found to be sufficient for M protein binding. Expression of AP3B1-derived, M-binding polypeptides prevented M protein association with cellular membranes and inhibited the budding of Nipah and Hendra VLPs, suggesting that the M protein: AP3B1 binding interface could prove useful as a target in future efforts to inhibit these viruses using small molecules. Significant colocalization between M protein and AP3B1 was observed in transfected mammalian cells, and siRNA-mediated depletion of AP3B1 impaired the production of Nipah VLPs, suggesting that the presence of functioning AP-3 complexes benefits the assembly and release of henipavirus particles.

AP-3 adapter protein complexes in mammalian cells direct the trafficking of membrane proteins from tubular sorting endosomes to late endosomes and lysosomes (51, 157, 172). A role for AP-3 complexes in enveloped virus assembly and release has already been well established in the case of HIV-1. HIV-1 Gag protein was shown to interact with the Delta subunit of AP-3(58), and siRNA-mediated depletion of AP-3 complexes impaired the assembly and release of HIV-1 particles (58). HIV-1 particle assembly was also impaired in cells derived from human patients with AP-3 deficiency, caused by mutations to AP3B1 (114). An N-

terminal fragment of the AP-3 Delta subunit (AP-3D-5') was sufficient for binding to HIV-1 Gag, and this polypeptide could inhibit HIV-1 particle release and interfere with Gag protein trafficking to multivesicular bodies (58). Although interaction with AP-3 appears to be mediated through the MA component of Gag protein, as judged by GST pulldown assays (58), the molecular details of this interaction are not completely understood and evidence for direct binding between MA and the protein interactive domain of the AP-3 Delta subunit in vitro using NMR could not be obtained (107).

AP-3 interaction with henipavirus M proteins was mapped to the acidic, serine-rich Hinge domain of the AP-3 Beta subunit, AP3B1. Interestingly, this AP3B1 Hinge region has been studied previously in the context of two different cellular binding partners: kinesin family member 3A (Kif3A) (7), and rabip4' (93). The interaction between AP3B1 and Kif3A was identified in a yeast two-hybrid screen, using a Hinge-containing fragment of AP3B1 as bait (7). Here, the serine-rich Hinge region of AP3B1 had been characterized as a target for IP7-directed pyrophosphorylation, and the yeast two-hybrid investigation was carried out to determine if the pyrophosphorylation modification might impact protein-protein interactions. The screen identified Kif3A protein, and the Kif3A-AP3B1 interaction was confirmed in pulldown experiments (7). The interaction was found to be negatively regulated by AP3B1 pyrophosphorylation. In addition, the interaction was found to be important for HIV-1 particle release, as release of HIV-1 Gag VLPs could be inhibited either through siRNA depletion of Kif3A, or by expression of a motorless Kif3A polypeptide

that binds AP3B1 and presumably acts as a competitive inhibitor to block AP3B1 interaction with full-length, endogenous Kif3A (7). In a separate study, binding partners for the endosomal protein rabip4' were isolated using an affinity pulldown procedure followed by mass spectrometry, and this identified an interaction between rabip4' and AP3B1 (93). Mapping studies showed that the Hinge domain of AP3B1 bound to the FYVE domain of rabip4', and knockdown studies suggested that AP-3:rabip4' complexes are likely important for proper control of lysosome distribution within cells (93). Taken together with our results obtained with the henipavirus M proteins, these studies suggest that the AP3B1 Hinge domain is capable of directing protein interactions with a variety of partners. It will be important in future studies to determine whether these different viral and cellular proteins can bind simultaneously to AP3B1, or if instead these proteins compete with one another for binding to the same site within the Hinge domain.

AP3B1-derived polypeptides were potent inhibitors of Nipah and Hendra VLP production. The shortest of these fragments, Hinge1B, caused ten-fold reduction in VLP production yet is only 29 amino acid residues in length. Consistent with these results, earlier studies have found that short polypeptides derived from various host proteins that bind to viral Gag or M proteins are often potent inhibitors of virus budding. For example, expression of a Gag-binding fragment of Tsg101 (TSG-5') caused a 60% reduction in HIV-1 particle production (56, 66), and expression of a Gag-binding fragment of Aip1/Alix caused a 5-fold reduction of HIV-1 particle production (38, 67, 122, 130). Likewise, budding of the paramyxovirus PIV5 was

reduced by more than 3-fold upon expression of an M-binding polypeptide derived from the host protein AmotL1 (159). These findings support the overall concept that binding interfaces between host factors and budding-relevant viral proteins can be targeted for disruption as an effective antiviral approach (15, 23). In the cases of Aip1/Alix and AmotL1, even overexpression of the full-length host proteins caused moderate negative effects on viral particle production (38, 159), drawing a further parallel with the results described here, in which full-length AP3B1 overexpression reduced Nipah VLP production to approximately 35% of its normal level. In this case, it is likely that the imbalance in AP-3 complex components caused by AP3B1 overexpression leads to some of the M protein binding to free AP3B1 that has not interacted with the other AP-3 components to form a functioning complex. Interestingly, although full-length AP3B1 overexpression moderately reduced VLP production, it did not have any noticeable effect on M protein membrane binding. Expression of AP3B1 Hinge polypeptide, in contrast, caused a more severe impairment in VLP production, along with significant impairment of M protein membrane binding. It is possible that Hinge and other AP3B1-derived polypeptides bind more strongly to M protein than full-length AP3B1 does and that the functional VLP assay is more sensitive at detecting these differences than the sucrose flotation-based membrane-binding assay. Another possibility is that the AP3B1-derived polypeptides and full-length AP3B1 could affect M protein in different ways, with the AP3B1-derived polypeptides disrupting the M protein conformation such that membrane-binding function is lost, while overexpressed full-length AP3B1 might

cause moderate levels of inhibition merely by occupying M protein binding sites and preventing fully formed AP-3 complexes from interacting at these sites. Overall, the inhibition of M protein function by both AP3B1-derived polypeptides and overexpressed full-length AP3B1 supports the general concept that binding interfaces between host factors and budding-relevant viral proteins can be targeted for disruption as an effective antiviral approach (66, 82). Indeed, small-molecule budding inhibitors have recently been identified that target the PTAP-Tsg101 interface in the case of HIV-1 (195, 207) or the PPxY-Nedd4 interface in the cases of Ebola virus, Marburg virus, Lassa virus, and rabies virus (78). Similar approaches that target the AP3B1-M binding interface may prove useful in the identification of new therapeutics for paramyxovirus infections.

CHAPTER 4

Trafficking and Assembly of Hendra Virus Glycoproteins with Matrix Protein

4.1 Introduction

The paramyxoviruses life cycle has to be initiated by the surface glycoproteins, the attachment protein and fusion protein. Henipavirus attachment protein is designated as G protein as it lacks both hemagglutinin and neuraminidase activities. Henipavirus G protein is required for binding protein receptor ephrin-B2/3 on cell surface (21, 137, 138). It has a receptor-binding ‘‘head’’ domain connected to its transmembrane anchor via a ‘‘stalk’’ domain, as well as a short cytoplasmic tail (Fig. 4-1A). Henipavirus F protein is mainly responsible for mediating membrane fusion for the purpose of virus entry. Fusogenic F protein consists of a disulfide linked F_1 -F_2 complex. Within F_1, there is a fusion peptide located just C-terminal to the cleavage site of a precursor form of the protein. This is followed by two heptad repeat domains, a transmembrane (TM) domain and a cytoplasmic tail (CT) (Fig. 4-1B). Like other F proteins of paramyxoviruses, HeV F protein is synthesized as an inactive precursor (F_0) in ER, which is subsequently cleaved into disulfide linked F_1-F_2 complex by cellular protease (129). Cleavage of F_0 is thought to play an important role that influences both infectivity and pathogenicity of paramyxoviruses. In terms of proteolytic cleavage, the type I viral glycoproteins fall into two groups—those with a

single basic residue cleavage site and those with multiple basic residues at the cleavage site. In general, viral glycoproteins containing a single basic cleavage site have restricted cleavability and they are usually activated by exogenous protease (101). For example SeV replicates poorly in tissue culture; however, after addition of exogenous protease, infectivity significantly increased (100) (Table 4-1A). On the other hand, viral glycoproteins that have multibasic cleavage sites containing a consensus sequence R-X-K/R-R have higher cleavability. They are usually activated during transport through the trans-Golgi network by endoprotease, most commonly, a substilisin-like serine protease called furin (136) (Table 4-1B). Interestingly, although HeV F has a single basic residue cleavage site, it does not require exogenous protease for cleavage. Instead, it is cleaved intracellularly. The protease responsible for cleavage is not furin, as inhibitors against furin such as EGTA and A23187 could prevent cleavage of PIV5 F but not HeV F protein (125, 148). To determine the protease that cleaves HeV F protein, inhibitors against a variety of proteases were tested. Only inhibitors against an endosomal protease called cathespin L, such as E-64d, could block processing of HeV F protein, but not PIV5 F protein (148). This demonstrated that unlike other paramyxovirus F proteins, HeV F protein was cleaved by the cellular endosomal protease, cathepsin L.

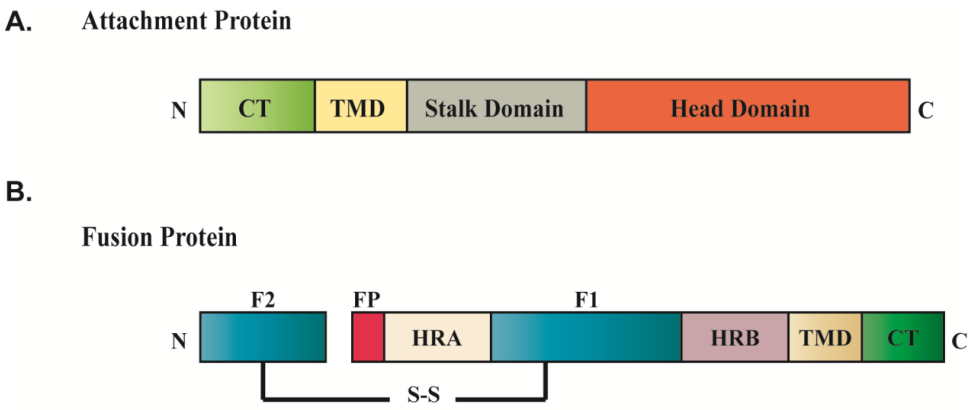

Figure 4-1. Schematic illustration of paramyxovirus glycoproteins domain structures. (A) Domain structure of paramyxovirus attachment protein. **(B)** Domain structure of paramyxovirus fusion protein. Abbreviations: fusion peptide (FP); heptad repeat region (HRA, HRB); transmembrane domain (TMD); cytoplasmic tail (CT); disulfide bond (S-S). This figure was adapted from (62).

A

Virus	Glycoprotein	Cleavage site	Ref.
Orthomyxoviridae			
A/WSN/33 (H1)	HA	PSIQY**R**GL	6
A/Japan/305/57 (H2)	HA	PQIES**R**GL	7
A/Memphis/102/72 (H3)	HA	PEKQT**R**GL	8
B/Lee/40	HA	KLLKE**R**GF	9
C/JHB/1/66	HEF	TKPKS**R**IF	10
Paramyxoviridae			
Sendai virus	F	GAPQS**R**FF	11
Newcastle disease virus La Sota	F	GGRQS**R**FI	12
Newcastle disease virus Ulster	F	GGKQS**R**LI	12

B

Virus	Glycoprotein	Cleavage site	Ref.
Orthomyxoviridae			
A/fowl plague virus/Rostock/34 (H7)	HA	KK**R**E**KR**GL	13
A/Tern/SA/61 (H5)	HA	TR**RQKR**GL	14
Paramyxoviridae			
Newcastle disease virus Miyadera	F	GR**RQRR**FI	12
Human parainfluenza virus 3	F	DP**R**T**KR**FF	15
Mumps virus	F	SR**R**H**KR**FA	16
Measles virus	F	SR**R**H**KR**FA	17
Simian virus 5	F	TR**RRRR**FA	18
Respiratory syncytial virus	F	KK**R**K**RR**FL	19
Flaviviridae			
Yellow fever virus	M	SG**R**S**RR**SV	20
Togaviridae			
Sindbis virus	E2	SG**R**S**KR**SV	21
Coronaviridae			
Infectious bronchitis virus	E2	TR**R**F**RR**SI	22
Retroviridae			
HIV-1	env	VQ**R**E**KR**AV	23
Rous sarcoma virus	env	GI**R**R**KR**SV	24
Herpesviridae			
Human cytomegalovirus	gB	TH**R**T**RR**ST	25
Varicella–zoster virus	gB	NT**R**S**RR**SV	26
Epstein–Barr virus	gB	LR**RRRR**DA	27

Table 4-1. Proteolytic cleavages sites of viral type I glycoproteins. (A) Monobasic cleavage sites of viral glycoproteins with restricted cleavability **(B)** The consensus sequence R-X-K/R-R at the multibasic cleavage sites of viral glycoproteins with high cleavability. These tables were adapted from (101).

Based on this discovery, unique trafficking of Hendra virus fusion protein was subsequently characterized shown in Fig. 4-2A (165). Cathepsin L is primarily thought to locate in late endosome or lysosomes. In order to determine what compartments must be reached to facilitate cathepsin L cleavage, cell surface expression and cleavage of HeV F in the presence of the DN Rab5 which inhibits early endosomal fusion, or the DN Rab7 which inhibits late endosomal fusion were examined. It was found that expression of DN Rab5 significantly reduced F protein processing while Rab7 did not have such effects, indicating that trafficking to early endosomes is important to F cleavage whereas trafficking to late endosomes is not necessary for F processing (165). It was also found that overexpression of DN Rab5 significantly delayed F processing (Fig 4-2B). Furthermore, F has been found to co-localize with GFP-Rab4 and GFP-Rab5 but not GFP-Rab7. Since F internalization could be finished within 30mins (124), an antibody capture assay was developed to dissect each stage of F protein endocytosis and recycling (165). This study suggested that F protein reached the Rab5-EEs right after it was endocytosed and colocalized with Rab4 positive endosomes mainly after proteolytic cleavage as they returned back to the plasma membrane (Fig. 4-2A).

Above-mentioned studies demonstrated a unique trafficking pathway of HeV F protein, where the precursor F_0 protein is initially trafficked to the plasma membrane in its uncleaved form through the secretory pathway. F_0 protein is subsequently internalized through endocytosis and enters Rab5 positive early endosomes. Then F_0 is proteolytically processed by endosomal protease cathepsin L

into disulfide-linked F_1 and F_2. At last, fusion active F protein returns back to the plasma membrane through Rab4 positive vesicular membrane compartments (Fig. 4-2A).

A

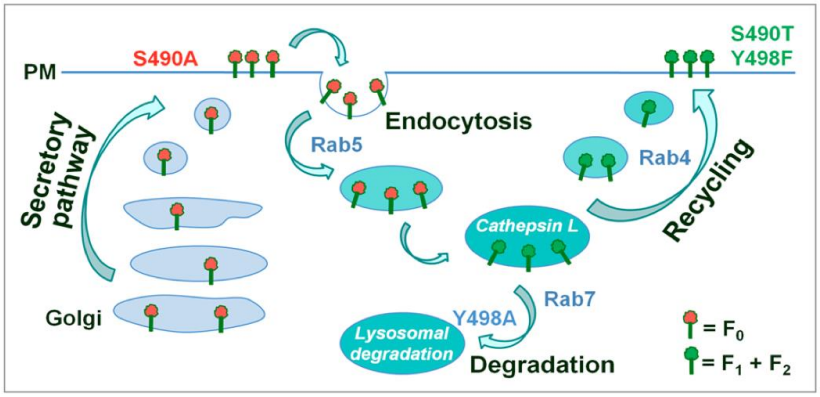

B

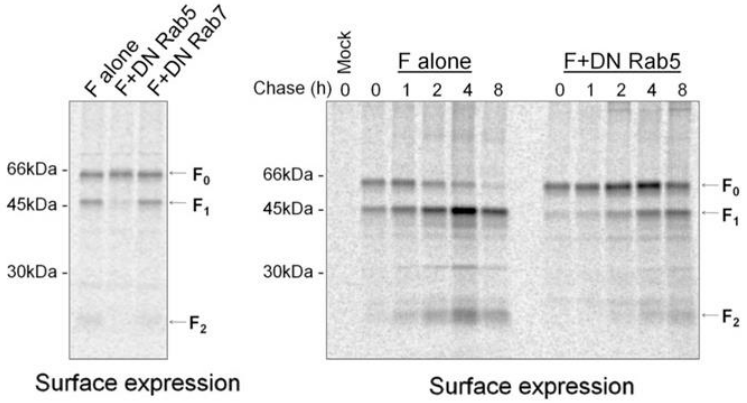

Figure 4-2. Unique trafficking pathway of Hendra virus F protein. (A) Model of Hendra virus F protein trafficking and proteolytic processing. Uncleaved F protein is sorted to PM through secretory pathway, after which it is endocytosed into EEs where it is cleaved into F1 + F2. Processed F is then returned back to PM. (**B)** Hendra virus F proteolytic cleavage requires delivery to the early endosomes but not the late endosomes. Expression of a DN Rab5 significantly slows the kinetics of Hendra virus F cleavage. This figure was adapted from (165).

The assembly of paramyxovirus M protein with glycoproteins is thought to be mediated through interactions between M proteins with cytoplasmic tails of glycoprotein (4, 13, 65, 117, 150, 180). However, details within this process remain largely unknown, including those for henipaviruses. Here, we hypothesized that HeV M and F proteins traffic to Rab11-REs separately, with M trafficking faciliated by AP-3 complex. Then M and cathepsin-cleaved biologically active F protein assemble together within these compartment prior to their delivery to the cell surface for particles budding. This hypothesis is supported by the evidence we obtained that M and F protein partially localized to Rab11-REs, and a lack of M protein in Rab11-REs was observed in the presence of inhibitory Hinge domain of AP3B1. Moreover, we demonstrated that endocytic trafficking of F protein is necessary for proper assembly of F into M-containing VLPs. On the other hand, we showed that M protein mediates G recruitment into M-VLPs, which is supported by colocalization of G with M protein at plasma membrane in transfected cells.

4.2 Results

M trafficking to Rab11a recycling endosomes is important for Hendra M-VLPs production

In chapter 3, we have shown that henipavirus M protein binds host protein AP3B1, a subunit of adaptor protein complex 3. In transfected 293T cells, M protein is also found to colocalize with endogenous AP3B1, which suggested a biologically relevant role of AP-3 complex in M protein functions. However, the biological function of AP-

3 in M protein trafficking is still unclear. To gather more insights on M protein trafficking, we also looked at M localization relative to other protein markers representing different cellular compartments, such as trans-Golgi marker TGN46, cis-Golgi marker GM130, late endosome/lysosome marker LAMP-1, early endosome marker EEA1, ER marker E-Cadherin and recycling endosome marker Rab11a. Here, Vero cells were transfected to produce Hendra virus M protein, endogenous protein markers mentioned above were detected using corresponding antibodies. Co-localization between a portion of M protein and endogenous Rab11a is observed by fluorescence microscopy, where endogenous Rab11a was mainly found in peri-nuclear compartments, and small portion of M protein was detected to overlap with Rab11a in large peri-nuclear compartments (Fig. 4-3A). No other colocalization was detected between M and other protein markers (data not shown). This observation indicated M proteins likely trafficked to Rab11-REs.

We know that M protein likely traffics through AP-3 positive vesicles based on our earlier immunofluorescence microscopy results in chapter 3. So we wondered if trafficking to AP-3 positive vesicles was required for M trafficking to Rab11-REs. Our strategy was to overexpress M-binding inhibitory polypeptide derived from AP3B1 in order to out-compete M interaction from endogenous AP3B1. Here, Vero cells were transfected to co-express Hendra virus M protein together with the Hinge domain of AP3B1. M localization relative to endogenous Rab11a was evaluated again by immunofluorescence microscopy. M proteins in the cells were found to be re-distributed into a more diffused pattern throughout the cytoplasm upon co-

expression of inhibitory Hinge domain. Importantly, when Hinge was present, M protein no longer was found in the Rab11-REs (Fig. 4-3B). This observation is consistent with the possibility that AP-3 complex is necessary for trafficking of M protein to REs.

We know that overexpression of a DN Rab11a (S25N), which is preferentially GDP bound, would inhibit protein cargos, such as transferrin, recycling from the later recycling endosome to the cell surface (171, 198). To gather more insights on the role of Rab11 in M protein function, we examined Hendra M-VLPs production in the presence of either wt GFP-Rab11a or DN GFP-Rab11a. HEK293T cells were transfected to produce Myc-tagged Hendra virus M protein alone, or together with wild type Rab11a or DN Rab11a. After replacing media, VLPs were collected from the culture supernatants and pelleted through sucrose cushion. Proteins were resolved on SDS gel and detected by western blot using mouse anti-Myc mAb and rabbit anti-Rab11a pAb. The result showed that overexpression of DN Rab11 significantly reduced Hendra M-VLPs production (Fig. 4-3C). This suggests an important role for Rab11-REs in Hendra VLP production.

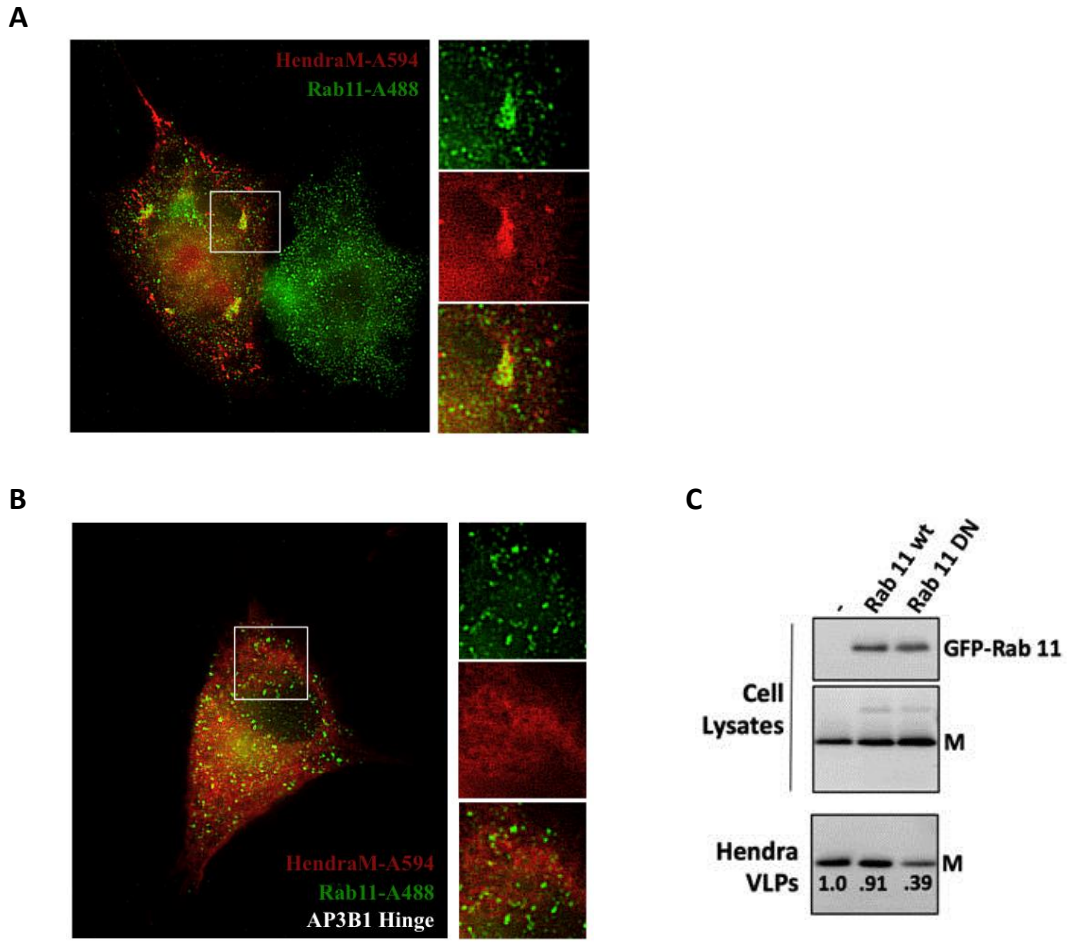

Figure 4-3. Hendra virus M protein trafficking to Rab11a-REs is necessary for M-VLPs production. (A) Vero cells on glass coverslips were transfected to produce Myc-tagged Hendra virus M protein, and subcellular localization of M protein (red) and endogenous Rab11a protein (green) were visualized by immunofluorescence microscopy at 24 h posttransfections. Representative of *n=3* shown.**(B)** Flag-tagged Hinge domain derived from AP3B1 was co-expressed with Myc-tagged Hendra virus M protein in transfected Vero cells, M protein and endogenous Rab11a were visualized as described in (A). Representative of *n=3* shown. **(C)** HEK293T cells were transfected to produce Myc-tagged Hendra virus M protein alone, M protein together with wild type GFP-Rab11a or with a DN GFP-Rab11a. After replacing media with DMEM containing 2% FBS, cell lysates were prepared. VLPs from cell culture supernatants were purified by centrifugation through sucrose cushions. Lysed cell lysates and purified VLPs were loaded directly onto 10% SDS-PAGE, and proteins were detected by western blot using a mouse anti-Myc mAb, and a rabbit anti-Rab11a pAb, and proteins were visualized by a phosphorimager. Representative of *n=3* shown.

F trafficking to Rab11a recycling endosomes is important for Hendra F-VLPs production

Our earlier data show that M protein is likely trafficking through Rab11 positive recycling endosomes, and this suggested a possible scenario in which coordination with the glycoprotein F could occur during virus assembly due to the unique trafficking pathway of Hendra virus F proteins as described earlier. Under the model that has been described for Hendra virus F trafficking (Fig. 4-2A), it is likely that F protein would be returned to the surface by recycling endosomes, however F protein localization with Rab11 had not been formally tested. So here we examined Hendra virus F protein localization relative to GFP-Rab11a in transfected Vero cells by immunofluorescence microscopy. We found F protein could in fact localize to Rab11-positive recycling endosomes in Vero cells producing Hendra virus F protein and GFP-Rab11a (Fig. 4-4A). Additionally, we also performed budding assay to test F release into particles in the presence of wt Rab11a or DN Rab11a. HEK293T cells were transfected to express F alone, F together with wt GFP-Rab11a or F together with DN GFP-Rab11a. Cell lysates and VLPs were prepared as described earlier, and proteins were resolved on SDS gel and detected by western blot using mouse anti-HeV F pAb and rabbit anti-Rab11a pAb. We found, similarly to M protein, F protein release into particles was also inhibited when DN Rab11a is expressed (Fig. 4-4C). Based on this result, we hypothesized that the viral M and F proteins independently traffic to Rab11 recycling endosomes, where they assemble and then transport together to the cell surface. Interestingly, we also found that a portion of G proteins

localized to enlarged GFP-Rab11 containing compartments (Fig. 4-4B). It is unclear at this point what is the putative role of Rab11-REs in G protein trafficking and assembly, but it is consistent with the possibility that Rab11 recycling endosomes might serve as a key platform for assembly of Hendra virus M protein with both of its glycoproteins.

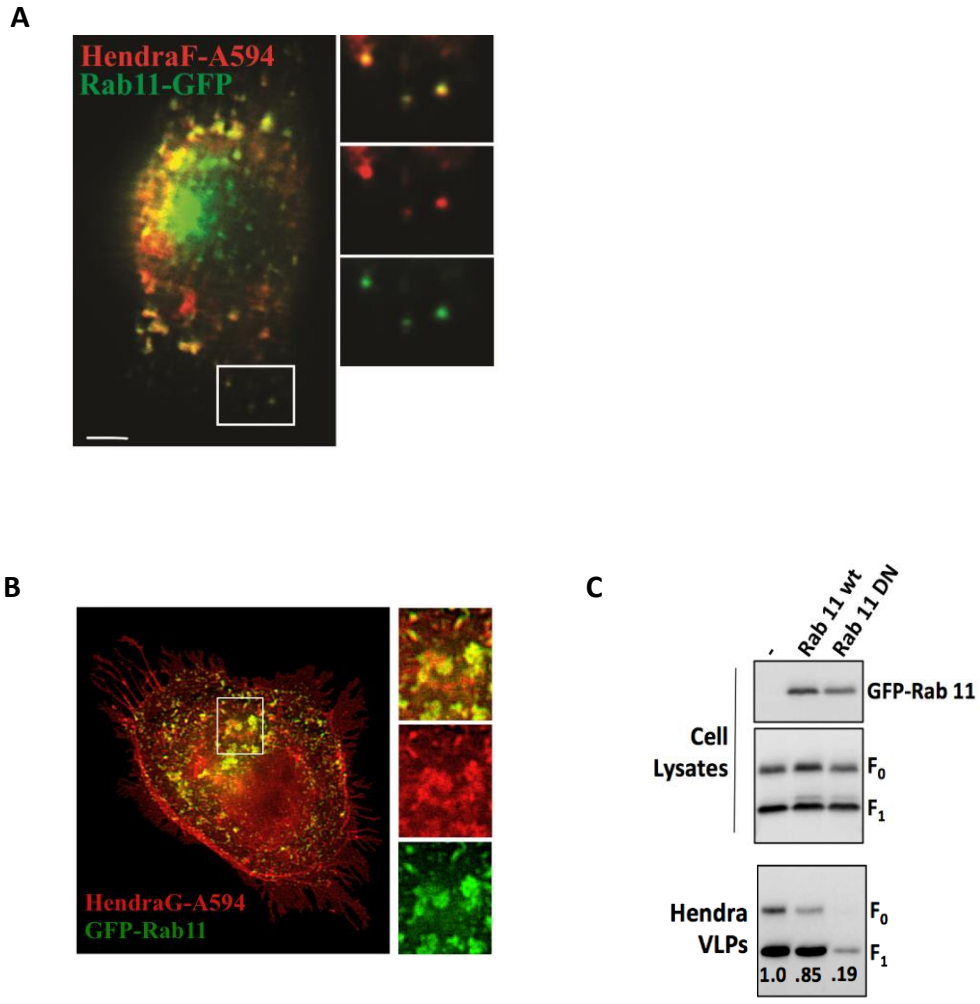

Figure 4-4. Rab11-REs co-localize with Hendra virus glycoproteins and are necessary for F-VLPs production. Vero cells on glass coverslips were transfected to produce **(A)** Hendra virus F protein together with GFP-Rab11a or **(B)** Hendra virus G protein together with GFP-Rab11a.The subcellular localization of F protein or G protein (red) and GFP-Rab11a protein (green) were visualized by immunofluorescence microscopy at 24 h posttransfections. Representative of *n=3* shown. **(C)** HEK293T cells were transfected to produce Hendra virus F protein alone, F protein together with wild type GFP-Rab11a or F protein together with DN GFP-Rab11a. After replacing media with DMEM containing 2% FBS, cell lysates were prepared. VLPs from cell culture supernatants were purified by centrifugation through sucrose cushions. Lysed cell lysates and purified VLPs were loaded directly onto 10% SDS-PAGE, and proteins were detected by western blot using rabbit anti-HeV F pAb, and rabbit anti-Rab11a pAb. Proteins were visualized by a phosphorimager. Representative of *n=3* shown.

Endocytic trafficking of Hendra virus F protein is required for assembly into M-VLPs

In order to fully characterize Hendra virus F protein trafficking, the Dutch group has constructed a series of F mutants that are defective at various stages of F trafficking. The mutant F proteins harboring mutations in their TM domains or cytoplasmic tails are defective in either endocytosis or recycling to various degrees. For example, some mutants are significantly defective in endocytosis such as HeV F S490A, which is retained as uncleaved F on the cell surface (165) (Fig. 4-2A); some mutants are only defective at the stage of recycling, such as HeV F Y498A and F S490V (165) (Fig. 4-2A). Others showed minor or no defects in both trafficking events. In order to determine if endocytosis of F is required for F release into particles, we looked at F S490A incorporation into M-VLPs compared to wild type F protein. Here, 293T cells were transfected to produce Myc-tagged Hendra virus M protein together with either wt F protein or mutant F S490A, VLPs were purified and proteins were detected as described earlier. We found that the mutant F protein was uncleaved, and significantly defective for incorporation into M-VLPs (Fig. 4-5A). As F490A did not undergo either endocytosis or proteolytic cleavage, there is one possibility that cleavage of F protein is required for its incorporation into M-VLPs, while the second possibility is that the whole process of endocytosis and recycling is required for F incorporation into M-VLPs. To distinguish between them, we prevented F cleavage using a cathepsin L inhibitor, E64-d, which did not have any effects on F endocytosis and recycling. The VLP result showed that E-64d (10 uM) treated wt F incorporated perfectly well into M-VLPs even though it is in the

uncleaved state (Fig. 4-5A). This observation provided strong evidence to demonstrate that it is the endocytic trafficking of F protein and not its proteolytic cleavage that is required for F incorporation into M-VLPs.

To further assure that F and M protein assemble into the same virus-like particles, a sucrose gradient fractionation was performed where 293T cells were transfected to produce Hendra virus M protein, F protein or M together with F protein. VLPs were pelleted through sucrose cushion, and separated through sedimentation on continuous sucrose gradients. We found M-VLPs were mainly recovered in fraction 7-10 with a peak in 8. Differently, F-VLPs were mainly found in fraction 10-12. However, when M and F proteins were co-expressed in the cells, both M and F proteins showed a shift of fractionation profile with a more concentration of both proteins in fraction 8-11 with a peak in fraction 9, suggesting they were packed into the same VLPs. Consistently, treatment of E-64d did not change the fractionation profile of M, F or M with F together (Fig. 4-5B). This reinforces our early observation that Hendra virus M and F assembly required F protein endocytosis trafficking instead of proteolytic cleavage.

A

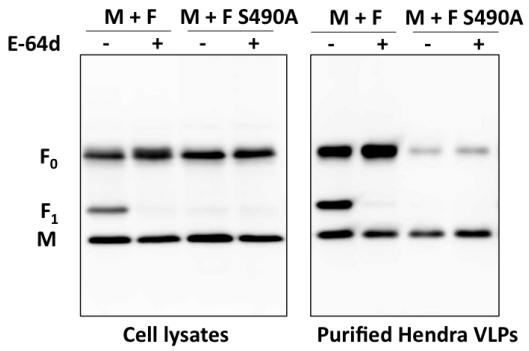

B

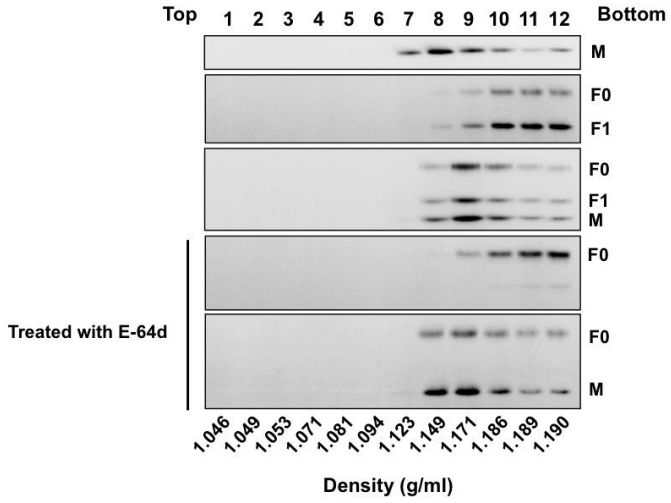

Figure 4-5. Endocytosis but not proteolytic processing of F protein is required for Hendra virus M and F proteins assembly into the same particles. (A) HEK293T cells were transfected to produce Myc-tagged Hendra virus M protein together with wild type Hendra virus F protein or with mutant F S490A in the absence or presence of cathepsin L inhibitor E-64d. Cell lysates were prepared and VLPs were purified through sucrose cushion as described earlier. Proteins were detected by western blot using a mouse anti-Myc mAb and a rabbit anti-HeV F pAb. Representative of *n=3* shown. **(B)** Hendra M-VLPs, F-VLPs and M/F-VLPs produced with or without treatment of E-64d were prepared as describe in (A), and loaded on top of 5%-45% continuous sucrose gradients for a subsequent ultracentrifugation in a Sovrall AH650 swinging bucket rotor for 16 h at 4C. 12 fractions were collected, 1/20 of each fraction was resolved on 10% SDS-PAGE. Proteins were detected by western blot using a mouse anti-Myc mAb and a rabbit anti-HeV F pAb. All proteins were visualized by a phosphoimager.

Evidence for M-mediated recruitment of HeV G into VLPs

Authentic Hendra virions are densely packed with both glycoproteins, F and G. Expression of G by itself in cells do not result in significant release of VLPs (152). This is in contrast to the F and M proteins, each of which is capable of driving efficient VLP release when expressed alone. Presumably, G is recruited into the budding particles by F and/or M. To determine which of these two proteins is responsible for G recruitment into VLPs, we performed budding assay to examine G incorporation into M or F VLPs. HEK293T cells were transfected to express G alone, G together with M protein, or G together with F protein. VLPs were purified and proteins were analyzed on SDS gel by western blot. The result showed that G protein was not released into supernatant very well when expressed alone (Fig. 4-6). When F protein was co-expressed with G protein, G incorporation into F-VLP was still poor, even though G protein was thought to associate with F protein at the plasma membrane (214). However, co-expression of M significantly increased G protein incorporation into M-VLPs (Fig. 4-6). This observation is consistent with the idea that M-G interactions, most likely involving the G cytoplasmic tail, drive the incorporation of G into budding particles.

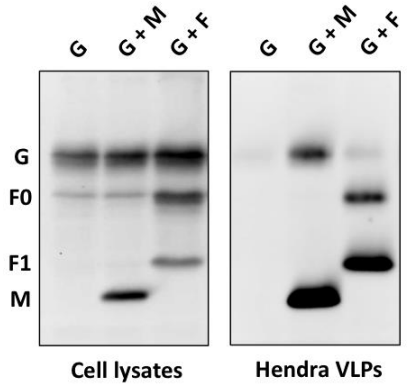

Figure 4-6. Hendra virus G protein incorporation into VLPs is enhanced by M protein instead of F protein. HEK293T cells were transfected to produce Hendra virus G protein alone, G protein together with Myc-tagged M protein or G protein together with F protein. After replacing media with DMEM containing 2% FBS, cell lysates were prepared. VLPs from cell culture supernatants were purified by centrifugation through sucrose cushions. Lysed cell lysates and purified VLPs were loaded directly onto 10% SDS-PAGE, and proteins were detected by western blot using a rabbit anti-HeV G pAb, a mouse anti-Myc and a rabbit anti-HeV F pAb. Proteins were visualized using a phosphorimager. Representative of *n=2* shown.

Hendra virus G protein colocalizes with M protein in transfected cells

We observed that Hendra virus G protein could incorporate into M-VLPs but not F-VLPs. We next performed immunofluorescence microscopy, where Vero cells were transfected to express Hendra virus M and G proteins together. 24 h p.t., cells were fixed and stained with rabbit anti-HeV G pAb and mouse anti-Myc mAb to detect G and M respectively. We found that a portion of G protein could colocalize with M protein in filamentous structures on the plasma membrane (Fig. 4-7), which indicated that G and M interaction might occur at the plasma membrane during assembly. We have also examined HeV F and M proteins in transfected cells by immunofluorescence microscopy, we did not observed significant colocalization between F and M proteins (data not shown). It may be that F and M protein interaction is transient and difficult to detect using our current methods. Taken together, our data suggests that M and G proteins assemble together in a coordinated way at the plasma membrane prior to particle budding.

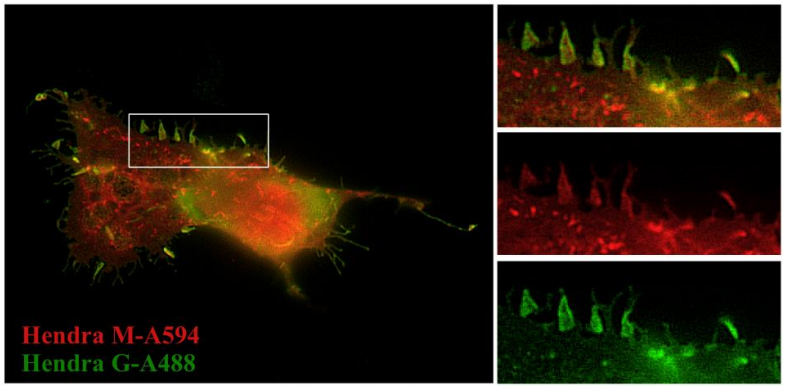

Figure 4-7. Colocalization of Hendra virus G protein with M protein in transfected Vero cells. Vero cells seeded on glass coverslips were transfected to produce Flag-tagged Hendra virus M protein and Hendra virus G protein. Subcellular localization of M protein (red) and G protein (green) were visualized by immunofluorescence microscopy at 24 h posttransfections. Representative of *n=3* shown.

4.3 Discussion

Here, we studied HeV M protein assembly with glycoproteins. We used immunofluorescence microscopy to observe partial localization of HeV M, G and F in Rab11-REs. Overexpression of DN Rab11 significantly reduced production of both M-VLPs and F-VLPs, suggesting Rab11-REs are likely important for Hendra virus assembly and budding. M-binding Hinge domain derived from AP3B1 was used to dissociate M protein from endogenous AP3B1. This resulted in an absence of M in Rab11-REs, indicating AP-3 likely facilitated M protein trafficking to Rab11-REs. By using an endocytosis defective HeV F mutant, S490A, we found that endocytic trafficking was required for F incorporation into M-VLPs. During this process, prevention of F cleavage did not negatively affect F incorporation, suggesting that coordinated assembly of F with M depends on F protein recycling. Additionally, we found HeV G incorporation into particles was significantly increased in the presence of M protein. Coexpression of F protein did not enhance G incorporation into F-VLPs. Consistent with this observation, G and M were found to partially colocalize at plasma membrane.

Based on these findings, we proposed an overall model for HeV M assembly with F in which HeV M and F proteins have separate mechanisms for trafficking to Rab11-REs, with the M protein trafficking facilitated by its interaction with AP3B1. Then M and cathepsin-cleaved fusogenic F proteins must assemble together within these compartments prior to their delivery to the cell surface for particle budding (Fig. 4-8). For many paramyxoviruses, M assembly with the glycoproteins most likely

occurs at the plasma membrane, where the glycoproteins are concentrated (14, 62, 181). It is also true for some other enveloped RNA virus, such as HIV-1 and influenza virus (34, 174). Our studies suggested that HeV M protein assemble with F protein in Rab11-REs instead of plasma membrane, which is quite unusual.

The incorporation of paramyxovirus glycoproteins into particles is thought to be mediated by interactions between their cytoplasmic tails with M protein. This is proved to be true for many paramyxoviruses, such as PIV5 and SeV, where truncation of HN and/or F protein cytoplasmic tail severely impaired particle assembly (4, 183). Our results with HeV G protein suggested an interaction between its cytoplasmic tail and M protein at the plasma membrane, as G incorporation into particles appeared to be mediated by M protein, and colocalization between G and M proteins was observed at the plasma membrane in transfected cells. We attempted to examine G and M interaction biochemically. However, no precipitation of G was detected with M by coimmunoprecipitation assay (data not shown). This may indicate any weak or transient interaction between M protein and cytoplasmic tails of G protein, which could not be detected by classical coimmunoprecipitation. Alternatively, the conformational of the relatively short G protein cytoplasmic tail (44 aa residues) could be changed upon solubilization of membrane with detergents in coimmunoprecipitation assays.

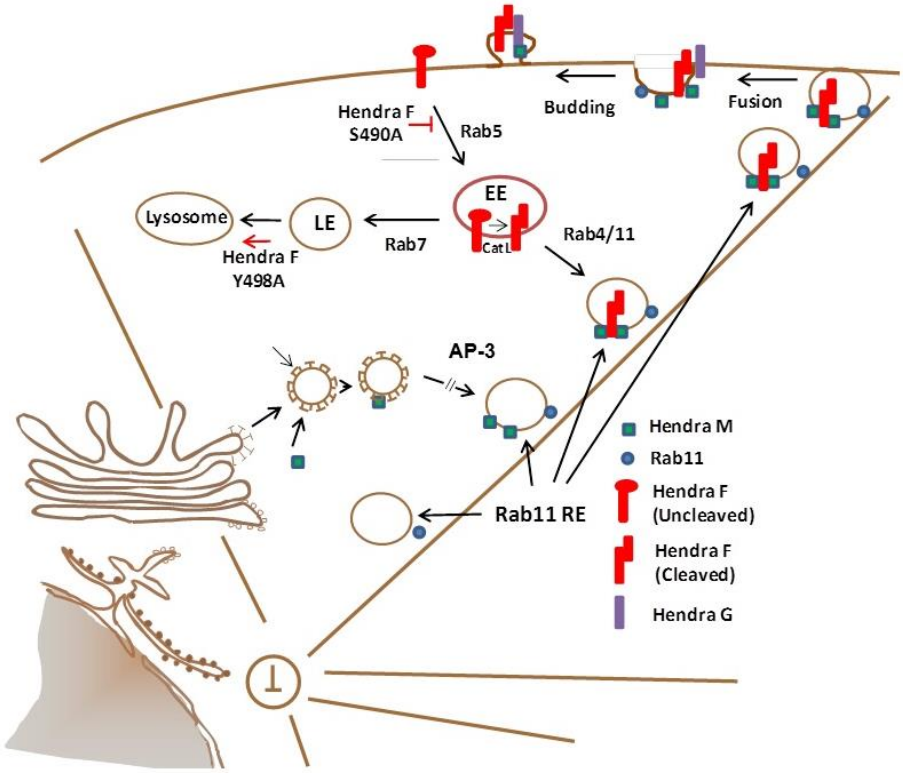

Figure 4-8. An overall model for Hendra virus M assembly with Hendra virus glycoproteins. Uncleaved Hendra virus F precursor F0 is transported to plasma membrane through secretory pathway, then F0 is internalized into the cells by endocytosis in Rab5-EEs and cleaved into disulfide linked F1+F2. It is subsequently sorted into Rab4/Rab11-REs. On the other hand, Hendra virus M protein traffics to Rab11-REs under the help of AP-3 complex. In Rab11-REs, Hendra virus fusogenic F1+F2 assemble with M protein and are returned back to the cell surface together, where Hendra virus G protein assemble into particles through its interaction with M protein.

Rab11a is a member of Rab11 small GTPase family, the other two members are Rab11b and Rab25. Rab11 GTPases was mainly found to execute functions in recycling endosomes shown as centralized peri-nuclear compartments (16). It is well established that Rab11 is involved in several cellular processes of intracellular vesicles trafficking including secretion of protein factors, targeting proteins to tubular structures and directing apical membrane trafficking in polarized cells (16). Interestingly, several negative-strand RNA viruses have been found to utilize Rab11 positive recycling endosome for trafficking of viral components and assembly. Examples include IAV, MeV and SeV, their vRNPs were found in Rab11 positive vesicles (6, 37, 135). In terms of virus assembly and budding, it was first observed with RSV that overexpression of a DN Rab11 effector, Rab11-FIP2, inhibited virus release (30). Furthermore, siRNA-depletion of Rab11 was found to negatively affect ANDV release (177). Taken together with our results obtained with Hendra virus M protein and glycoproteins, these studies suggest that Rab11 pathway could be hijacked by multiple components of negative-strand RNA viruses. It will be important to further determine the role of Rab11-REs in viral components of HeV, such as G protein. We know that HeV G protein trafficking to the plasma membrane is through the secretory pathway (213). We observed partial localization of G in Rab11-REs. One possibility is that during the G trafficking through secretory pathway, G trafficking route somehow intersects with Rab11 pathway and recycled back to the plasma membrane by REs, as Rab11 was detected in association with TGN and possibly be involved in transport from TGN to cell surface (200). As G protein is

found to traffic at a slower rate than F protein (214), this possibility suggested a scenario where G protein encounters the internalized and cleaved F protein in the recycling endosomes and traffic back together to the plasma membrane. Henipavirus G protein was found to be internalized in both infected and transfected cells during membrane turnover (205). Therefore, the other possibility for HeV G being found in the Rab11 REs is that similar to NiV G proteins, HeV G proteins are also endocytosed after they initially reach the cell surface. Then a portion of internalized G proteins are returned to the plasma membrane through Rab11 pathway. However, more investigations are needed to characterize the role of Rab11-REs in HeV G trafficking and assembly.

Overall, our studies on HeV M assembly with F or G proteins raise an interesting possibility that HeV F and G are recruited into particles through different mechanisms, in which F protein assembles with M protein in Rab11-REs and G assembles with M at the plasma membrane (Fig. 4-8). It will be important to determine how this assembly model benefits virus in general. Firstly, this is all due to the unique trafficking pathway of henipavirus F protein, in which extra endocytosis of F occurs. We speculate that this is likely for efficient production of infectious particles. We know that paramyxovirus virions need to incorporate cleaved fusogenic F protein to be infectious. HeV F endocytic trafficking and entering endosomes for cleavage provide a platform in Rab11-REs, where biologically active F proteins are enriched, and separated from the inactive uncleaved form of F proteins on the plasma membrane. Therefore, when F and M proteins assembly occurs in

Rab11-REs, mainly fusogenic F protein get incorporated into particles, generating mostly infectious virions. As HeV G proteins are synthesized in their active form, extra endocytic trafficking is not necessary in this case. To verify the importance of this model for HeV assembly, more efforts are required for future investigations.

CHAPTER 5

Summary and Future Directions

5.1 Summary

Within virus life cycle, host factors often play an indispensable role as many of them are involved in assisting each step to achieve successful virus replication. This is also true for virus assembly and budding, the last step of virus life cycle. As paramyxovirus M protein is the main organizer for virus assembly and budding, we set out to identify M-interacting host proteins that are required for henipavirus M-VLPs formation. By using a proteomics-based approach, affinity purification of viral M protein and a following identification of co-purifying host polypeptides by mass spectrometry, we have identified AP3B1, the beta subunit of AP-3 complex as one of the host factors that bind M protein. We were able to confirm the binding through a secondary screening using coimmunoprecipitation assay. Also, we were able to identify small polypeptides derived from AP3B1 that bound M protein as inhibitors of M-VLPs formation. Furthermore, our investigation suggested AP-3 complex is quite likely biologically relevant to M protein function as depletion of AP3B1 by siRNA severely decreased Nipah M-VLPs production. This was also supported by experiments showing that Brefeldin A (BFA) treatment that dissociated AP-3 complex from cellular membrane significantly impaired Nipah M-VLPs production, shown in Appendix A, Fig. 1.

In addition to characterizing host factors that are important for henipavirus particle formation, we also set out to identify determinants of henipavirus M assembly with viral glycoproteins, where we were mainly focusing on the assembly of HeV M protein with F protein. Based on the unique trafficking pathway of HeV F protein characterized by the Dutch group, we have identified another host protein, Rab11a, that might play a critical role in coordinating M and F assembly as we observed colocalization of both M and F protein with Rab11a, and overexpression of a DN Rab11a inhibited both M-VLPs and F-VLPs. These results suggested that trafficking to Rab11a-REs was important for both F-VLPs and M-VLPs particles formation and pointed a role for REs as potential assembly sites for M and F. This was further supported by a PI3P depletion assay using a PI3K inhibitor, as we know that membrane of Rab11-REs are enriched in PI3P (187). In this study shown in Appendix E, both M-VLPs and F-VLPs productions in PI3P depleted cells were significantly impaired. Furthermore, we have examined how the intrinsic properties of F could contribute to its incorporation into M-VLPs, such as its endocytosis trafficking and proteolytic cleavage. By using an endocytosis defective mutant HeV F S490A, we found the endocytic trafficking of F protein was required for its incorporation into M-VLPs. Additionally, we prevented F cleavage through inhibiting cathepsin L activity, and we found the fully-trafficked uncleaved F protein also succeeded in incorporating into M-VLPs, indicating proteolytic cleavage of F protein is not necessary.

HeV G protein was also found in Rab11-REs. Moreover, we observed that G incorporation into particles appeared to depend on co-expression of M protein instead of F protein, although G and F were thought to associate with each other at plasma membrane for effective virus entry (2, 19, 27, 28). The association of G with M likely occurs at the plasma membrane, as immunofluorescence microscopy showed an overlap of G and M at the plasma membrane in transfected cells, although no biochemistry assays could detect HeV M interaction with both glycoproteins so far.

5.2 Future Directions

Develop antiviral-strategies against henipaviruses using inhibitory polypeptides derived from AP3B1

Part of our work has studied one of M-interacting host proteins, AP3B1, identified by the proteomics-based approach. Small inhibitory polypeptides against henipavirus-like particles productions were developed based on subsequent mapping studies. Likely, these inhibitory small polypeptides could also inhibit virion particles production in the context of henipavirus infection. In order to assess their ability to inhibit virus egress in addition to VLPs production, stable cells lines that constitutively express small inhibitory polypeptides are under development, where 293T cells were used to select for clones that stably express either the minimal inhibitory fragment Hinge 1B or non-binding Hinge 1A as a control. Hinge 1B mutants, such as Hinge 1B D691/E693/695A, that failed to bind and did not inhibit

VLPs production are identified using mutagenesis shown in Appendix D, Fig. 1 and Fig. 2. These M-binding defective Hinge 1B mutants could be used as alternative negative controls, and they have a more similar amino acids composition as Hinge 1B than Hinge 1A. Stable cell lines expressing such Hinge 1B mutants will also be developed. Eventually, we would like to send these cell lines to our collaborator Dr. Linfa Wang at Australian Animal Health Laboratory, where they are able to conduct henipavirus infection under BSL-4 containment and evaluate the inhibitory efficacy of these small polypeptides derived from AP3B1 against henipavirus infection. In long-term, this might provide important insights on identification of novel targets against henipavirus infection in vivo and also provide valuable information on antivirals development.

However, the biggest challenges to translate M-AP3B1 interaction to antivirals development are the ones also faced by most therapeutic peptides at present, such as poor bio-stability in vivo. One strategy is to chemically modify the peptides with polymeric conjugates such as polyethylene glycol (PEG) or monoclonal antibodies, which make the peptides less easily degradable. Another important hurdle is bioavailability. To improve penetration of peptides across biological barriers, one strategy is to fuse the peptides with ligands that bind cell surface receptors, where they could be subsequently delivered into the cells by receptor-mediated uptake. This approach is supposed to be safer than just simply ligating the peptides to positively charged amino acids rich sequences containing arginines and lysines. Even though that positively charged sequences could actively penetrate through the cell

or tissue, polycations could often destroy cell membrane and cause toxicity (147). Overall, future efforts that could optimize peptide stability and delivery would definitely take our research one big step further to become therapeutics against henipavirus infection.

Explore the biological role of AP-3 complex in M protein functions

To fully characterize the biological role of AP-3, one strategy is to identify M mutants that fail to bind AP3B1 so that we could obtain important information on AP-3 function based on defects of mutant M proteins. In order to do this, we firstly mapped AP3B1 binding region within M protein by constructing N-terminally GST fused M fragments and examined their co-precipitation with full length AP3B1. These experiments are shown in Appendix B, Fig. 1. Here, we were able to narrow down AP3B1 binding region within M protein to residue 237-282, a 45 amino acids stretch at the C-terminus. Then we subsequently made mutagenesis to residues within this 45 amino acids stretch. We were mainly focusing on residues that are relatively conserved among 5 paramyxovirus M proteins that have been shown to bind AP3B1 to various degrees in chapter 3, including NiV, HeV, PIV5, SeV and MuV, as well as residues that are positively charged. More conserved residues were selected based on amino acids sequence alignment shown in Appendix C, Fig. 1A. We have identified several mutant M protein candidates that appeared to not interact with AP3B1 by coimmunoprecipitation assay shown in Appendix C, Fig. 1B. These mutant M proteins are also proved to be defective on VLP production shown

in Appendix C, Fig. 2. These preliminary data provided us important information to further screen for M mutants whose defects are specifically due to their loss of AP3B1 binding, as it is also likely that some of the mutations would cause abnormality of other functions of M protein first, where loss of AP3B1 binding is just a side effect. Therefore, it is important to develop a secondary screening to confirm the specificity of the mutation. For example, we now have found that the mutation on K258 to either A or acidic residues (E or D) severely impaired mutant M protein ability to bind AP3B1, and conveyed defects on their VLPs production. A previous study has also reported that K258A mutation disrupted M protein putative nuclear localization signal (NLS), resulting in M being excluded from the nucleus (210). Here, the lack of M entering the nucleus complicated the situation. There will be an argument that missing of possible modifications on M protein in the nucleus could result in the defect on M-VLPs production as well, although the lack of these modifications might have side effects such as altering M distribution in the cells where M proteins do not have good access to interact with AP3B1. Therefore, in this case, loss of AP3B1 interaction is not the only cause that would explain the out-coming phenotypes. One strategy to resolve this issue is to identify another mutant M protein whose NLS is also disrupted but could still bind AP3B1, such as the M R244/245A. This M mutant has also been observed to have a significantly higher cytoplasmic localization relative to wild type M protein, which is similar to K258A (210). However, unlike M K258A, M R244/245A bound AP3B1 as well as the wild type, examined by our group and shown in Appendix C, Fig. 1B. Therefore, we would

like to compare the budding ability of these two mutants, to see if it correlates with their ability to bind AP3B1. Likewise, other mutant M protein candidates that are trapped in the nucleus could compare in parallel with previously reported mutant M proteins with the putative L-domain like motif YMYL or YPLGVG deleted at the N-terminus, which were also trapped in the nucleus (42, 153), to rule out the possibility that localization to the nucleus restrict their ability to get access to cytoplasmic AP3B1.

Alternatively, it will be informative to examine M protein functions in AP-3 complex depleted cells. We have recently obtained cell lines derived from pearl mice (AP-3 beta subunit-deficient) and mocha mice (AP-3 delta subunit-deficient) from Dr. Andrew Peden at University of Sheffield, as well as the corresponding control cell lines engineered to express intact AP-3 complex (158). We will also generate stable human cell lines with shRNA-mediated depletion of AP3B1, as well as control cell lines with scrambled shRNAs. Successful knockdown will be verified by western blotting. We anticipate a knockdown efficiency of at least 3-fold, as was the case for our transient siRNA knockdown of AP3B1 shown in chapter 3. To verify the importance of AP-3 complex, we will examine M protein functions such as its membrane association, its subcellular distribution and budding ability in these AP-3 deficient cells. Furthermore, virus budding in these AP-3 deficient cells will be examined in the context of henipavirus infection in collaboration with BSL-4 facility. Taken together, these approaches that disrupt M-AP3B1 interactions would provide

valuable insights on the biological role of AP-3 complex in M protein trafficking and budding.

Identify other M-interacting host factors in both human cells and bat cells

Moreover, we could investigate other host proteins candidates identified by mass spectrometry. We will perform a secondary screening by coimmunoprecipitation assay in the presence of cross-linker, as many interactions could be low affinity and transient, but important. In that case, we would expect stronger co-precipitation of M with host proteins other than AP3B1, including protein candidates that have already been tested, as we already observed weak co-precipitation of M protein with certain host protein including TCOF1, ZC3HAV1 and VPRBP described in chapter 3. We would also expect host restriction factors other than helpers of henipavirus M protein assembly and budding to be identified, as we have previously reported 14-3-3 as the restriction factor for PIV5 assembly and budding by yeast two-hybrid approach using PIV5 M as the bait. PIV5 M mutants that failed to bind 14-3-3 could actually produce more VLPs (160).

We know that fruit bats are the natural host for henipavirus, so we could study henipavirus assembly and budding in bat cells lines as well. As a joint effort, we have obtained three cell lines of a fruit bat species *P. alecto,* a lung cell line (PaLu), a kidney cell line (PaKi) and a brain cell line (PaBr) from our collaborator Dr. Christopher Broder at Uniformed Services University of Health Science. Once we manage to transfect these cell lines more efficiently, we would like to affinity-purify

henipavirus M protein in bat cells in order to further identify M interacting host factors in bats. With that information, it will be interesting to compare the list of bat host candidates with human host candidates, which might provide insights to the pathogenesis of henipavirus in humans and other mammalian species but not in bats. The *P. alecto* genome has been sequenced and compared to human genome earlier. In part, Guojie Zhang and colleagues have looked at genes related to immunity, and found differences including the absence of two families of natural killer (NK) cells receptors: killer cell lectin-like receptors (KLRs) and killer-cell immunoglobulin like receptors (KIR); and mutation of a member in NF-kB transcription family, c-REL, which could affect IkB binding (223). These comparative data provided important information for the possibility of obtaining eventual explanation to how could bats react so differently from other mammals to fatal viral pathogens. Therefore, we think it will be very useful to identify host proteins that are likely involved in henipavirus assembly and budding in both human cells and bat cells.

Explore the trafficking of HeV M and assembly of HeV M protein with G and F proteins

In addition to characterizing M-interacting host proteins, we have also worked on the assembly of HeV M protein with G protein and F protein. Rab11-REs were found to be likely important for both M and F trafficking. We would like to perform experiments in which F trafficking is manipulated by overexpression of DN Rabs or Rab effector proteins. We know that Rabs and Rab effector proteins have been

implicated in the assembly of negative-strand RNA viruses, including Rab8 (177), Rab11 (31, 37), and Rab11-FIPs (201). Our preliminary data indicate that DN Rab11 blocks Hendra F-VLPs and M-VLPs productions. Therefore, we would like to test the effects of other DN Rabs which were characterized earlier in the HeV F recycling pathway such as Rab4 and Rab5 (165), as well as those that are not predicted to be in F trafficking pathway such as Rab7 and Rab8 on both Hendra F-VLPs and M-VLPs formation. We have previously examined HeV M localization in LEs and EEs in transfected cells, and no colocalization was observed for M with LEs marker LAMP-1, neither with EEs marker EEA-1 (data not shown). We would thereby expect that, for example, DN Rab5 will have no negative effects on Hendra M-VLPs formation, whereas it quite likely will block Hendra F-VLPs formation. Overall, this will allow us to selectively manipulate F trafficking or M trafficking components during HeV assembly. Additionally, we would like to test the effect of DN Rab11 effectors such as Rab11-FIPs including Rab11-FIP1C, Rab11-FIP2 and Rab11-FIP3 that have been reported to be involved in enveloped RNA virus trafficking and assembly (30, 31, 168) to further dissect the role of Rab11-REs. We observed that M protein preferentially associated with endogenous Rab11a rather than GFP-Rab11a, where Rab11 effectors were likely involved in physical interaction with M protein. As different Rab11-FIPs define spatially and temporally distinct regions within the dynamic Rab11a-dependent recycling system with FIP1A, FIP2 and FIP5 mainly associating with wildly distributed mobile tubules and vesicles, and FIP1B, FIP1C and FIP3 mostly found in perinuclear tubules and vesicles (11), to determine the role of Rab11-FIPs

will provide more insights on M protein trafficking. Similarly, F-VLPs assembly could also be examined upon expression of DN Rab11-FIPs.

Our initial data indicated that both HeV M and HeV F partially colocalize to Rab11-REs. However, the physical interaction between HeV M and F proteins was not verified, as no co-localization and co-precipitation between M and F was observed (data not shown). One possibility that F-M interaction could not be easily captured by our current approaches such as coimmunoprecipiration and immunofluorescence microscopy is that this interaction could be very transient, where only a small amount of M and F proteins colocalize within cells at certain times. In order to test whether M and F in Rab11-REs co-localize, alternative proximity ligation assays (PLAs) will be performed to detect more transient interaction. This method requires close localization (<40nm) of the two proteins for signal generation. It was recently used to demonstrate influenza virus NP association with Rab11 (6). This would be a joint effort with an expert in PLA methods, Dr. Daniel DiMaio at Yale University (112). Once interaction between M and F proteins is verified by PLA, we would like to determine the requirements for F-M interaction, such as various stages of F protein trafficking as well as F protein cytoplasmic tail. Here, we would like to test HeV F mutants that are defective at different stages of trafficking or cytoplasmic tail depleted F Δ 519-546 for their interactions with M protein. To decide the locations that F-M interaction occurs, cellular markers of membrane compartments, especially REs marker Rab11, will be examined relative to PLA signals generated by F-M interaction. Also, we would like to examine M-F interaction in cells lacking or having

reduced levels of AP3B1. Our preliminary data show a defect in M localization to Rab11 compartments upon expression of Hinge, which likely acts as a competitive inhibitor preventing M interaction with endogenous full-length AP3B1 shown in chapter 4. Therefore, M localization to Rab11-REs as well as M-F interaction measured by PLA will be examined in earlier described pearl cells, mocha cells and human cells line that we would like to generate with AP-3 knockdown by shRNA.

On the other hand, we would like to test the importance of the G protein cytoplasmic tail and AP3B1 for G packaging into M-VLPs. We found that the presence of HeV M led to both accumulation of G protein within M enriched region at plasma membrane, and increased release of G protein in VLPs shown in chapter 4. These were likely due to M-G interaction through G protein cytoplasmic tail. To test this, HeV G Δ32 or Δ44, which remove all or part of the cytoplasmic tail (214) will be tested for incorporation into both M-VLPs and co-localization with M protein. Stability of these CT truncated G proteins as well as full length G will be monitored by radio-labeled pulse-chase assay, both in the presence or absence of M protein. We hypothesize that truncation of G protein cytoplasmic tail will impair M-G assembly, thereby affecting G protein stability and/or G protein incorporation into M-VLPs. In addition, we will examine packaging of G into VLPs when M protein trafficking to Rab11 REs has been disrupted through AP3B1 depletion or expression of AP3B1 Hinge domain. G colocalization with M will also be examined in AP3B1 depletion cells mentioned earlier or in the presence of AP3B1 Hinge domain by immunofluorescence microscopy.

Taken together, these experiments will allow us to gain more insights on the trafficking of henipavirus M protein and glycoproteins, as well as to gather more information on identifying platforms where coordinated assembly of M protein with glycoproteins occur. Furthermore, they will provide us possibilities of unveiling important interactions between M protein and glycoproteins that are necessary for assembly and characterizing virus-host interactions including but not limited to AP-3, complex, Rabs and Rab effector proteins that are involved in this assembly process of henipavirus. Importantly, these interaction interfaces could be further targeted for antivirals development in order to combat lethal henipavirus infections.

APPENDICES

Appendix A: Brefeldin A treatment disrupts M protein intracellular localization and impairs M-VLP productions

Brefeldin A (BFA) is a fugal metabolite that could interfere with transport of protein from Endoplasmic Reticulum (ER) to Golgi apparatus. BFA has also been reported to interfere with Arf1 GTPase cycle, which is used to recruit AP-3 complex to the endosomal membrane. BFA treatment leads to accumulation of GDP-bound Arf1, and therefore prevents the binding of AP-3 to membranes (97, 139). So we would like to test what change could be caused to M protein distribution in cells when treated with BFA. Here, by immunofluorescence microscopy, we found 20 ug/ml BFA treatment significantly disrupted AP-3 complex perinuclear localization and turned it in to more diffused pattern (data not shown) in transfected Vero cells, reinforcing what it has been observed previously by the Freed group (97). Without BFA, a substantial amount of M protein appeared to associate with vesicular compartments forming protein clusters as described in chapter 3. On the contrary, in the presence of BFA, M distribution was more diffused throughout the cells (Fig. A-1A). We think this is due to the lack of M protein association with membrane, as a subsequent membrane flotation experiment on sucrose gradient showed that BFA treatment significantly reduced M protein binding to the membranes (Fig. A-1B). Furthermore, we examined Nipah M-VLPs production in HEK 293T cells under the treatment of BFA. Here, HIV-1 GFP-Gag was used as a control, since we know that

Gag protein of HIV-1 expressed in the cell alone could also result in Gag-VLPs production, and a role of AP-3 complex in HIV-1 assembly has been established, where HIV-1 Gag protein is found to bind to the delta subunit of AP-3 (58). Disruption of this interaction prevents Gag trafficking to multivesicular bodies and AP-3 deficiency in cells impaired HIV-1 particles assembly (58, 114). Generally, HEK 293T cells were transfected to express either NiV M protein or HIV-1 GFP-Gag. After metabolic labeling, VLPs were collected from the culture supernatants, pelleted through sucrose cushion, further purified by flotation on sucrose gradients and analyzed on SDS gels. We found BFA treatment substantially decreased Nipah M-VLPs production, however, surprisingly had no negative effect on HIV-1 GFP-Gag-VLPs production (Fig. A-1C). This generates conflicting result to the importance of AP-3 complex in HIV-1 assembly and budding that has been suggested in previous studies (58, 114). It is noteworthy that this assay has certain limitations, as BFA treatment could impair the functions of multiple cellular membrane organelles (113) . It was found to cause tubulation of endosomal system, TGN and lysosomes (113). Therefore, there is a possibility that the effect of BFA on NiV M protein is a combined result caused by several malfunction cellular membrane organelles upon BFA treatment. However, in contrast to un-affected HIV-1 GFP-Gag-VLPs, defective NiV M-VLPs production upon BFA treatment is at least consistent with the possibility that AP-3 trafficking is important for M protein function, even though BFA treatment does not exclusively impair AP-3 complex function.

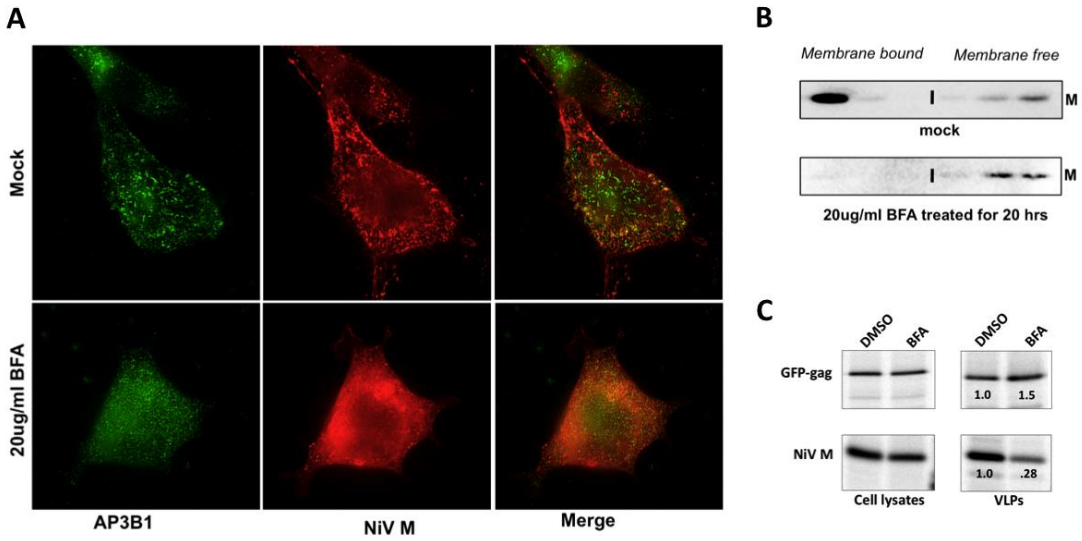

Figure A-1. Brefeldin A treatment impaires Nipah M-VLPs production by disrupting M membrane association. (A) Vero cells were transfected to produce Flag-tagged Nipah virus M protein. Cells were mock treated or treated with 20 ug/ml BFA at 4 h posttransfections. Subcellular localization of M protein (red) and endogenous AP3B1 (green) were visualized by immunofluorescence microscopy at 24 h posttransfections. **(B)** Membrane flotation assay was performed as described earlier. HEK293T cells were transfected to produce Myc-tagged NiV M protein treated with or without 20 ug/ml BFA at 4 h p.t. Cells were harvested 24 h p.t., and homogenized cell lysates were loaded to the bottom of sucrose gradients for flotation through ultracentrifugation. M protein was detected by western blot using a mouse anti-Myc mAb. **(C)** HEK293T cells were transfected to produce Myc-tagged NiV M and HIV-1 GFP-Gag. After metabolic labeling, cell lysates were prepared and VLPs were purified as described earlier. Proteins were resolved on 10% SDS-PAGE and detected using a phosphorimager.

Appendix B: Mapping AP3B1 binding sites within NiV M protein

To gain insights into the biological relevance of the AP3B1-M protein interaction, it will be important to construct and functionally analyze mutant M proteins that fail to bind AP3B1. Towards this end, we have generated a series of NiV M protein-derived truncated polypeptides fused to GST. Firstly, a total of six NiV M fragments were made using PCR, which are 1-128, 129-352, 1-190, 191-352, 1-282 and 283-352. These constructs were N-terminally fused to GST and cloned into pCAGGS expression vector and subsequently co-expressed with full-length AP3B1 in 293T cells. Coimmunoprecipitation assay was performed to examine the binding ability of these NiV M-derived fragments. As indicated in the Fig. B-1A, GST-fused NiV M protein fragments 1-282, 129-352 and 191-352 all coimmunoprecipitated with AP3B1. This result narrowed down the AP3B1-binding region within NiV M protein to the amino acids residues 191-282. The binding activity of this mapped region was further confirmed by coimmunoprecipitation assay including the GST-fused NiV M 191-282 construct (Fig. B-1A). Furthermore, we divided residue 191-282 to even smaller fragments including 191-236, 191-262, 237-262, 237-282 and 263-282. By coimmunoprecipiration assay, we found NiV M 237-282 appeared to be the smallest fragment that was sufficient to bind AP3B1. This result suggested that AP3B1-binding region is likely within this 45 amino acids stretch at the C-terminal domain of NiV M protein (Fig. B-1B).

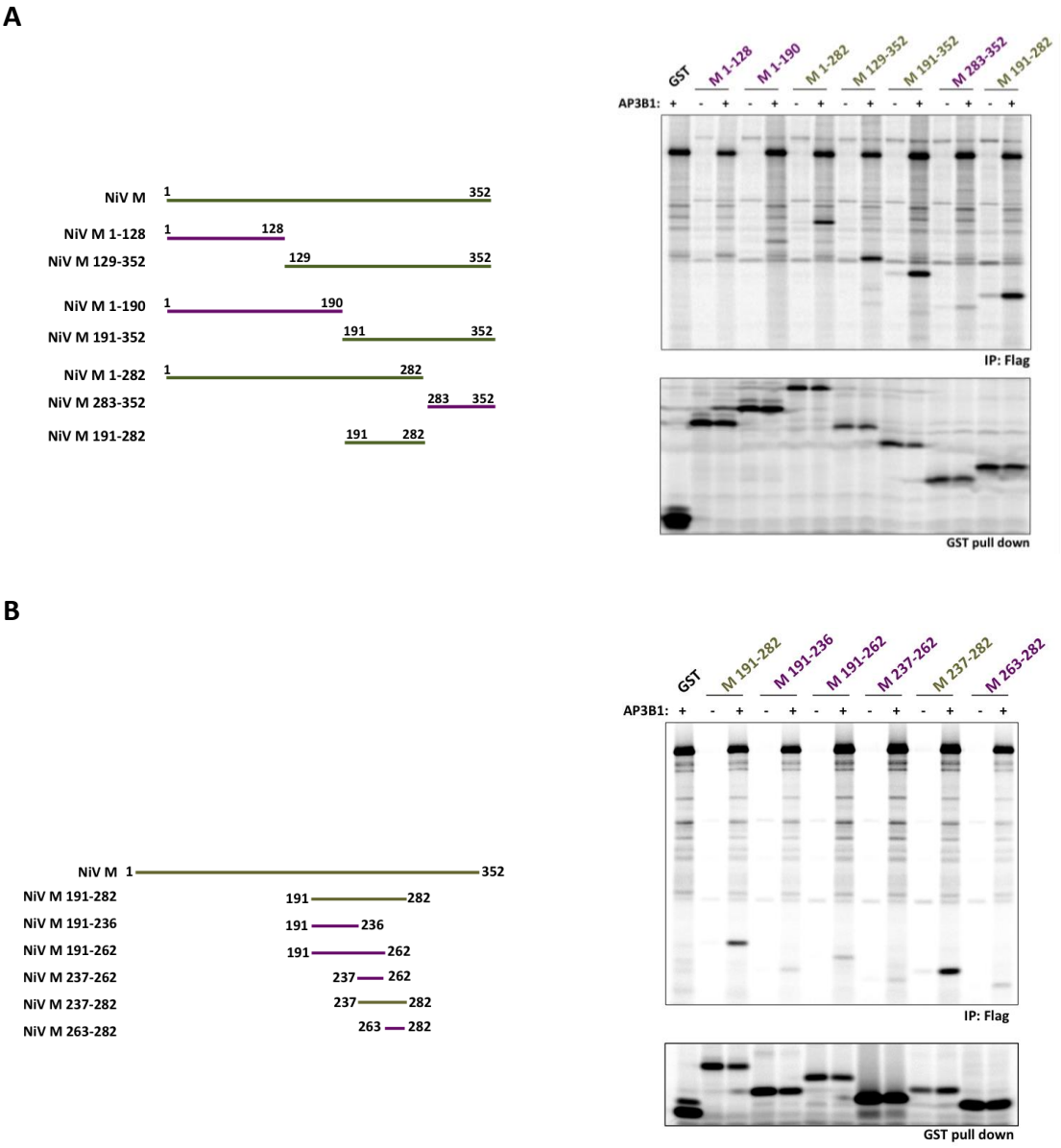

Figure B-1. Mapping AP3B1-binding region within Nipah virus M protein. HEK293T cells were transfected to produce Flag-tagged AP3B1 together with larger GST-M fragments as illustrated on the left of panel **(A)** or smaller fragments as illusated on the left of panel **(B)** Proteins synthesized in the transfected cells were metabolically labeled, and cells were lysed in a solution containing 1% NP-40. Imunoprecipation was carried out using anti-Flag M2 magnetic bead or anti-GST sepharose. Proteins were detected using a phosphorimager.

Appendix C: Generating M mutants that fail to bind AP3B1

Since we have narrowed down AP3B1-binding region within NiV M protein to residues 237-282, eventually, we would like to generate M mutants that fail to bind AP3B1 in order to define the biological role of AP-3 complex in M protein functions. We performed mutagenesis on residues mainly within the stretch of 237-282 of NiV M protein. We were focusing on two groups of residues within this region: (1) Conserved amino acid residues among NiV, HeV, SeV, PIV5 and MuV M proteins (Fig. C-1A) as our previous data showed that the M proteins from these five paramyxoviruses bind AP3B1 with various efficiency. (2) The positively charged residues, such as lysines (K) and arginines (R), as the Hinge domain of AP3B1 is highly negatively charged. So we firstly mutated selected residues as indicated in Fig. C-1B into alanines (A), then the wild type NiV M proteins or mutant NiV M proteins were co-expressed with full length AP3B1 in 293T cells and a radio-labeled coimmunoprecipitation assay was performed to assess interaction between AP3B1 with wt/mutant M proteins. For the majority of conserved residues, mutagenesis to alanine resulted in substantially reduced protein level, so it was difficult to conclude whether there was reduced interaction to AP3B1 (Fig. C-1B and data not shown). For positively charged residues, mutating most of them into alanine did not cause significant change on AP3B1 binding, except one residue K258, which conveyed mutant M protein similar expression level as the wt M protein, but a significantly decreased binding with AP3B1. Furthermore, we even made harsher mutation by turning positively charged residues to either negatively charged glutamic acid (E) or

aspartic acid (D). This resulted in several more M mutants AP3B1 that have reduced AP3B1 binding in addition to M K258A, such as M RR244/245ED, R257D, K258D and R261D (Fig. C-1B). Then a subsequent budding assay was performed to test if they are defective on VLPs production (Fig. C-2). Indeed, all the M mutants that were identified to lose AP3B1 binding were significantly defective on VLP production with at least 7-fold reduction. However, extra assays needs to be developed to secondarily screen for M mutants whose budding defects are more specifically due to their loss of AP3B1 binding, as it is likely that for some of the mutants, mutagenesis affects M other functions first which subsequently results in the loss of AP3B1 interaction. For example, mutations to residue K258 are already known to affect nuclear-cytoplasmic shuttling of M protein (210), and it is possible that the nuclear trafficking defects impact AP3B1 binding, or vice-versa.

A

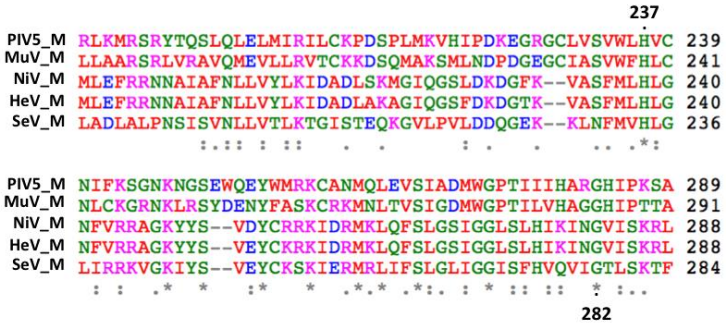

B

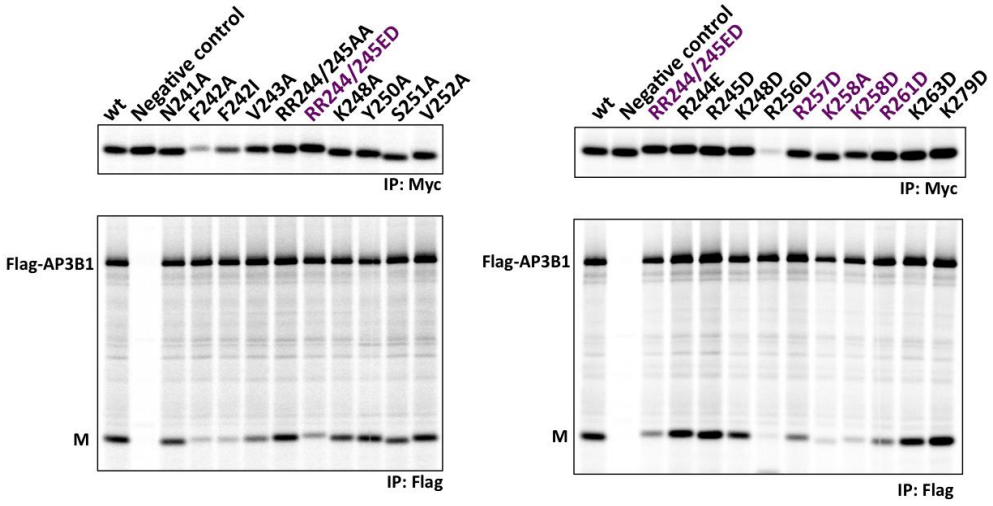

Figure C-1. Identification of Nipah virus M mutants that are defective on AP3B1 binding. (A) Amino acid sequence alignment of five paramyxovirus M proteins corresponding to NiV M protein residue 237-282. **(B)** Coimmunoprecipitation of AP3B1 with mutant Nipah virus M proteins. HEK293T cells were tranfected to produce Flag-tagged AP3B1 together with Myc-tagged wild type or mutant NiV M proteins. Proteins synthesized in the transfected cells were metabolically labeled, and cells were lysed in a solution containing 1% NP-40. Imunoprecipation was carried out using anti-Myc antibody or anti-Flag M2 magnetic beads, and proteins were detected using a phosphorimager.

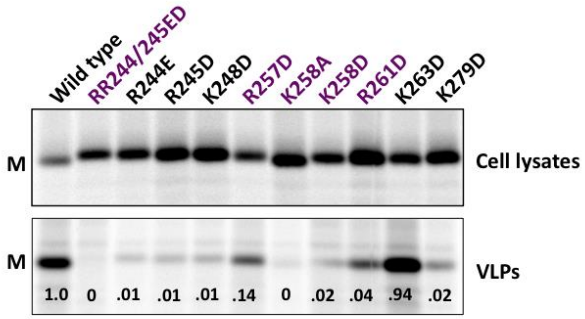

Figure C-2. Mutant Nipah virus M proteins that fail to bind AP3B1 are also defective on VLP production. HEK293Tcells were transfected to produce Myc-tagged wilde type NiV M or NiV M mutants as indicated (purple) that were identified earlier as the candidates that lost binding to AP3B1. After metabolic labeling of cells, lysates were prepared and M protein was immunoprecipitated using anti-Myc mAb. VLPs from culture supernatants were purified by centrifugation through sucrose cushions. Purified VLPs were loaded directly onto SDS gels, and proteins were visualized using a phosphorimager. VLP production efficiencies were calculated as the amount of viral M protein detected in VLPs divided by the amount of M protein detected in the corresponding cell lysate fraction and were normalized to the values obtained for wild type M protein.

Appendix D: Mutations within Hinge 1B screen for amino acids residues that are more important for M-binding

AP3B1 Hinge 1B was identified as the minimal fragment that could bind M protein. It also includes the 10 amino acids stretch that is shared by Hinge 1 and Hinge 3. Here, we further made mutagenesis to the residues within Hinge 1B to examine which residues play more critical role in M-binding. Hinge 1B is concentrated with serine (S), glutamic acid (E) and aspartic acid (D) (Fig. D-1A). We mutated these serines or acidic residues individually to alanine (A), and found that no significant effects on M-binding were caused (data not shown). This indicates that interaction between M proteins with Hinge 1B is the accumulative contribution of multiple residues. Next, we mutated multiple serine residues or acidic residues to alanine in combinations as indicated in Fig. D-1A. The Hinge 1B mutants were flag-tagged at the N terminus, and co-expressed with NiV M protein in 293T cells. Wild type Hinge 1B was used as a positive control, whereas Hinge 1A was used a negative control. By radio-labeled coimmunoprecipitation, binding is evaluated by co-precipitation of M protein with Hinge 1B wt and its mutants. It was quite clear that mutation E678/680A did not convey much defect on Hinge 1B-M interaction. Mutations S677/679/685/686A, S692/694/696A and D684/687A all appeared to have intermediate reduction on M-binding, whereas mutation S688/689/690A, E681/682/683A and D691/E693/695A significantly impaired Hinge 1B M-binding ability (Fig. D-1B). Although these results did not define a specific motif that is

responsible for M protein binding within Hinge 1B, they suggested some residues are more important than others in terms of directing Hinge 1B-M protein interaction.

Next, we tested whether the Hinge 1B mutants that lost M-binding also lacked the ability to inhibit M-VLPs production. We selected one the three Hinge 1B mutants that appeared to be most defective on M-binding, Hinge 1B D691/E693/695A (Fig.D-2A). By budding assay, we found the Hinge 1B mutant that lost M-binding did not inhibit M-VLPs production anymore just as we expected, while Hinge 1B inhibited M-VLPs production very efficiently (Fig. D-2B) This provided an alternative negative control which has a more similar amino acids composition background with Hinge 1B than Hinge 1A, with a few residues changed, which could be used in the future when evaluating Hinge 1B properties other than M-binding for antiviral development against henipviruses.

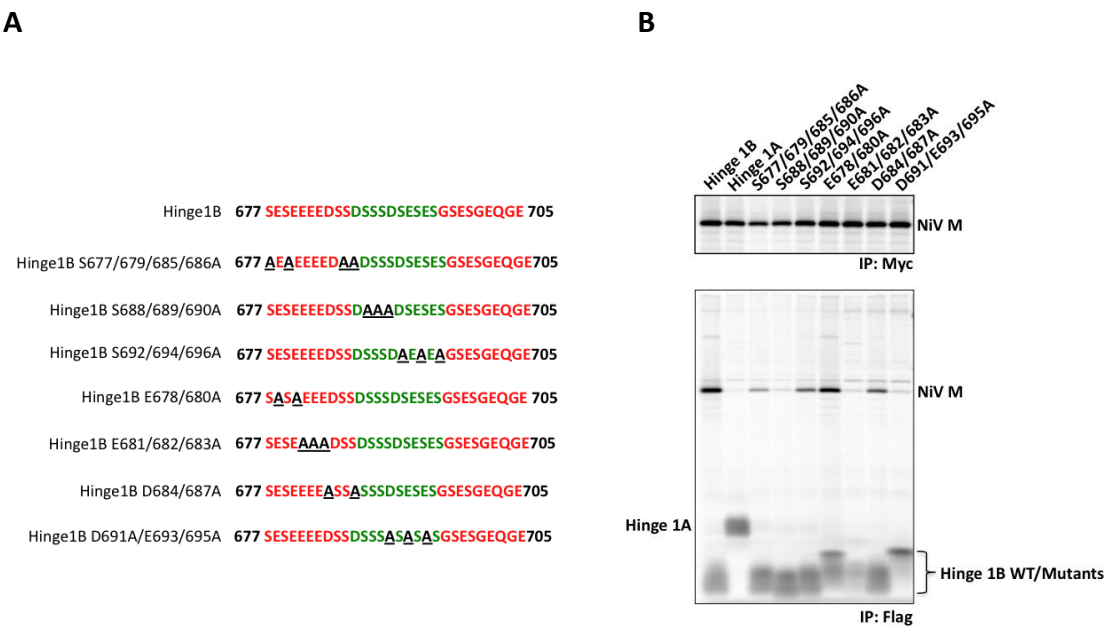

Figure D-1. Generating Hinge 1B mutants that are defective on M-binding. (A) Amino acids sequence illusatration of Hinge 1B mutants that were constructed. They are all N-terminally flag-tagged. **(B)** Coimmunoprecipitation of M with Hinge 1B mutants. HEK293T cells were transfected to produce Nipah virus M protein together with Flag-tagged Hinge 1B wild type or mutant proteins as indicated. Flag-tagged Hinge 1A was used as a negative control. Proteins synthesized in the transfected cells were metabolically labeled and cells were lysed in a solution containing 1% NP-40. Immunoprecipiration was carried out using anti-Myc mAb or anti-Flag M2 magnetic beads, and proteins were detected using a phosphorimager.

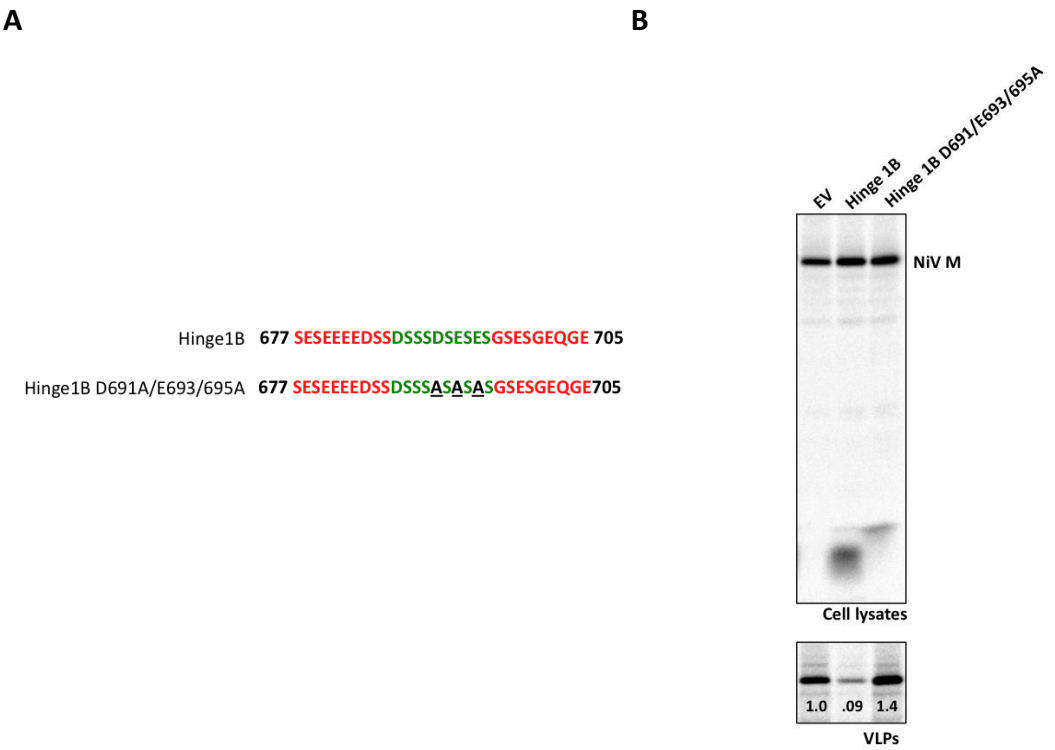

Figure D-2. Hinge 1B mutant that fail to bind M protein do not inhibit Nipah M-VLPs production. (A) Amino acid sequence illustration of one Hinge 1B mutant, Hinge 1B D691A/E693/695A. **(B)** HEK293Tcells were transfected to produce Myc-tagged Nipah virus M alone, M protein together with wild type Hinge 1B or M protein together with mutant Hinge 1B D691/E693/695A. After metabolic labeling of cells, lysates were prepared and M protein was immunoprecipitated using anti-Myc mAb and Hinge 1B wild type and mutant were immunoprecipitated using anti-Flag M2 magnetic beads. VLPs from culture supernatants were purified by centrifugation through sucrose cushions followed by flotation on sucrose gradient. Purified VLPs were loaded directly onto SDS gels, and proteins were visualized using a phosphorimager. VLP production efficiencies were calculated as the amount of viral M protein detected in VLPs divided by the amount of M protein detected in the corresponding cell lysate fraction and were normalized to the values obtained for wild type M protein.

Appendix E: Hendra F and M VLPs productions are inhibited upon PI3P depletion

Although HeV F protein and M protein were both found to colocalize with Rab11 positive recycling endosomes, it is still unclear at what platform that M and F assembly occurs at this point. To further explore, on one hand, we set out to propose assays to detect M and F interaction even though it could be transient. On the other hand, we wanted to examine what cellular membrane could support the coordinated assembly of M and F protein. We know that phosphatidylinositides (PIPs) could serve as lipid signals to regulate membrane-bound protein cargo trafficking as well as lipid markers that represent different cellular membrane compartments (187).For example, phosphatidylinositol 4-phosphate (PI4P) is mainly present at the membrane of Golgi apparatus, phosphatidylinositol 3-phosphate (PI3P) was mostly found at the membrane of early endosome, recycling endosomes and phosphatidylinositol 4,5-biphosphate (PI (4,5) P2) is concentrated at the plasma membrane (187). We have examined M and F protein localization relative to PI (4,5) P2 and PI4P in the cells by immunofluorescence microscopy and found no significant colocalization (data now shown). We depleted PI3P in the cells by using a phosphatidylinositide kinase (PI3K) inhibitor LY294002 to assess the role of PI3P in M and F protein assembly and budding. We performed budding assay in the absence or presence of increasing amount of LY294002 to see how it would affect M-VLPs and F-VLPs formation individually. We found when using 50 uM LY294002, there was hardly any F_1 expressed in the cells, suggesting a processing defect of F protein. Meanwhile, F-VLPs production was severely impaired when treated with 50 uM

LY294002 (Fig. E-1A). Similar effect of 50uM LY294002 on M-VLPs was also observed. However, while LY294002 inhibited both Hendra F and M VLPs significantly, it showed much less effects on HIV-1 Gag-VLPs (Fig. E-1B). This result was consistent with the previous studies where HIV-1 gag proteins were reported to mainly form VLPs at PI (4,5) P2 containing lipid rafts microdomains at plasma membrane. This result suggested PI3P or PI3P containing compartments were likely to be indispensable during M and F trafficking or assembly and budding process.

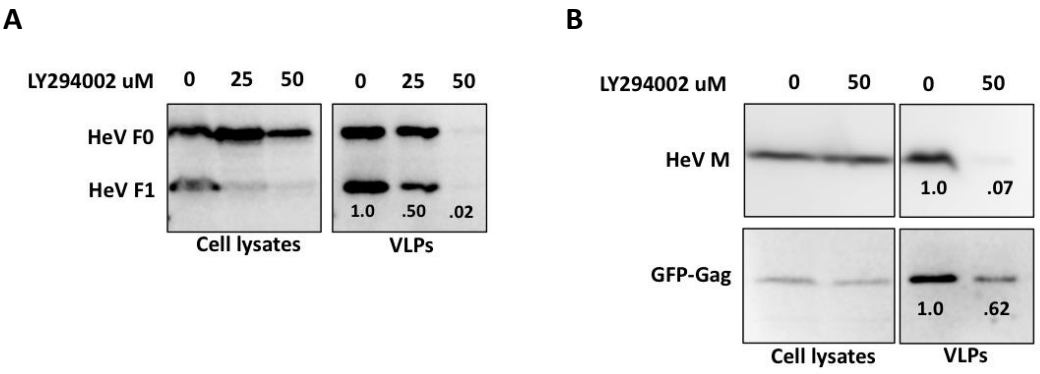

Figure E-1. PI3K inhibitor LY294002 treatment severely impairs both Hendra virus M-VLPs and F-VLPs. HEK293T cells were transfected to produce **(A)** Hendra virus F protein, **(B)** Myc-tagged Hendra virus M protein or HIV-1 GFP-Gag. 24 h p.t, media were replaced with DMEM containing 2% FBS with increasing amount of PI3K inhibitor LY294002 as indicated. Cell lysates were prepared and VLPs were purified through centrifugation on sucrose cushion. Proteins were resolved on SDS-PAGE and detected by western blot using rabbit anti-HeV F, mouse anti-Myc mAb and rabbit anti-GFP pAb. Proteins were visualized using a phosphorimager.

Appendix F: HeV M and F are in vesicles resembling Rab11a positive compartments

As we observed colocalization of HeV M and F with Rab11a, we set out to obtain more evidence of HeV M and F in Rab11 positive vesicles. Here we performed subcellular fractionation to separate cellular membrane compartments with different densities. 293T cells were mock transfected or transfected to express Myc-HeV M proteins or F proteins. 24 h p.t, cells were harvested and homogenized. Nuclei were removed through centrifugation. The supernatant was subjected to subcellular fractionation in discontinuous iodixanol gradients as described in the material and methods, which is modified from the method of Yeaman et al (220). This pilot experiment allows a rough separation of proteins associated with plasma membranes (fractions 1 and 2), late endosomal/ER membranes (fractions 3-7) and small vesicles membranes (fractions 8-11) from soluble proteins (fractions 12 and 13) (Fig. F-1A) (102, 220). Endogenous LAMP-1 and Rab11a were also shown as indicators of different membrane compartments in untransfected cells, as LAMP-1 is mainly found in late endosomes and could be recycled back to the plasma membrane (Fig. F-1A), whereas Rab11a is the protein marker of recycling endosomes whose density is similar to late endosomes. Consistently, a substantial portion of Rab11a is found at PM, while some of Rab11a proteins were also found in small vesicles which were likely derived from recycling endosomes as small carriers for proteins recycling (Fig. F-1A). When HeV M proteins were expressed in the cells, fractions enriched in M proteins are also enriched in Rab11a (fraction 1, 5 and 9), indicating M proteins are likely in Rab11 positive compartments (Fig. F-1B). Similarly,

when HeV F proteins were expressed in the cells, the peak fractions of F (fraction 10 and 11) contained the majority of Rab11a (Fig. F-1C). The expression of HeV F also caused a significant change on the fractionation profile of Rab11a compared to untransfected cells. These preliminary results provide further evidence to demonstrate that HeV M and F are in vesicles that resemble Rab11 positive compartments due to similar densities, and reinforce the possibility that HeV M and F assemble within Rab11-REs. Although M and F were not suggested to be in the same Rab11 positive compartments in this experiment, it is possible they would enter the same Rab11 containing compartments due to F-M interaction when co-expressed together.

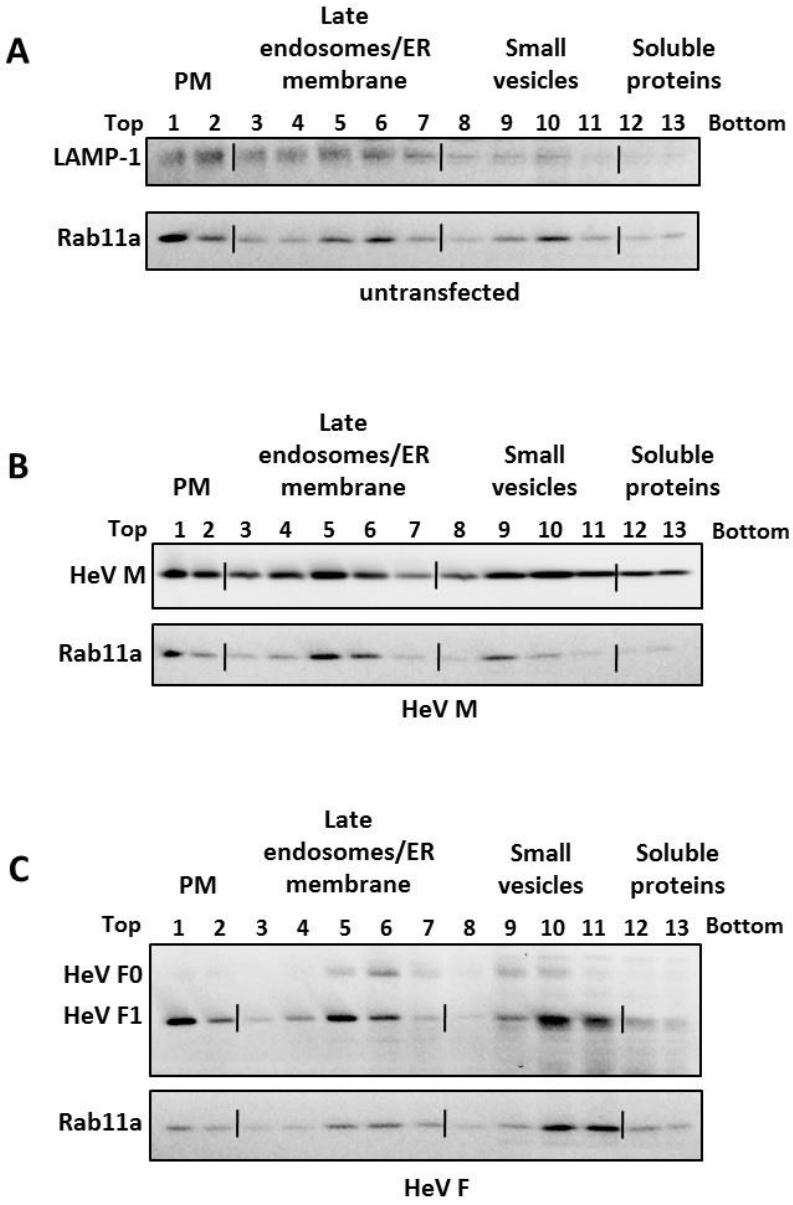

Figure F-1 Subcellular fractionation in an iodixanol gradient to examine HeV M and F localization to Rab11 positive compartments. (A) Detection of cellular proteins in the iodixanol gradients. **(B)** Deterction of HeV M in fractions relative to Rab11a in fractions from iodixanol gradients of HeV M-expressing HEK 293T cells. **(C)** Deterction of HeV F in fractions relative to Rab11a in fractions from iodixanol gradients of HeV F-expressing HEK 293T cells. Plasma membrane: fractions 1 and 2; late endosomes/ER membrane: fractions 3-7; Small vesicles: fractions 8-11; Soluble proteins: fractions 12 and 13.

BIBLIOGRAPHY

1. **Agrawal, T., P. Schu, and G. R. Medigeshi.** 2013. Adaptor protein complexes-1 and 3 are involved at distinct stages of flavivirus life-cycle. Sci Rep **3:**1813.
2. **Aguilar, H. C., K. A. Matreyek, D. Y. Choi, C. M. Filone, S. Young, and B. Lee.** 2007. Polybasic KKR motif in the cytoplasmic tail of Nipah virus fusion protein modulates membrane fusion by inside-out signaling. Journal of virology **81:**4520-4532.
3. **Aguilar, R. C., M. Boehm, I. Gorshkova, R. J. Crouch, K. Tomita, T. Saito, H. Ohno, and J. S. Bonifacino.** 2001. Signal-binding specificity of the mu4 subunit of the adaptor protein complex AP-4. The Journal of biological chemistry **276:**13145-13152.
4. **Ali, A., and D. P. Nayak.** 2000. Assembly of Sendai virus: M protein interacts with F and HN proteins and with the cytoplasmic tail and transmembrane domain of F protein. Virology **276:**289-303.
5. **Aljofan, M.** 2013. Hendra and Nipah infection: emerging paramyxoviruses. Virus research **177:**119-126.
6. **Amorim, M. J., E. A. Bruce, E. K. Read, A. Foeglein, R. Mahen, A. D. Stuart, and P. Digard.** 2011. A Rab11- and microtubule-dependent mechanism for cytoplasmic transport of influenza A virus viral RNA. Journal of virology **85:**4143-4156.
7. **Azevedo, C., A. Burton, E. Ruiz-Mateos, M. Marsh, and A. Saiardi.** 2009. Inositol pyrophosphate mediated pyrophosphorylation of AP3B1 regulates HIV-1 Gag release. Proceedings of the National Academy of Sciences of the United States of America **106:**21161-21166.
8. **Bache, K. G., A. Brech, A. Mehlum, and H. Stenmark.** 2003. Hrs regulates multivesicular body formation via ESCRT recruitment to endosomes. The Journal of cell biology **162:**435-442.
9. **Bache, K. G., C. Raiborg, A. Mehlum, and H. Stenmark.** 2003. STAM and Hrs are subunits of a multivalent ubiquitin-binding complex on early endosomes. The Journal of biological chemistry **278:**12513-12521.
10. **Baczko, K., U. G. Liebert, M. Billeter, R. Cattaneo, H. Budka, and V. ter Meulen.** 1986. Expression of defective measles virus genes in brain tissues of patients with subacute sclerosing panencephalitis. Journal of virology **59:**472-478.
11. **Baetz, N. W., and J. R. Goldenring.** 2013. Rab11-family interacting proteins define spatially and temporally distinct regions within the dynamic Rab11a-dependent recycling system. Molecular biology of the cell **24:**643-658.
12. **Bandyopadhyay, S., S. Ray, A. Mukhopadhyay, and U. Maulik.** 2014. A review of in silico approaches for analysis and prediction of HIV-1-human protein-protein interactions. Brief Bioinform.

13. **Batonick, M., and G. W. Wertz.** 2011. Requirements for Human Respiratory Syncytial Virus Glycoproteins in Assembly and Egress from Infected Cells. Adv Virol **2011**.
14. **Battisti, A. J., G. Meng, D. C. Winkler, L. W. McGinnes, P. Plevka, A. C. Steven, T. G. Morrison, and M. G. Rossmann.** 2012. Structure and assembly of a paramyxovirus matrix protein. Proceedings of the National Academy of Sciences of the United States of America **109:**13996-14000.
15. **Beyer, T., M. Herrmann, C. Reiser, W. Bertling, and J. Hess.** 2001. Bacterial carriers and virus-like-particles as antigen delivery devices: role of dendritic cells in antigen presentation. Curr Drug Targets Infect Disord **1:**287-302.
16. **Bhuin, T., and J. K. Roy.** 2014. Rab proteins: the key regulators of intracellular vesicle transport. Experimental cell research **328:**1-19.
17. **Bieniasz, P. D.** 2006. Late budding domains and host proteins in enveloped virus release. Virology **344:**55-63.
18. **Bishop KA, B. C.** 2008. Hendra and Nipah viruses: lethal zoonotic paramyxoviruses,p 155-187. In Scheld WM, Hammer SM, Hughes JM (ed), Emerging infections. ASM press, Washington, DC.
19. **Bishop, K. A., T. S. Stantchev, A. C. Hickey, D. Khetawat, K. N. Bossart, V. Krasnoperov, P. Gill, Y. R. Feng, L. Wang, B. T. Eaton, L. F. Wang, and C. C. Broder.** 2007. Identification of Hendra virus G glycoprotein residues that are critical for receptor binding. Journal of virology **81:**5893-5901.
20. **Boman, A. L.** 2001. GGA proteins: new players in the sorting game. Journal of cell science **114:**3413-3418.
21. **Bonaparte, M. I., A. S. Dimitrov, K. N. Bossart, G. Crameri, B. A. Mungall, K. A. Bishop, V. Choudhry, D. S. Dimitrov, L. F. Wang, B. T. Eaton, and C. C. Broder.** 2005. Ephrin-B2 ligand is a functional receptor for Hendra virus and Nipah virus. Proceedings of the National Academy of Sciences of the United States of America **102:**10652-10657.
22. **Bonney, D., H. Razali, A. Turner, and A. Will.** 2009. Successful treatment of human metapneumovirus pneumonia using combination therapy with intravenous ribavirin and immune globulin. Br J Haematol **145:**667-669.
23. **Bossart, K. N., G. Crameri, A. S. Dimitrov, B. A. Mungall, Y. R. Feng, J. R. Patch, A. Choudhary, L. F. Wang, B. T. Eaton, and C. C. Broder.** 2005. Receptor binding, fusion inhibition, and induction of cross-reactive neutralizing antibodies by a soluble G glycoprotein of Hendra virus. Journal of virology **79:**6690-6702.
24. **Bossart, K. N., T. W. Geisbert, H. Feldmann, Z. Zhu, F. Feldmann, J. B. Geisbert, L. Yan, Y. R. Feng, D. Brining, D. Scott, Y. Wang, A. S. Dimitrov, J. Callison, Y. P. Chan, A. C. Hickey, D. S. Dimitrov, C. C. Broder, and B. Rockx.** 2011. A neutralizing human monoclonal antibody protects african green monkeys from hendra virus challenge. Sci Transl Med **3:**105ra103.
25. **Bossart, K. N., B. Rockx, F. Feldmann, D. Brining, D. Scott, R. LaCasse, J. B. Geisbert, Y. R. Feng, Y. P. Chan, A. C. Hickey, C. C. Broder, H. Feldmann, and T. W. Geisbert.** 2012. A Hendra virus G glycoprotein subunit vaccine protects

African green monkeys from Nipah virus challenge. Sci Transl Med **4:**146ra107.

26. **Bossart, K. N., M. Tachedjian, J. A. McEachern, G. Crameri, Z. Zhu, D. S. Dimitrov, C. C. Broder, and L. F. Wang.** 2008. Functional studies of host-specific ephrin-B ligands as Henipavirus receptors. Virology **372:**357-371.
27. **Bossart, K. N., L. F. Wang, B. T. Eaton, and C. C. Broder.** 2001. Functional expression and membrane fusion tropism of the envelope glycoproteins of Hendra virus. Virology **290:**121-135.
28. **Bossart, K. N., L. F. Wang, M. N. Flora, K. B. Chua, S. K. Lam, B. T. Eaton, and C. C. Broder.** 2002. Membrane fusion tropism and heterotypic functional activities of the Nipah virus and Hendra virus envelope glycoproteins. Journal of virology **76:**11186-11198.
29. **Bossart, K. N., Z. Zhu, D. Middleton, J. Klippel, G. Crameri, J. Bingham, J. A. McEachern, D. Green, T. J. Hancock, Y. P. Chan, A. C. Hickey, D. S. Dimitrov, L. F. Wang, and C. C. Broder.** 2009. A neutralizing human monoclonal antibody protects against lethal disease in a new ferret model of acute nipah virus infection. PLoS pathogens **5:**e1000642.
30. **Brock, S. C., J. R. Goldenring, and J. E. Crowe, Jr.** 2003. Apical recycling systems regulate directional budding of respiratory syncytial virus from polarized epithelial cells. Proceedings of the National Academy of Sciences of the United States of America **100:**15143-15148.
31. **Bruce, E. A., P. Digard, and A. D. Stuart.** 2010. The Rab11 pathway is required for influenza A virus budding and filament formation. Journal of virology **84:**5848-5859.
32. **Bruce, E. A., A. Stuart, M. W. McCaffrey, and P. Digard.** 2012. Role of the Rab11 pathway in negative-strand virus assembly. Biochemical Society transactions **40:**1409-1415.
33. **Byland, R., and M. Marsh.** 2005. Trafficking of viral membrane proteins. Current topics in microbiology and immunology **285:**219-254.
34. **Campbell, S. M., S. M. Crowe, and J. Mak.** 2001. Lipid rafts and HIV-1: from viral entry to assembly of progeny virions. Journal of clinical virology : the official publication of the Pan American Society for Clinical Virology **22:**217-227.
35. **Cathomen, T., B. Mrkic, D. Spehner, R. Drillien, R. Naef, J. Pavlovic, A. Aguzzi, M. A. Billeter, and R. Cattaneo.** 1998. A matrix-less measles virus is infectious and elicits extensive cell fusion: consequences for propagation in the brain. EMBO J **17:**3899-3908.
36. **Centers for Disease Control and Prevention** 2015, posting date. Measles Cases and Outbreaks. [Online.]
37. **Chambers, R., and T. Takimoto.** 2010. Trafficking of Sendai virus nucleocapsids is mediated by intracellular vesicles. PloS one **5:**e10994.
38. **Chen, C., O. Vincent, J. Jin, O. A. Weisz, and R. C. Montelaro.** 2005. Functions of early (AP-2) and late (AIP1/ALIX) endocytic proteins in equine

infectious anemia virus budding. The Journal of biological chemistry **280:**40474-40480.

39. **Chroboczek, J., I. Szurgot, and E. Szolajska.** 2014. Virus-like particles as vaccine. Acta Biochim Pol **61:**531-539.
40. **Chua, K. B., W. J. Bellini, P. A. Rota, B. H. Harcourt, A. Tamin, S. K. Lam, T. G. Ksiazek, P. E. Rollin, S. R. Zaki, W. Shieh, C. S. Goldsmith, D. J. Gubler, J. T. Roehrig, B. Eaton, A. R. Gould, J. Olson, H. Field, P. Daniels, A. E. Ling, C. J. Peters, L. J. Anderson, and B. W. Mahy.** 2000. Nipah virus: a recently emergent deadly paramyxovirus. Science **288:**1432-1435.
41. **Chua, K. B., S. K. Lam, C. T. Tan, P. S. Hooi, K. J. Goh, N. K. Chew, K. S. Tan, A. Kamarulzaman, and K. T. Wong.** 2000. High mortality in Nipah encephalitis is associated with presence of virus in cerebrospinal fluid. Annals of neurology **48:**802-805.
42. **Ciancanelli, M. J., and C. F. Basler.** 2006. Mutation of YMYL in the Nipah virus matrix protein abrogates budding and alters subcellular localization. Journal of virology **80:**12070-12078.
43. **Ciancanelli, M. J., and C. F. Basler.** 2006. Mutation of YMYL in the Nipah virus matrix protein abrogates budding and alters subcellular localization. Journal of virology **80:**12070-12078.
44. **Clayton, B. A., L. F. Wang, and G. A. Marsh.** 2013. Henipaviruses: an updated review focusing on the pteropid reservoir and features of transmission. Zoonoses Public Health **60:**69-83.
45. **Coronel, E. C., K. G. Murti, T. Takimoto, and A. Portner.** 1999. Human parainfluenza virus type 1 matrix and nucleoprotein genes transiently expressed in mammalian cells induce the release of virus-like particles containing nucleocapsid-like structures. Journal of virology **73:**7035-7038.
46. **Coronel, E. C., T. Takimoto, K. G. Murti, N. Varich, and A. Portner.** 2001. Nucleocapsid incorporation into parainfluenza virus is regulated by specific interaction with matrix protein. Journal of virology **75:**1117-1123.
47. **Cowles, C. R., G. Odorizzi, G. S. Payne, and S. D. Emr.** 1997. The AP-3 adaptor complex is essential for cargo-selective transport to the yeast vacuole. Cell **91:**109-118.
48. **Cowles, C. R., W. B. Snyder, C. G. Burd, and S. D. Emr.** 1997. Novel Golgi to vacuole delivery pathway in yeast: identification of a sorting determinant and required transport component. EMBO J **16:**2769-2782.
49. **Craig, H. M., T. R. Reddy, N. L. Riggs, P. P. Dao, and J. C. Guatelli.** 2000. Interactions of HIV-1 nef with the mu subunits of adaptor protein complexes 1, 2, and 3: role of the dileucine-based sorting motif. Virology **271:**9-17.
50. **CSIRO.** 2012. Vaccine arrives to boost the frontline fight against Hendra virus.
51. **Dell'Angelica, E. C.** 2009. AP-3-dependent trafficking and disease: the first decade. Current opinion in cell biology **21:**552-559.
52. **Dell'Angelica, E. C., J. Klumperman, W. Stoorvogel, and J. S. Bonifacino.** 1998. Association of the AP-3 adaptor complex with clathrin. Science **280:**431-434.

53. **Dell'Angelica, E. C., H. Ohno, C. E. Ooi, E. Rabinovich, K. W. Roche, and J. S. Bonifacino.** 1997. AP-3: an adaptor-like protein complex with ubiquitous expression. EMBO J **16:**917-928.
54. **Dell'Angelica, E. C., C. E. Ooi, and J. S. Bonifacino.** 1997. Beta3A-adaptin, a subunit of the adaptor-like complex AP-3. The Journal of biological chemistry **272:**15078-15084.
55. **Dell'Angelica, E. C., V. Shotelersuk, R. C. Aguilar, W. A. Gahl, and J. S. Bonifacino.** 1999. Altered trafficking of lysosomal proteins in Hermansky-Pudlak syndrome due to mutations in the beta 3A subunit of the AP-3 adaptor. Molecular cell **3:**11-21.
56. **Demirov, D. G., A. Ono, J. M. Orenstein, and E. O. Freed.** 2002. Overexpression of the N-terminal domain of TSG101 inhibits HIV-1 budding by blocking late domain function. Proceedings of the National Academy of Sciences of the United States of America **99:**955-960.
57. **Di Pietro, S. M., J. M. Falcon-Perez, D. Tenza, S. R. Setty, M. S. Marks, G. Raposo, and E. C. Dell'Angelica.** 2006. BLOC-1 interacts with BLOC-2 and the AP-3 complex to facilitate protein trafficking on endosomes. Molecular biology of the cell **17:**4027-4038.
58. **Dong, X., H. Li, A. Derdowski, L. Ding, A. Burnett, X. Chen, T. R. Peters, T. S. Dermody, E. Woodruff, J. J. Wang, and P. Spearman.** 2005. AP-3 directs the intracellular trafficking of HIV-1 Gag and plays a key role in particle assembly. Cell **120:**663-674.
59. **Eaton, B. T., C. C. Broder, D. Middleton, and L. F. Wang.** 2006. Hendra and Nipah viruses: different and dangerous. Nature reviews. Microbiology **4:**23-35.
60. **Eaton, B. T., C. C. Broder, D. Middleton, and L. F. Wang.** 2006. Hendra and Nipah viruses: different and dangerous. Nat Rev Microbiol **4:**23-35.
61. **Edwards, K. M., Y. Zhu, M. R. Griffin, G. A. Weinberg, C. B. Hall, P. G. Szilagyi, M. A. Staat, M. Iwane, M. M. Prill, J. V. Williams, and N. New Vaccine Surveillance.** 2013. Burden of human metapneumovirus infection in young children. N Engl J Med **368:**633-643.
62. **El Najjar, F., A. P. Schmitt, and R. E. Dutch.** 2014. Paramyxovirus glycoprotein incorporation, assembly and budding: a three way dance for infectious particle production. Viruses **6:**3019-3054.
63. **Escaffre, O., V. Borisevich, J. R. Carmical, D. Prusak, J. Prescott, H. Feldmann, and B. Rockx.** 2013. Henipavirus pathogenesis in human respiratory epithelial cells. Journal of virology **87:**3284-3294.
64. **Flicek, P., M. R. Amode, D. Barrell, K. Beal, K. Billis, S. Brent, D. Carvalho-Silva, P. Clapham, G. Coates, S. Fitzgerald, L. Gil, C. G. Giron, L. Gordon, T. Hourlier, S. Hunt, N. Johnson, T. Juettemann, A. K. Kahari, S. Keenan, E. Kulesha, F. J. Martin, T. Maurel, W. M. McLaren, D. N. Murphy, R. Nag, B. Overduin, M. Pignatelli, B. Pritchard, E. Pritchard, H. S. Riat, M. Ruffier, D. Sheppard, K. Taylor, A. Thormann, S. J. Trevanion, A. Vullo, S. P. Wilder, M. Wilson, A. Zadissa, B. L. Aken, E. Birney, F. Cunningham, J. Harrow, J.**

Herrero, T. J. Hubbard, R. Kinsella, M. Muffato, A. Parker, G. Spudich, A. Yates, D. R. Zerbino, and S. M. Searle. 2014. Ensembl 2014. Nucleic acids research **42:**D749-755.

65. **Fouillot-Coriou, N., and L. Roux.** 2000. Structure-function analysis of the Sendai virus F and HN cytoplasmic domain: different role for the two proteins in the production of virus particle. Virology **270:**464-475.
66. **Freed, E. O.** 2003. The HIV-TSG101 interface: recent advances in a budding field. Trends in microbiology **11:**56-59.
67. **Fujii, K., J. H. Hurley, and E. O. Freed.** 2007. Beyond Tsg101: the role of Alix in 'ESCRTing' HIV-1. Nat Rev Microbiol **5:**912-916.
68. **Ganar, K., M. Das, S. Sinha, and S. Kumar.** 2014. Newcastle disease virus: current status and our understanding. Virus research **184:**71-81.
69. **Garcia, E., D. S. Nikolic, and V. Piguet.** 2008. HIV-1 replication in dendritic cells occurs through a tetraspanin-containing compartment enriched in AP-3. Traffic **9:**200-214.
70. **Geisbert, T. W., C. E. Mire, J. B. Geisbert, Y. P. Chan, K. N. Agans, F. Feldmann, K. A. Fenton, Z. Zhu, D. S. Dimitrov, D. P. Scott, K. N. Bossart, H. Feldmann, and C. C. Broder.** 2014. Therapeutic treatment of Nipah virus infection in nonhuman primates with a neutralizing human monoclonal antibody. Sci Transl Med **6:**242ra282.
71. **Gheysen, D., E. Jacobs, F. de Foresta, C. Thiriart, M. Francotte, D. Thines, and M. De Wilde.** 1989. Assembly and release of HIV-1 precursor Pr55gag virus-like particles from recombinant baculovirus-infected insect cells. Cell **59:**103-112.
72. **Goh, K. J., C. T. Tan, N. K. Chew, P. S. Tan, A. Kamarulzaman, S. A. Sarji, K. T. Wong, B. J. Abdullah, K. B. Chua, and S. K. Lam.** 2000. Clinical features of Nipah virus encephalitis among pig farmers in Malaysia. N Engl J Med **342:**1229-1235.
73. **Gomis-Ruth, F. X., A. Dessen, J. Timmins, A. Bracher, L. Kolesnikowa, S. Becker, H. D. Klenk, and W. Weissenhorn.** 2003. The matrix protein VP40 from Ebola virus octamerizes into pore-like structures with specific RNA binding properties. Structure **11:**423-433.
74. **Gotoh, B., F. Yamauchi, T. Ogasawara, and Y. Nagai.** 1992. Isolation of factor Xa from chick embryo as the amniotic endoprotease responsible for paramyxovirus activation. FEBS Lett **296:**274-278.
75. **Gurley, E. S., J. M. Montgomery, M. J. Hossain, M. Bell, A. K. Azad, M. R. Islam, M. A. Molla, D. S. Carroll, T. G. Ksiazek, P. A. Rota, L. Lowe, J. A. Comer, P. Rollin, M. Czub, A. Grolla, H. Feldmann, S. P. Luby, J. L. Woodward, and R. F. Breiman.** 2007. Person-to-person transmission of Nipah virus in a Bangladeshi community. Emerg Infect Dis **13:**1031-1037.
76. **Halpin, K., A. D. Hyatt, R. Fogarty, D. Middleton, J. Bingham, J. H. Epstein, S. A. Rahman, T. Hughes, C. Smith, H. E. Field, P. Daszak, and G. Henipavirus Ecology Research.** 2011. Pteropid bats are confirmed as the reservoir hosts

of henipaviruses: a comprehensive experimental study of virus transmission. The American journal of tropical medicine and hygiene **85:**946-951.

77. **Halpin, K., P. L. Young, H. E. Field, and J. S. Mackenzie.** 2000. Isolation of Hendra virus from pteropid bats: a natural reservoir of Hendra virus. J Gen Virol **81:**1927-1932.
78. **Han, Z., J. Lu, Y. Liu, B. Davis, M. S. Lee, M. A. Olson, G. Ruthel, B. D. Freedman, M. J. Schnell, J. E. Wrobel, A. B. Reitz, and R. N. Harty.** 2014. Small-molecule probes targeting the viral PPxY-host Nedd4 interface block egress of a broad range of RNA viruses. Journal of virology **88:**7294-7306.
79. **Harrion MS, S. T., Schmitt AP.** 2011. Paramyxovirus budding mechanisms, p 193-218. *In* Luo M (ed), Negative strand RNA virus. World Scientific, Hackensack, NJ.
80. **Harrison, M. S., T. Sakaguchi, and A. P. Schmitt.** 2010. Paramyxovirus assembly and budding: building particles that transmit infections. The international journal of biochemistry & cell biology **42:**1416-1429.
81. **Harrison, M. S., P. T. Schmitt, Z. Pei, and A. P. Schmitt.** 2012. Role of ubiquitin in parainfluenza virus 5 particle formation. Journal of virology **86:**3474-3485.
82. **Harty, R. N.** 2009. No exit: targeting the budding process to inhibit filovirus replication. Antiviral Res **81:**189-197.
83. **Harty, R. N., M. E. Brown, F. P. Hayes, N. T. Wright, and M. J. Schnell.** 2001. Vaccinia virus-free recovery of vesicular stomatitis virus. J Mol Microbiol Biotechnol **3:**513-517.
84. **Harty, R. N., M. E. Brown, G. Wang, J. Huibregtse, and F. P. Hayes.** 2000. A PPxY motif within the VP40 protein of Ebola virus interacts physically and functionally with a ubiquitin ligase: implications for filovirus budding. Proceedings of the National Academy of Sciences of the United States of America **97:**13871-13876.
85. **Hausmann, S., D. Garcin, C. Delenda, and D. Kolakofsky.** 1999. The versatility of paramyxovirus RNA polymerase stuttering. Journal of virology **73:**5568-5576.
86. **Hermansky, F., and P. Pudlak.** 1959. Albinism associated with hemorrhagic diathesis and unusual pigmented reticular cells in the bone marrow: report of two cases with histochemical studies. Blood **14:**162-169.
87. **Hirano, A., M. Ayata, A. H. Wang, and T. C. Wong.** 1993. Functional analysis of matrix proteins expressed from cloned genes of measles virus variants that cause subacute sclerosing panencephalitis reveals a common defect in nucleocapsid binding. Journal of virology **67:**1848-1853.
88. **Hirst, J., L. D. Barlow, G. C. Francisco, D. A. Sahlender, M. N. Seaman, J. B. Dacks, and M. S. Robinson.** 2011. The fifth adaptor protein complex. PLoS Biol **9:**e1001170.
89. **Hirst, J., N. A. Bright, B. Rous, and M. S. Robinson.** 1999. Characterization of a fourth adaptor-related protein complex. Molecular biology of the cell **10:**2787-2802.

90. **Hirst, J., and M. S. Robinson.** 1998. Clathrin and adaptors. Biochimica et biophysica acta **1404:**173-193.
91. **Honing, S., I. V. Sandoval, and K. von Figura.** 1998. A di-leucine-based motif in the cytoplasmic tail of LIMP-II and tyrosinase mediates selective binding of AP-3. EMBO J **17:**1304-1314.
92. **Ihrke, G., A. Kyttala, M. R. Russell, B. A. Rous, and J. P. Luzio.** 2004. Differential use of two AP-3-mediated pathways by lysosomal membrane proteins. Traffic **5:**946-962.
93. **Ivan, V., E. Martinez-Sanchez, L. E. Sima, V. Oorschot, J. Klumperman, S. M. Petrescu, and P. van der Sluijs.** 2012. AP-3 and Rabip4' coordinately regulate spatial distribution of lysosomes. PloS one **7:**e48142.
94. **Iwasaki, M., M. Takeda, Y. Shirogane, Y. Nakatsu, T. Nakamura, and Y. Yanagi.** 2009. The matrix protein of measles virus regulates viral RNA synthesis and assembly by interacting with the nucleocapsid protein. Journal of virology **83:**10374-10383.
95. **Jacobs, E., D. Gheysen, D. Thines, M. Francotte, and M. de Wilde.** 1989. The HIV-1 Gag precursor Pr55gag synthesized in yeast is myristoylated and targeted to the plasma membrane. Gene **79:**71-81.
96. **Jane S. Flint, V. R. R., Robert Krug** 2009. Principles of Virology: Molecular Biology, Pathogenesis, and Control
97. **Joshi, A., H. Garg, K. Nagashima, J. S. Bonifacino, and E. O. Freed.** 2008. GGA and Arf proteins modulate retrovirus assembly and release. Molecular cell **30:**227-238.
98. **Kantheti, P., X. Qiao, M. E. Diaz, A. A. Peden, G. E. Meyer, S. L. Carskadon, D. Kapfhamer, D. Sufalko, M. S. Robinson, J. L. Noebels, and M. Burmeister.** 1998. Mutation in AP-3 delta in the mocha mouse links endosomal transport to storage deficiency in platelets, melanosomes, and synaptic vesicles. Neuron **21:**111-122.
99. **Keen, J. H.** 1987. Clathrin assembly proteins: affinity purification and a model for coat assembly. The Journal of cell biology **105:**1989-1998.
100. **Kido, H., M. Murakami, K. Oba, Y. Chen, and T. Towatari.** 1999. Cellular proteinases trigger the infectivity of the influenza A and Sendai viruses. Mol Cells **9:**235-244.
101. **Klenk, H. D., and W. Garten.** 1994. Host cell proteases controlling virus pathogenicity. Trends in microbiology **2:**39-43.
102. **Kolesnikova, L., S. Bamberg, B. Berghofer, and S. Becker.** 2004. The matrix protein of Marburg virus is transported to the plasma membrane along cellular membranes: exploiting the retrograde late endosomal pathway. Journal of virology **78:**2382-2393.
103. **Komarova, A. V., C. Combredet, L. Meyniel-Schicklin, M. Chapelle, G. Caignard, J. M. Camadro, V. Lotteau, P. O. Vidalain, and F. Tangy.** 2011. Proteomic analysis of virus-host interactions in an infectious context using recombinant viruses. Mol Cell Proteomics **10:**M110 007443.

104. **Kondo, T., T. Yoshida, N. Miura, and M. Nakanishi.** 1993. Temperature-sensitive phenotype of a mutant Sendai virus strain is caused by its insufficient accumulation of the M protein. The Journal of biological chemistry **268:**21924-21930.
105. **Ksiazek, T. G., P. A. Rota, and P. E. Rollin.** 2011. A review of Nipah and Hendra viruses with an historical aside. Virus research **162:**173-183.
106. **Kulkarni, S., V. Volchkova, C. F. Basler, P. Palese, V. E. Volchkov, and M. L. Shaw.** 2009. Nipah virus edits its P gene at high frequency to express the V and W proteins. Journal of virology **83:**3982-3987.
107. **Kyere, S. K., P. Y. Mercredi, X. Dong, P. Spearman, and M. F. Summers.** 2012. The HIV-1 matrix protein does not interact directly with the protein interactive domain of AP-3delta. Virus research **169:**411-414.
108. **Lamb, R. A., and G.D. Parks** 2006. Paramyxovirividae: the viruses and their replication, p. p.1449-1496, In D.M. Knipe and P.M. Howley (ed.), Field of Virology, Fifth ed. Lippincott, Willians and Wilkins, Philadelhpia.
109. **Larkin, M. A., G. Blackshields, N. P. Brown, R. Chenna, P. A. McGettigan, H. McWilliam, F. Valentin, I. M. Wallace, A. Wilm, R. Lopez, J. D. Thompson, T. J. Gibson, and D. G. Higgins.** 2007. Clustal W and Clustal X version 2.0. Bioinformatics **23:**2947-2948.
110. **Li, M., P. T. Schmitt, Z. Li, T. S. McCrory, B. He, and A. P. Schmitt.** 2009. Mumps virus matrix, fusion, and nucleocapsid proteins cooperate for efficient production of virus-like particles. Journal of virology **83:**7261-7272.
111. **Liljeroos, L., and S. J. Butcher.** 2013. Matrix proteins as centralized organizers of negative-sense RNA virions. Front Biosci (Landmark Ed) **18:**696-715.
112. **Lipovsky, A., A. Popa, G. Pimienta, M. Wyler, A. Bhan, L. Kuruvilla, M. A. Guie, A. C. Poffenberger, C. D. Nelson, W. J. Atwood, and D. DiMaio.** 2013. Genome-wide siRNA screen identifies the retromer as a cellular entry factor for human papillomavirus. Proceedings of the National Academy of Sciences of the United States of America **110:**7452-7457.
113. **Lippincott-Schwartz, J., L. Yuan, C. Tipper, M. Amherdt, L. Orci, and R. D. Klausner.** 1991. Brefeldin A's effects on endosomes, lysosomes, and the TGN suggest a general mechanism for regulating organelle structure and membrane traffic. Cell **67:**601-616.
114. **Liu, L., J. Sutton, E. Woodruff, F. Villalta, P. Spearman, and X. Dong.** 2012. Defective HIV-1 particle assembly in AP-3-deficient cells derived from patients with Hermansky-Pudlak syndrome type 2. Journal of virology **86:**11242-11253.
115. **Lloyd, V., M. Ramaswami, and H. Kramer.** 1998. Not just pretty eyes: Drosophila eye-colour mutations and lysosomal delivery. Trends in cell biology **8:**257-259.
116. **Lo, M. K., B. H. Harcourt, B. A. Mungall, A. Tamin, M. E. Peeples, W. J. Bellini, and P. A. Rota.** 2009. Determination of the henipavirus

phosphoprotein gene mRNA editing frequencies and detection of the C, V and W proteins of Nipah virus in virus-infected cells. J Gen Virol **90:**398-404.

117. **Loo, L. H., M. R. Jumat, Y. Fu, T. C. Ayi, P. S. Wong, N. W. Tee, B. H. Tan, and R. J. Sugrue.** 2013. Evidence for the interaction of the human metapneumovirus G and F proteins during virus-like particle formation. Virol J **10:**294.
118. **Lu, Q., L. W. Hope, M. Brasch, C. Reinhard, and S. N. Cohen.** 2003. TSG101 interaction with HRS mediates endosomal trafficking and receptor down-regulation. Proceedings of the National Academy of Sciences of the United States of America **100:**7626-7631.
119. **Lyles, D. S.** 2013. Assembly and budding of negative-strand RNA viruses. Adv Virus Res **85:**57-90.
120. **Maisner, A., J. Neufeld, and H. Weingartl.** 2009. Organ- and endotheliotropism of Nipah virus infections in vivo and in vitro. Thromb Haemost **102:**1014-1023.
121. **Marsh, G. A., C. de Jong, J. A. Barr, M. Tachedjian, C. Smith, D. Middleton, M. Yu, S. Todd, A. J. Foord, V. Haring, J. Payne, R. Robinson, I. Broz, G. Crameri, H. E. Field, and L. F. Wang.** 2012. Cedar virus: a novel Henipavirus isolated from Australian bats. PLoS pathogens **8:**e1002836.
122. **Martin-Serrano, J., A. Yarovoy, D. Perez-Caballero, and P. D. Bieniasz.** 2003. Divergent retroviral late-budding domains recruit vacuolar protein sorting factors by using alternative adaptor proteins. Proceedings of the National Academy of Sciences of the United States of America **100:**12414-12419.
123. **Mayer, D., K. Molawi, L. Martinez-Sobrido, A. Ghanem, S. Thomas, S. Baginsky, J. Grossmann, A. Garcia-Sastre, and M. Schwemmle.** 2007. Identification of cellular interaction partners of the influenza virus ribonucleoprotein complex and polymerase complex using proteomic-based approaches. Journal of proteome research **6:**672-682.
124. **Meulendyke, K. A., M. A. Wurth, R. O. McCann, and R. E. Dutch.** 2005. Endocytosis plays a critical role in proteolytic processing of the Hendra virus fusion protein. Journal of virology **79:**12643-12649.
125. **Michalski, W. P., G. Crameri, L. Wang, B. J. Shiell, and B. Eaton.** 2000. The cleavage activation and sites of glycosylation in the fusion protein of Hendra virus. Virus research **69:**83-93.
126. **Middleton, D., J. Pallister, R. Klein, Y. R. Feng, J. Haining, R. Arkinstall, L. Frazer, J. A. Huang, N. Edwards, M. Wareing, M. Elhay, Z. Hashmi, J. Bingham, M. Yamada, D. Johnson, J. White, A. Foord, H. G. Heine, G. A. Marsh, C. C. Broder, and L. F. Wang.** 2014. Hendra virus vaccine, a one health approach to protecting horse, human, and environmental health. Emerg Infect Dis **20:**372-379.
127. **Mimnaugh, E. G., H. Y. Chen, J. R. Davie, J. E. Celis, and L. Neckers.** 1997. Rapid deubiquitination of nucleosomal histones in human tumor cells caused by proteasome inhibitors and stress response inducers: effects on replication,

transcription, translation, and the cellular stress response. Biochemistry **36:**14418-14429.

128. **Mire, C. E., J. B. Geisbert, K. N. Agans, Y. R. Feng, K. A. Fenton, K. N. Bossart, L. Yan, Y. P. Chan, C. C. Broder, and T. W. Geisbert.** 2014. A recombinant Hendra virus G glycoprotein subunit vaccine protects nonhuman primates against Hendra virus challenge. Journal of virology **88:**4624-4631.
129. **Morrison, T. G.** 1988. Structure, function, and intracellular processing of paramyxovirus membrane proteins. Virus research **10:**113-135.
130. **Munshi, U. M., J. Kim, K. Nagashima, J. H. Hurley, and E. O. Freed.** 2007. An Alix fragment potently inhibits HIV-1 budding: characterization of binding to retroviral YPXL late domains. The Journal of biological chemistry **282:**3847-3855.
131. **Munster, V. J., J. B. Prescott, T. Bushmaker, D. Long, R. Rosenke, T. Thomas, D. Scott, E. R. Fischer, H. Feldmann, and E. de Wit.** 2012. Rapid Nipah virus entry into the central nervous system of hamsters via the olfactory route. Sci Rep **2:**736.
132. **Murray, K., R. Rogers, L. Selvey, P. Selleck, A. Hyatt, A. Gould, L. Gleeson, P. Hooper, and H. Westbury.** 1995. A novel morbillivirus pneumonia of horses and its transmission to humans. Emerg Infect Dis **1:**31-33.
133. **Murray, K., P. Selleck, P. Hooper, A. Hyatt, A. Gould, L. Gleeson, H. Westbury, L. Hiley, L. Selvey, B. Rodwell, and et al.** 1995. A morbillivirus that caused fatal disease in horses and humans. Science **268:**94-97.
134. **Nakatsu, F., and H. Ohno.** 2003. Adaptor protein complexes as the key regulators of protein sorting in the post-Golgi network. Cell Struct Funct **28:**419-429.
135. **Nakatsu, Y., X. Ma, F. Seki, T. Suzuki, M. Iwasaki, Y. Yanagi, K. Komase, and M. Takeda.** 2013. Intracellular transport of the measles virus ribonucleoprotein complex is mediated by Rab11A-positive recycling endosomes and drives virus release from the apical membrane of polarized epithelial cells. Journal of virology **87:**4683-4693.
136. **Nakayama, K.** 1997. Furin: a mammalian subtilisin/Kex2p-like endoprotease involved in processing of a wide variety of precursor proteins. The Biochemical journal **327 (Pt 3):**625-635.
137. **Negrete, O. A., E. L. Levroney, H. C. Aguilar, A. Bertolotti-Ciarlet, R. Nazarian, S. Tajyar, and B. Lee.** 2005. EphrinB2 is the entry receptor for Nipah virus, an emergent deadly paramyxovirus. Nature **436:**401-405.
138. **Negrete, O. A., M. C. Wolf, H. C. Aguilar, S. Enterlein, W. Wang, E. Muhlberger, S. V. Su, A. Bertolotti-Ciarlet, R. Flick, and B. Lee.** 2006. Two key residues in ephrinB3 are critical for its use as an alternative receptor for Nipah virus. PLoS pathogens **2:**e7.
139. **Newell-Litwa, K., E. Seong, M. Burmeister, and V. Faundez.** 2007. Neuronal and non-neuronal functions of the AP-3 sorting machinery. Journal of cell science **120:**531-541.

140. **Newman, L. S., M. O. McKeever, H. J. Okano, and R. B. Darnell.** 1995. Beta-NAP, a cerebellar degeneration antigen, is a neuron-specific vesicle coat protein. Cell **82:**773-783.
141. **Nishimura, N., H. Plutner, K. Hahn, and W. E. Balch.** 2002. The delta subunit of AP-3 is required for efficient transport of VSV-G from the trans-Golgi network to the cell surface. Proceedings of the National Academy of Sciences of the United States of America **99:**6755-6760.
142. **Niwa, H., K. Yamamura, and J. Miyazaki.** 1991. Efficient selection for high-expression transfectants with a novel eukaryotic vector. Gene **108:**193-199.
143. **O'Sullivan, J. D., A. M. Allworth, D. L. Paterson, T. M. Snow, R. Boots, L. J. Gleeson, A. R. Gould, A. D. Hyatt, and J. Bradfield.** 1997. Fatal encephalitis due to novel paramyxovirus transmitted from horses. Lancet **349:**93-95.
144. **Odorizzi, G., C. R. Cowles, and S. D. Emr.** 1998. The AP-3 complex: a coat of many colours. Trends in cell biology **8:**282-288.
145. **Ohno, H., R. C. Aguilar, D. Yeh, D. Taura, T. Saito, and J. S. Bonifacino.** 1998. The medium subunits of adaptor complexes recognize distinct but overlapping sets of tyrosine-based sorting signals. The Journal of biological chemistry **273:**25915-25921.
146. **Ooi, C. E., E. C. Dell'Angelica, and J. S. Bonifacino.** 1998. ADP-Ribosylation factor 1 (ARF1) regulates recruitment of the AP-3 adaptor complex to membranes. The Journal of cell biology **142:**391-402.
147. **Otvos, L., Jr., and J. D. Wade.** 2014. Current challenges in peptide-based drug discovery. Front Chem **2:**62.
148. **Pager, C. T., and R. E. Dutch.** 2005. Cathepsin L is involved in proteolytic processing of the Hendra virus fusion protein. Journal of virology **79:**12714-12720.
149. **Pallister, J., D. Middleton, L. F. Wang, R. Klein, J. Haining, R. Robinson, M. Yamada, J. White, J. Payne, Y. R. Feng, Y. P. Chan, and C. C. Broder.** 2011. A recombinant Hendra virus G glycoprotein-based subunit vaccine protects ferrets from lethal Hendra virus challenge. Vaccine **29:**5623-5630.
150. **Pantua, H. D., L. W. McGinnes, M. E. Peeples, and T. G. Morrison.** 2006. Requirements for the assembly and release of Newcastle disease virus-like particles. Journal of virology **80:**11062-11073.
151. **Parks, G. D. a. L., R.A.** 2013. Paramyxoviruses and Rubella Virus, Jawetz, Melnick & Adelberg's Medical Microbiology, 26ed.
152. **Patch, J. R., G. Crameri, L. F. Wang, B. T. Eaton, and C. C. Broder.** 2007. Quantitative analysis of Nipah virus proteins released as virus-like particles reveals central role for the matrix protein. Virol J **4:**1.
153. **Patch, J. R., Z. Han, S. E. McCarthy, L. Yan, L. F. Wang, R. N. Harty, and C. C. Broder.** 2008. The YPLGVG sequence of the Nipah virus matrix protein is required for budding. Virol J **5:**137.
154. **Patch, J. R., Z. Han, S. E. McCarthy, L. Yan, L. F. Wang, R. N. Harty, and C. C. Broder.** 2008. The YPLGVG sequence of the Nipah virus matrix protein is required for budding. Virology journal **5:**137.

155. **Patnaik, A., V. Chau, and J. W. Wills.** 2000. Ubiquitin is part of the retrovirus budding machinery. Proceedings of the National Academy of Sciences of the United States of America **97:**13069-13074.
156. **Pearse, B. M.** 1975. Coated vesicles from pig brain: purification and biochemical characterization. J Mol Biol **97:**93-98.
157. **Peden, A. A., V. Oorschot, B. A. Hesser, C. D. Austin, R. H. Scheller, and J. Klumperman.** 2004. Localization of the AP-3 adaptor complex defines a novel endosomal exit site for lysosomal membrane proteins. The Journal of cell biology **164:**1065-1076.
158. **Peden, A. A., R. E. Rudge, W. W. Lui, and M. S. Robinson.** 2002. Assembly and function of AP-3 complexes in cells expressing mutant subunits. J Cell Biol **156:**327-336.
159. **Pei, Z., Y. Bai, and A. P. Schmitt.** 2010. PIV5 M protein interaction with host protein angiomotin-like 1. Virology **397:**155-166.
160. **Pei, Z., M. S. Harrison, and A. P. Schmitt.** 2011. Parainfluenza virus 5 m protein interaction with host protein 14-3-3 negatively affects virus particle formation. Journal of virology **85:**2050-2059.
161. **Philbey, A. W., P. D. Kirkland, A. D. Ross, R. J. Davis, A. B. Gleeson, R. J. Love, P. W. Daniels, A. R. Gould, and A. D. Hyatt.** 1998. An apparently new virus (family Paramyxoviridae) infectious for pigs, humans, and fruit bats. Emerg Infect Dis **4:**269-271.
162. **Pinney, J. W., J. E. Dickerson, W. Fu, B. E. Sanders-Beer, R. G. Ptak, and D. L. Robertson.** 2009. HIV-host interactions: a map of viral perturbation of the host system. AIDS **23:**549-554.
163. **Playford, E. G., B. McCall, G. Smith, V. Slinko, G. Allen, I. Smith, F. Moore, C. Taylor, Y. H. Kung, and H. Field.** 2010. Human Hendra virus encephalitis associated with equine outbreak, Australia, 2008. Emerg Infect Dis **16:**219-223.
164. **Pohl, C., W. P. Duprex, G. Krohne, B. K. Rima, and S. Schneider-Schaulies.** 2007. Measles virus M and F proteins associate with detergent-resistant membrane fractions and promote formation of virus-like particles. J Gen Virol **88:**1243-1250.
165. **Popa, A., J. R. Carter, S. E. Smith, L. Hellman, M. G. Fried, and R. E. Dutch.** 2012. Residues in the hendra virus fusion protein transmembrane domain are critical for endocytic recycling. Journal of virology **86:**3014-3026.
166. **Prasad, K., and J. H. Keen.** 1991. Interaction of assembly protein AP-2 and its isolated subunits with clathrin. Biochemistry **30:**5590-5597.
167. **Prevention, C. f. D. C. a.** 2015, posting date. Mumps Cases and Outbreaks. [Online.]
168. **Qi, M., J. A. Williams, H. Chu, X. Chen, J. J. Wang, L. Ding, E. Akhirome, X. Wen, L. A. Lapierre, J. R. Goldenring, and P. Spearman.** 2013. Rab11-FIP1C and Rab14 direct plasma membrane sorting and particle incorporation of the HIV-1 envelope glycoprotein complex. PLoS pathogens **9:**e1003278.

169. **Raiborg, C., K. G. Bache, D. J. Gillooly, I. H. Madshus, E. Stang, and H. Stenmark.** 2002. Hrs sorts ubiquitinated proteins into clathrin-coated microdomains of early endosomes. Nat Cell Biol **4:**394-398.
170. **Rao, V. S., K. Srinivas, G. N. Sujini, and G. N. Kumar.** 2014. Protein-protein interaction detection: methods and analysis. Int J Proteomics **2014:**147648.
171. **Ren, M., G. Xu, J. Zeng, C. De Lemos-Chiarandini, M. Adesnik, and D. D. Sabatini.** 1998. Hydrolysis of GTP on rab11 is required for the direct delivery of transferrin from the pericentriolar recycling compartment to the cell surface but not from sorting endosomes. Proceedings of the National Academy of Sciences of the United States of America **95:**6187-6192.
172. **Robinson, M. S., and J. S. Bonifacino.** 2001. Adaptor-related proteins. Current opinion in cell biology **13:**444-453.
173. **Rodriguez, L., I. Cuesta, A. Asenjo, and N. Villanueva.** 2004. Human respiratory syncytial virus matrix protein is an RNA-binding protein: binding properties, location and identity of the RNA contact residues. J Gen Virol **85:**709-719.
174. **Rossman, J. S., and R. A. Lamb.** 2011. Influenza virus assembly and budding. Virology **411:**229-236.
175. **Rossman, J. S., and R. A. Lamb.** 2013. Viral membrane scission. Annual review of cell and developmental biology **29:**551-569.
176. **Rous, B. A., B. J. Reaves, G. Ihrke, J. A. Briggs, S. R. Gray, D. J. Stephens, G. Banting, and J. P. Luzio.** 2002. Role of adaptor complex AP-3 in targeting wild-type and mutated CD63 to lysosomes. Molecular biology of the cell **13:**1071-1082.
177. **Rowe, R. K., J. W. Suszko, and A. Pekosz.** 2008. Roles for the recycling endosome, Rab8, and Rab11 in hantavirus release from epithelial cells. Virology **382:**239-249.
178. **Runkler, N., C. Pohl, S. Schneider-Schaulies, H. D. Klenk, and A. Maisner.** 2007. Measles virus nucleocapsid transport to the plasma membrane requires stable expression and surface accumulation of the viral matrix protein. Cell Microbiol **9:**1203-1214.
179. **Salazar, G., B. Craige, B. H. Wainer, J. Guo, P. De Camilli, and V. Faundez.** 2005. Phosphatidylinositol-4-kinase type II alpha is a component of adaptor protein-3-derived vesicles. Molecular biology of the cell **16:**3692-3704.
180. **Sanderson, C. M., H. H. Wu, and D. P. Nayak.** 1994. Sendai virus M protein binds independently to either the F or the HN glycoprotein in vivo. Journal of virology **68:**69-76.
181. **Schmitt, A. P., and R. A. Lamb.** 2004. Escaping from the cell: assembly and budding of negative-strand RNA viruses. Current topics in microbiology and immunology **283:**145-196.
182. **Schmitt, A. P., G. P. Leser, E. Morita, W. I. Sundquist, and R. A. Lamb.** 2005. Evidence for a new viral late-domain core sequence, FPIV, necessary for budding of a paramyxovirus. Journal of virology **79:**2988-2997.

183. **Schmitt, A. P., G. P. Leser, D. L. Waning, and R. A. Lamb.** 2002. Requirements for budding of paramyxovirus simian virus 5 virus-like particles. Journal of virology **76:**3952-3964.
184. **Schmitt, P. T., G. Ray, and A. P. Schmitt.** 2010. The C-terminal end of parainfluenza virus 5 NP protein is important for virus-like particle production and M-NP protein interaction. Journal of virology **84:**12810-12823.
185. **Schubert, U., D. E. Ott, E. N. Chertova, R. Welker, U. Tessmer, M. F. Princiotta, J. R. Bennink, H. G. Krausslich, and J. W. Yewdell.** 2000. Proteasome inhibition interferes with gag polyprotein processing, release, and maturation of HIV-1 and HIV-2. Proceedings of the National Academy of Sciences of the United States of America **97:**13057-13062.
186. **Scott, A., J. Gaspar, M. D. Stuchell-Brereton, S. L. Alam, J. J. Skalicky, and W. I. Sundquist.** 2005. Structure and ESCRT-III protein interactions of the MIT domain of human VPS4A. Proceedings of the National Academy of Sciences of the United States of America **102:**13813-13818.
187. **Simonsen, A., A. E. Wurmser, S. D. Emr, and H. Stenmark.** 2001. The role of phosphoinositides in membrane transport. Current opinion in cell biology **13:**485-492.
188. **Simpson, F., N. A. Bright, M. A. West, L. S. Newman, R. B. Darnell, and M. S. Robinson.** 1996. A novel adaptor-related protein complex. The Journal of cell biology **133:**749-760.
189. **Simpson, F., A. A. Peden, L. Christopoulou, and M. S. Robinson.** 1997. Characterization of the adaptor-related protein complex, AP-3. The Journal of cell biology **137:**835-845.
190. **Stepp, J. D., K. Huang, and S. K. Lemmon.** 1997. The yeast adaptor protein complex, AP-3, is essential for the efficient delivery of alkaline phosphatase by the alternate pathway to the vacuole. The Journal of cell biology **139:**1761-1774.
191. **Stricker, R., G. Mottet, and L. Roux.** 1994. The Sendai virus matrix protein appears to be recruited in the cytoplasm by the viral nucleocapsid to function in viral assembly and budding. J Gen Virol **75 (Pt 5):**1031-1042.
192. **Sugahara, F., T. Uchiyama, H. Watanabe, Y. Shimazu, M. Kuwayama, Y. Fujii, K. Kiyotani, A. Adachi, N. Kohno, T. Yoshida, and T. Sakaguchi.** 2004. Paramyxovirus Sendai virus-like particle formation by expression of multiple viral proteins and acceleration of its release by C protein. Virology **325:**1-10.
193. **Takimoto, T., K. G. Murti, T. Bousse, R. A. Scroggs, and A. Portner.** 2001. Role of matrix and fusion proteins in budding of Sendai virus. Journal of virology **75:**11384-11391.
194. **Takimoto, T., and A. Portner.** 2004. Molecular mechanism of paramyxovirus budding. Virus research **106:**133-145.
195. **Tavassoli, A., Q. Lu, J. Gam, H. Pan, S. J. Benkovic, and S. N. Cohen.** 2008. Inhibition of HIV budding by a genetically selected cyclic peptide targeting the Gag-TSG101 interaction. ACS Chem Biol **3:**757-764.

196. **Theos, A. C., D. Tenza, J. A. Martina, I. Hurbain, A. A. Peden, E. V. Sviderskaya, A. Stewart, M. S. Robinson, D. C. Bennett, D. F. Cutler, J. S. Bonifacino, M. S. Marks, and G. Raposo.** 2005. Functions of adaptor protein (AP)-3 and AP-1 in tyrosinase sorting from endosomes to melanosomes. Molecular biology of the cell **16:**5356-5372.
197. **Traub, L. M., and S. Kornfeld.** 1997. The trans-Golgi network: a late secretory sorting station. Current opinion in cell biology **9:**527-533.
198. **Ullrich, O., S. Reinsch, S. Urbe, M. Zerial, and R. G. Parton.** 1996. Rab11 regulates recycling through the pericentriolar recycling endosome. The Journal of cell biology **135:**913-924.
199. **Unanue, E. R., E. Ungewickell, and D. Branton.** 1981. The binding of clathrin triskelions to membranes from coated vesicles. Cell **26:**439-446.
200. **Urbe, S., L. A. Huber, M. Zerial, S. A. Tooze, and R. G. Parton.** 1993. Rab11, a small GTPase associated with both constitutive and regulated secretory pathways in PC12 cells. FEBS Lett **334:**175-182.
201. **Utley, T. J., N. A. Ducharme, V. Varthakavi, B. E. Shepherd, P. J. Santangelo, M. E. Lindquist, J. R. Goldenring, and J. E. Crowe, Jr.** 2008. Respiratory syncytial virus uses a Vps4-independent budding mechanism controlled by Rab11-FIP2. Proc Natl Acad Sci U S A **105:**10209-10214.
202. **Ventre, K., and A. G. Randolph.** 2007. Ribavirin for respiratory syncytial virus infection of the lower respiratory tract in infants and young children. Cochrane Database Syst Rev**:**CD000181.
203. **VerPlank, L., F. Bouamr, T. J. LaGrassa, B. Agresta, A. Kikonyogo, J. Leis, and C. A. Carter.** 2001. Tsg101, a homologue of ubiquitin-conjugating (E2) enzymes, binds the L domain in HIV type 1 Pr55(Gag). Proceedings of the National Academy of Sciences of the United States of America **98:**7724-7729.
204. **Vigers, G. P., R. A. Crowther, and B. M. Pearse.** 1986. Location of the 100 kd-50 kd accessory proteins in clathrin coats. EMBO J **5:**2079-2085.
205. **Vogt, C., M. Eickmann, S. Diederich, M. Moll, and A. Maisner.** 2005. Endocytosis of the Nipah virus glycoproteins. Journal of virology **79:**3865-3872.
206. **Votteler, J., and W. I. Sundquist.** 2013. Virus budding and the ESCRT pathway. Cell host & microbe **14:**232-241.
207. **Waheed, A. A., and E. O. Freed.** 2008. Peptide inhibitors of HIV-1 egress. ACS Chem Biol **3:**745-747.
208. **Wakefield, L., and G. G. Brownlee.** 1989. RNA-binding properties of influenza A virus matrix protein M1. Nucleic acids research **17:**8569-8580.
209. **Wang, J. W., and R. B. Roden.** 2013. Virus-like particles for the prevention of human papillomavirus-associated malignancies. Expert Rev Vaccines **12:**129-141.
210. **Wang, Y. E., A. Park, M. Lake, M. Pentecost, B. Torres, T. E. Yun, M. C. Wolf, M. R. Holbrook, A. N. Freiberg, and B. Lee.** 2010. Ubiquitin-regulated nuclear-cytoplasmic trafficking of the Nipah virus matrix protein is important for viral budding. PLoS pathogens **6:**e1001186.

211. **Weingartl, H., S. Czub, J. Copps, Y. Berhane, D. Middleton, P. Marszal, J. Gren, G. Smith, S. Ganske, L. Manning, and M. Czub.** 2005. Invasion of the central nervous system in a porcine host by nipah virus. Journal of virology **79:**7528-7534.
212. **Welliver, R. C.** 2003. Respiratory syncytial virus and other respiratory viruses. Pediatr Infect Dis J **22:**S6-10; discussion S10-12.
213. **Whitman, S. D., and R. E. Dutch.** 2007. Surface density of the Hendra G protein modulates Hendra F protein-promoted membrane fusion: role for Hendra G protein trafficking and degradation. Virology **363:**419-429.
214. **Whitman, S. D., E. C. Smith, and R. E. Dutch.** 2009. Differential rates of protein folding and cellular trafficking for the Hendra virus F and G proteins: implications for F-G complex formation. J Virol **83:**8998-9001.
215. **WHO.** 2009. Acute Respiratory infections.
216. **Williamson, M. M., P. T. Hooper, P. W. Selleck, L. J. Gleeson, P. W. Daniels, H. A. Westbury, and P. K. Murray.** 1998. Transmission studies of Hendra virus (equine morbillivirus) in fruit bats, horses and cats. Aust Vet J **76:**813-818.
217. **Wong, K. T., T. Robertson, B. B. Ong, J. W. Chong, K. C. Yaiw, L. F. Wang, A. J. Ansford, and A. Tannenberg.** 2009. Human Hendra virus infection causes acute and relapsing encephalitis. Neuropathol Appl Neurobiol **35:**296-305.
218. **Wyss, S., C. Berlioz-Torrent, M. Boge, G. Blot, S. Honing, R. Benarous, and M. Thali.** 2001. The highly conserved C-terminal dileucine motif in the cytosolic domain of the human immunodeficiency virus type 1 envelope glycoprotein is critical for its association with the AP-1 clathrin adaptor [correction of adapter]. Journal of virology **75:**2982-2992.
219. **Yamayoshi, S., T. Noda, H. Ebihara, H. Goto, Y. Morikawa, I. S. Lukashevich, G. Neumann, H. Feldmann, and Y. Kawaoka.** 2008. Ebola virus matrix protein VP40 uses the COPII transport system for its intracellular transport. Cell host & microbe **3:**168-177.
220. **Yeaman, C., K. K. Grindstaff, J. R. Wright, and W. J. Nelson.** 2001. Sec6/8 complexes on trans-Golgi network and plasma membrane regulate late stages of exocytosis in mammalian cells. The Journal of cell biology **155:**593-604.
221. **Yoshida, T., Y. Nagai, K. Maeno, M. Iinuma, M. Hamaguchi, T. Matsumoto, S. Nagayoshi, and M. Hoshino.** 1979. Studies on the role of M protein in virus assembly using a ts mutant of HVJ (Sendai virus). Virology **92:**139-154.
222. **Zamarin, D., and P. Palese.** 2012. Oncolytic Newcastle disease virus for cancer therapy: old challenges and new directions. Future Microbiol **7:**347-367.
223. **Zhang, G., C. Cowled, Z. Shi, Z. Huang, K. A. Bishop-Lilly, X. Fang, J. W. Wynne, Z. Xiong, M. L. Baker, W. Zhao, M. Tachedjian, Y. Zhu, P. Zhou, X. Jiang, J. Ng, L. Yang, L. Wu, J. Xiao, Y. Feng, Y. Chen, X. Sun, Y. Zhang, G. A. Marsh, G. Crameri, C. C. Broder, K. G. Frey, L. F. Wang, and J. Wang.** 2013.

Comparative analysis of bat genomes provides insight into the evolution of flight and immunity. Science **339:**456-460.

224. **Zhen, L., S. Jiang, L. Feng, N. A. Bright, A. A. Peden, A. B. Seymour, E. K. Novak, R. Elliott, M. B. Gorin, M. S. Robinson, and R. T. Swank.** 1999. Abnormal expression and subcellular distribution of subunit proteins of the AP-3 adaptor complex lead to platelet storage pool deficiency in the pearl mouse. Blood **94:**146-155.

225. **Zhu, Z., K. N. Bossart, K. A. Bishop, G. Crameri, A. S. Dimitrov, J. A. McEachern, Y. Feng, D. Middleton, L. F. Wang, C. C. Broder, and D. S. Dimitrov.** 2008. Exceptionally potent cross-reactive neutralization of Nipah and Hendra viruses by a human monoclonal antibody. J Infect Dis **197:**846-853.

226. **Zhu, Z., A. S. Dimitrov, K. N. Bossart, G. Crameri, K. A. Bishop, V. Choudhry, B. A. Mungall, Y. R. Feng, A. Choudhary, M. Y. Zhang, Y. Feng, L. F. Wang, X. Xiao, B. T. Eaton, C. C. Broder, and D. S. Dimitrov.** 2006. Potent neutralization of Hendra and Nipah viruses by human monoclonal antibodies. Journal of virology **80:**891-899.

VITA
Weina Sun

EDUCATIONAL BACKGROUND

2008-2015

Ph.D. in Pathobiology,
The Pennsylvania State University, University Park, PA.

2004-2008

B.S. in Biological Science
Jilin University, Changchun, China

CONFERENCES AND PRESETATIONS

Dec.10-11, 2013

Oral presentation with Dr. Anthony Schmitt "Characterization & Disruption of Host Protein Interactions Required for Budding of Hendra and Nipah Viruses", MARCE-2 Closeout Meeting.

Jul. 20-24, 2013

Conference volunteer, American Society for Virology 2013 Annual Meeting at The Pennsylvania State University.

Mar. 2013

Poster presentation "Interaction of Henipavirus Matrix Protein with Host Protein AP3B1" at 2013 Graduate Exhibition of The Pennsylvania State University.

Jul.16-20, 2011

Oral presentation "Paramyxovirus M Protein Interaction with AP-3 complex", American Society for Virology 2011 Annual Meeting at University of Minnesota.

HORNORS AND AWARDS

2008: Honored graduate of Jilin University.
2006-2007: The second-class scholarship of Jilin University; Honored student of Jilin University; Honored student cadre of life science college, Jilin University.
2005-2006: The first-class scholarship of Jilin University; Dong Rong social scholarship; Honored student of Jilin University.
2004-2005: The second-class scholarship of Jilin University; Honored student of Jilin University.

PUBLICATIONS

Weina Sun, Thomas S. McCrory, Wei Young Khaw, Stephanie Petzing, Terrel Myers, Anthony P. Schmitt. Matrix Proteins of Nipah and Hendra Viruses Interact with Beta Subunits of AP-3 Complexes J. Virol. published ahead of print 10 September 2014,doi:10.1128/JVI.02103-14